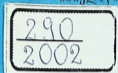


Proceedings of I. Javakhishvili Tbilisi State University

თვ. ჯავახიშვილის სახელობის თბილისის
სახელმწიფო უნივერსიტეტის შრომები



352

ISSN 1512-1461

PHYSICS
ფიზიკა

38



Proceedings of I. Javakhishvili Tbilisi State University

ივ. ჯავახიშვილის სახელობის თბილისის
სახელმწიფო უნივერსიტეტის შრომები



352

ISSN 1512-1461

www.tsu.edu.ge

PHYSICS

ფიზიკა

38

TBILISI UNIVERSITY PRESS



თბილისის უნივერსიტეტის გამომცემლობა

Tbilisi 2002 თბილისი

ББК 22.3

УДК 53

ფ 505

Editorial board

N. Amaglobeli, A. Gerasimov, Z. Kachlishvili, N. Kekelidze,
A. Khelashvili, Z. Khvedelidze, T. Kopalishvili (editor),
L. Kurdadze, R. Kvatadze, J. Mebonia, G. Mrevlishvili, T. Sanadze,
A. Ugulava (secretary).

სარედაქციო კოლეგია

ნ. ამაღლობელი, ა. გერასიმოვი, ნ. კეკელიძე,
თ. კოპალიშვილი (რედაქტორი), ჯ. მებონია,
გ. მრევლიშვილი, თ. სანაძე, ა. უგულავა (მდივანი),
ზ. ქაჩლიშვილი, რ. ქვათაძე, ლ. ქურდაძე, ზ. ხვედელიძე,
ა. ხელაშვილი.

© Tbilisi University Press, 2002

© თბილისის უნივერსიტეტის გამომცემლობა, 2002



THE INFLUENCE OF PRELIMINARY NONPOLARIZED EXPOSURE ON THE PHOTOANISOTROPY OF MORDANT AZODYES

G. Kakauridze, V. Shaverdova

Accepted for publication January, 2002

ABSTRACT. The influence of nonpolarized preillumination on photoanisotropy of media on the basis of Mordant azodyes in polymeric matrix has been experimentally investigated. It is shown that such action on the material increases the value of photoanisotropic sensitivity and also the absolute value of photoanisotropic parameters. The possible mechanism of influence of nonpolarized preillumination has been discussed.

The interest in polarization-sensitive media for the tasks of optical information storage and processing has recently increased. From this point of view the increase of the sensitivity of polarization-sensitive media is rather a task of current interest.

Quite a number of polarization-sensitive media with different mechanisms of the induction of anisotropy are known [1-4]. The media on the basis of organic dyes have quite a number of advantages: high resolution power, comparatively high light sensitivity. Among the investigated dyes mordant azodyes have turned out to be the most effective [5]. The chemical-technological optimization of media made earlier on the basis of mordant azodyes resulted in the essential increase of both light sensitivity and parameters of photoanisotropy. The matrix turned out to play an essential role under otherwise equal conditions. The carried out experiments have shown that the matrix on the basis of polyvinylpyrrolidone (PVP) with molecular mass $M = 35000$ is the most effective to achieve maximum values of photoanisotropy, and also photoanisotropic sensitivity [6,7].

In this work the influence of the preliminary exposure by nonpolarized light that are actinic wavelengths for the given media is being investigated in order to find out the possibility of further increase of photoanisotropic sensitivity in media on the basis of mordant azodyes.

63006030006
33600000000
22000000000
00000000000

The investigations were carried out on the samples with the dyes Mordant Pure Yellow (MPY) and specially synthesized dye with additional methyl group in a meta-position to azo-group (MPYM) [8] introduced into PVP matrix with $M = 35000$. The concentration of the dyes was 0.01 mol/l , concentration of PVP - 5 %; the thickness of the samples measured on a microinterferometer МИИ-10 was ~ 8.5 microns.

The preliminary non-polarized exposure was made by radiation of He-Cd laser ЛГ-62 ($\lambda = 441.6 \text{ nm}$). The power range of exposure was $2.6 - 54 \text{ J/cm}^2$ and as experiments have shown exposure $\sim 25 \text{ J/cm}^2$ turned out to be optimal. In order to receive exposure dependence $A_{ef} = f(H)$ the samples were exposed by polarized radiation of He-Cd laser ЛГ-70 ($\lambda = 441.6 \text{ nm}$) in exposure range $0.22 - 220 \text{ J/cm}^2$.

The anisotropy that appears in the medium was estimated by means of the parameter introduced into the work [9] - effective anisotropy A_{ef} , which is an anisotropic invariant of Jones matrix of the medium which is numerically equal to the transmission of the sample under investigation placed between crossed polarizers at the angle of 45° between the axis of anisotropy and the axis of transmission of one of the polarizers. Measurements A_{ef} were made on the modified spectrophotometer СФ-4А on the wavelength of the spectral maximum of photoanisotropy - 535 nm discovered earlier [9].

Fig. 1 shows the family of exposure curves for the dyes MPY and MPYM in PVP matrix: curve 1 - for sample MPY without preexposure, curve 2 - for the similar sample after preexposure; curve 3 - for the sample MPYM without preexposure, curve 4 - after preexposure. As we see from the Figure the preexposure by nonpolarized light for both dyes results in the increase of photoanisotropy.

From the above-mentioned exposure curves the values of polarization sensitivity of the material have been calculated. Polarization sensitivity is defined as the value which is inverse to exposure and which is necessary to achieve effective anisotropy that exceeds the original level by a predetermined value with the criterion of polarization sensitivity which is equal to 0.2 [9].

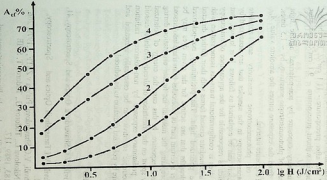


Fig.1. Exposure dependence $A_{eff} = \lg H$ (J/cm²) for the dye MPY and MPYM: curve 1 – for the dye MPY without preexposure; 2 – after preexposure; 3 – for the dye MPYM without preexposure; 4 – after preexposure.

The following results have been received. For the dye MPY in PVP matrix without preliminary exposure the polarization sensitivity is equal to $7.7 \text{ cm}^2/\text{J}$ and after preexposure - $11.1 \text{ cm}^2/\text{J}$. For the dye MPYM in PVP matrix without preexposure - $9.1 \text{ cm}^2/\text{J}$ and after preexposure - $12.5 \text{ cm}^2/\text{J}$.

Thus the preliminary exposure by non-polarized actinic light results in the increase of photoanisotropic sensitivity by ~ 1.5 times. Besides as we see from the exposure curves the absolute value A_{ef} also increases in all exposure interval.

The increase of photoanisotropic sensitivity and absolute maximums of photoanisotropy in the samples that are sensitized by non-polarized exposure can be explained as follows. It is known, that the mechanism which is responsible for the appearance of anisotropy in the investigated dyes is configurational trans-cis isomerization with the appearance of intermediate cisoid forms with their further directed orientation by the polarized light. The preliminary non-polarized exposure by wavelengths that are actinic for the given dyes may be presumed to transfer a certain part of molecules from trans into cisoid forms as though preparing the material for further orientation during subsequent polarized exposure. In this case the energy of polarized radiation is mainly spent on the orientation of already available cisoid forms. Thus the preliminary exposure by non-polarized radiation permits photoanisotropic sensitivity to be essentially increased and thereby the exposure by polarized radiation to be reduced.

REFERENCES

1. Sh.D.Kakichashvili, V.G.Shaverdova. Optics and Spectroscopy, **41**, 1976, 892.
2. Sh.D.Kakichashvili, V.I.Tarasashvili. Optics and Spectroscopy, **60**, 1986, 1071.
3. Sh.D.Kakichashvili, V.G.Shaverdova. Pis'ma v ZhTF, **5**, 1979, 266.
4. Markovsky P., Nikolova L., Todorov G., Todorov T. SPIE Proceedings, **1183**, 1989, 117.
5. Sh.D.Kakichashvili, V.G.Shaverdova. In: Photoanisotropic and Photogyrotropic Phenomenon in Condensed Media and Polarization



Holography, Mecniereba, Tbilisi, 1987, 48.

6. G.A.Kakauridze, V.G.Shaverdova, Y.A.Shvaitser, D.Shatalin. Pis'ma v ZhTF, 16, 1990, 59.

7. Sh.D.Kakichashvili, B.N.Kilosanidze, V.G.Shaverdova. Optics and Spectroscopy, 68, 1990, 1309.

8. A.Y.Zhel'tov, B.I.Stepanov, V.G.Shaverdova. Journ. of Applied Spectroscopy, 52, 1990, 280.

9. A.I.Balabanov, G.A.Kakauridze, Sh.D.Kakichashvili, A.V.Savickii, V.G.Shaverdova, Y.A.Shvaitser. Optics and Spectroscopy, 67, 1989, 409.

Georgian Academy of Sciences
Institute of Cybernetics

გ. კაკაურიძე, ვ. შავერდოვა

**წინასწარი არაპოლარიზებული დასხვივების მოქმედება
ამოსაღებავების ფოტოანიზოტროპიაზე**

დასკვნა

ექსპერიმენტულად გამოკვლეულია პოლიმერულ მატრიცაში ამოსაღებავების ბაზაზე შექმნილი არეების ფოტოანიზოტროპიაზე წინასწარი არაპოლარიზებული დასხვივების მოქმედება. ნაჩვენებია, რომ მასალაზე ასეთი შემოქმედება ზრდის როგორც ფოტოანიზოტროპული მგრძობიარობის მნიშვნელობას, ასევე ფოტოანიზოტროპიის პარამეტრების აბსოლუტურ მნიშვნელობებს. განიხილება არაპოლარიზებული დასხვივების მოქმედების შესაძლო მექანიზმები.

PHOTOANISOTROPY IN MEDIA ON THE BASIS OF ISOMERIC DYES METANILIC YELLOW AND TROPEOLIN 00

G. Kakauridze, V. Shaverdova

Accepted for publication January, 2002

ABSTRACT. Photoanisotropy of media on the basis of isomeric monoazodyes Metanilic yellow and Tropeolin 00 introduced into different polymeric matrices has been investigated. It is shown that the material on the basis of the dye Tropeolin 00 in PVP matrix with molecular mass 35000 has great photoanisotropic sensitivity compared with other discussed dyes and matrices. The influence of structural factors of molecular structure of dyes and their possible complex formation with PVP matrix on the value of photoanisotropic sensitivity is discussed.

Polarization-sensitive media which can fix the distribution of polarization of the exposing light beam have been used more often lately for optical information storing, coding and processing [1,2].

The method of polarization sensitometry [3] which enables complex and complex circular birefringence of the anisotropic sample to be defined has been developed to quantitatively describe anisotropy induced by polarized light. In order to make necessary calculations from 4 up to 8 transmission measurements of a differently oriented sample placed between parallel and crossed polarizers are required. Though this procedure gives the fullest description of anisotropy and permits the vector scalar reaction of the medium [3] to be calculated too, its use for investigating the induction kinetics and relaxation of photoanisotropy is hindered as it does not allow measurements to be made in the real scale of time.

The characteristic called effective anisotropy A_{ef} introduced in the work [4] allows to describe photoinduced anisotropy with the help of one measurement and is a modulus of anisotropic invariant of Johnes matrix of the medium:

$$A_{ef} = |\gamma^2| = \frac{1}{2} \exp\left\{-2kd(\overline{n\tau})\right\} [chkd\Delta(n\tau) - \cos kd\Delta n],$$

where $kd(\overline{n\tau})$ characterizes average absorption of the medium, $kd\Delta(n\tau)$ is dichroism and $kd\Delta n$ birefringence of the medium. The anisotropic invariant $|\gamma^2|$ is numerically equal to the transmission of the sample under investigation placed between the crossed polarizers when the angle between the axis of the induced anisotropy and the axis of transmission of one of the polarizers is equal to 45° . It follows from the above-mentioned expression for A_{ef} that this magnitude characterizes the joint contribution of dichroism, birefringence and scalar absorption to the induced anisotropy of the sample. The use of A_{ef} enables anisotropy to be induced and its parameters to be measured simultaneously and also the materials to be compared with different mechanisms of the induction of photoanisotropy.

In this work this method of sensitometry is used to investigate photoanisotropy in the media on the basis of isomeric azodyes: Metanilic yellow and Tropeolin 00 introduced into different polymeric matrices: to gelatine, nitrocellulose, polyvinylpyrrolidone with molecular mass $M = 12500$ and $M = 35000$. The concentration of dyes was $1.6 \times 10^{-2} \text{ mol/l}$, the concentration of polymers - 5%.

The measurements of A_{ef} were made in the real scale of time with the help of a photometric scheme in which the photoanisotropy in the sample was induced by He-Cd laser light ($\lambda = 441.6 \text{ nm}$) with power 12 mW and at the same time A_{ef} was measured with the help of the probing beam of the He-Ne laser ($\lambda = 632.8 \text{ nm}$) with power 2 mW. The polarization plane of the probing beam made an angle 45° with the polarization plane of the illuminating beam. Both beams were perpendicularly incident on one and the same area of the sample.

Having passed through the sample the beams were divided by a prism, in that case the illuminating beam reached a photoresistor the signal from which was given on one of the channels of the quick-operating recording device H 338-6П and the probing beam was

incident on the polarizer whose transmission axis made an angle of 90° with the initial direction of the polarization of that beam.

The preliminary experiments have shown, that the gyrotropy in all the samples is very small and we can think the axis of the induced anisotropy does not turn round and coincides with the direction of the polarization of an actinic beam.

In case the sample is isotropic the polarizer does not transmit the probing beam. When anisotropy is induced the probing beam passes through the polarizer and reaches the second photoresistor the signal from which is given on the other channel of the device H 338-6П. Another channel of this device served as a time marker. Energy density was calculated according to exposure duration and polarization exposure curves were plotted.

Fig. 1 shows the curves of exposure dependence $A_{ef} = f(H_\lambda)$ for the dye Metanilic yellow in different matrices: in nitrocellulose - curve 1, in gelatine- curve 2, in polyvinylpyrrolidone with $M = 12500$ - curve 3, in polyvinylpyrrolidone with $M = 35000$ - curve 4; the curves 5 and 6 are exposure curves for Tropeolin 00 in matrix polyvinylpyrrolidone $M = 12500$ and in polyvinylpyrrolidone with $M = 35000$. Exposure range was $0.048 - 2.2 \text{ J/cm}^2$ that permitted the saturation A_{ef} to be achieved for all the samples. The maximum value $A_{ef} \sim 27\%$ was received for the medium on the basis of dye Metanilic yellow in polyvinylpyrrolidone matrix with $M = 35000$.

Photoanisotropic sensitivity was calculated for the samples under investigation according to these curves. According to [4] photoanisotropic sensitivity is defined as the value which is inverse to the exposure necessary to achieve A_{ef} exceeding the initial level Q_0 on a definite value Q_{cr} called the criterion of photoanisotropic sensitivity

$$S = \left\{ H_{Q=Q_0+Q_{cr}} \right\}^{-1}, \quad Q = \lg A_{ef}.$$

$Q_0 = 0.3$ is usually accepted which is due to the sensitivity threshold of most of the devices and $Q_{cr} = 0.2$. Such a description of photoanisotropic sensitivity allows photoanisotropic materials to be compared with different mechanisms of induction of anisotropy.

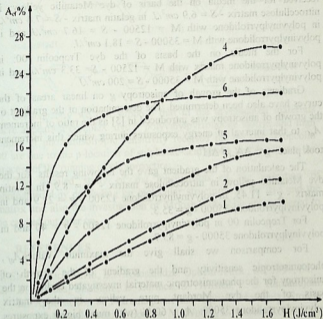


Fig.1. The family of the curves of exposure dependence $A_d = f(H_x)$:
 curve 1 – for the dye Metanilic yellow in nitrocellulose matrix,
 2 – in gelatine matrix, 3 – in PVP matrix ($M = 12500$), 4 — in
 PVP matrix ($M = 35000$); 5 – for dye Tropaeolin 00 in PVP
 matrix ($M = 12500$), 6 – in PVP matrix ($M = 135000$).



The following values of photoanisotropic sensitivity have been received for the media on the basis of dye Metanilic yellow: in nitrocellulose matrix - $S = 6.9 \text{ cm}^2/\text{J}$, in gelatin matrix - $S = 7.4 \text{ cm}^2/\text{J}$, in polyvinylpyrrolidone with $M = 12500$ - $S = 16.7 \text{ cm}^2/\text{J}$ and in polyvinylpyrrolidone with $M = 35000$ - $S = 18.1 \text{ cm}^2/\text{J}$.

For the media on the basis of the dye Tropeolin 00: in polyvinylpyrrolidone matrix with $M = 12500$ - $S = 33.3 \text{ cm}^2/\text{J}$ and in polyvinylpyrrolidone with $M = 35000$ - $S = 200 \text{ cm}^2/\text{J}$.

Gradients of the growth of anisotropy g on linear areas of the curves have also been determined. The determination of the gradient of the growth of anisotropy was introduced in [5] as the ratio of increment A_{ef} to that interval of energy exposures during which this increment took place: $g = \Delta A_{ef} / \Delta H$.

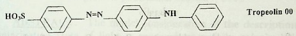
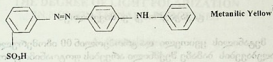
The calculation of the gradient gave the following results: for the dye Metanilic yellow in nitrocellulose matrix - $g = 8.9$, in gelatin matrix - $g = 11.45$, in polyvinylpyrrolidone 12500 - $g = 22.9$ and in polyvinylpyrrolidone 35000 - $g = 35.3$.

For Tropeolin 00 in polyvinylpyrrolidone 12500 - $g = 40$ and in polyvinylpyrrolidone 35000 - $g = 85.7$.

For comparison we shall give the maximum values A_{ef} , photoanisotropic sensitivity and the gradient of the growth of anisotropy for the photoanisotropic material investigated earlier on the basis of the dye Mordant pure yellow in the matrix polyvinylpyrrolidone 35000: $A_{ef} \sim 60\%$ (with much bigger exposures $\sim 17.5 \text{ J/cm}^2$), $S = 3.4 \text{ cm}^2/\text{J}$, $g \sim 12.2$ [4].

The carried out investigation has shown, that though in the media on the basis of isomeric dyes Metanilic yellow and Tropeolin 00 we do not succeed in achieving high values of the induced effective anisotropy, the sensitivity of such media is great, especially for Tropeolin 00. It should be especially noted the essential role of the polymer matrix when the molecular mass of one and the same polymer can change photoanisotropic sensitivity almost by an order.

It is known, that the mechanism of the induction of photoanisotropy in these azo dyes is trans-cis isomerization and Metanilic yellow differs from Tropeolin 00 only by the location of sulphonic-acid group.



Consequently we can suppose that in the investigated materials there appears a complex: dye + polyvinylpyrrolidone matrix and high values of photoanisotropic sensitivity received for the dye Tropocolin 00 are due to the p-location of sulphonic-acid group that facilitates the process of the running of photoreaction.

The detailed study of the mechanisms of the induction of photoanisotropy depending on molecular structures of the dye and the matrix and also the investigation of darkish relaxation are supposed to be carried out later on.

REFERENCES

1. Sh.D.Kakichashvili, B.N.Kilosanidze. Optical Journ., 64, 1997, 64.
2. B. Kerekes, Sz. Sajti., E. Lurincz, S. Hvilsted, P. S. Ramanujam. In: Applications of Ferromagnetic and Optical Materials, Storage and Magnetolectronics. Editors: M. Wuttig, L.Hesselink, H.J. Borg. MRS Proceedings, 2001, 674.
3. Sh. D. Kakichashvili. Polarization Holography, 1989.
4. A. I. Balabanov, G. A. Kakauridze, Sh. D. Kakichashvili, A. V. Savickii, V. G. Shaverdova, Y.A. Shvaitser. Optics and Spectroscopy, 67, 1989, 409.
5. Sh. D. Kakichashvili, V. G. Shaverdova. In: Photoanisotropic and Photogyrotropic Phenomenon in Condensed Media and Polarization Holography, 1987, 48.

Georgian Academy of Sciences
Institute of Cybernetics

გ. კაკაურიძე, ვ. შავერდია

მეტანილის ყვითელი და ტროპეოლინ 00 იზომერული
საღებავების ბაზაზე შექმნილი არეების ფოტოანიზოტროპია

დასკვნა

გამოკვლეულია სხვადასხვა პოლიმერულ მატრიცებში შეყვანით მეტანილის ყვითელი და ტროპეოლინ 00 მონოაზოსაღებავების ბაზაზე შექმნილი არეების ფოტოანიზოტროპია. ნაჩვენებია, რომ VP მატრიცაში მოლეკულური მასით 35000 ტროპეოლინ 00 საღებავის ბაზაზე მასალა სხვა განხილულ საღებავებსა და მატრიცებთან შედარებით მნიშვნელოვან ფოტოანიზოტროპულ მგრძნობიარობას ფლობს. განიხილება სტრუქტურული ფაქტორების მოქმედება საღებავების წყობაზე და მათი შესაძლებელი კომპლექსი VP მატრიცასთან ფოტოანიზოტროპულ მგრძნობიარობის სიდიდეზე.

REFERENCES

1. B. N. Kiselev, *Dokl. Akad. Nauk SSSR*, 197, 197 (1970).
2. B. N. Kiselev, *Dokl. Akad. Nauk SSSR*, 200, 197 (1971).
3. B. N. Kiselev, *Dokl. Akad. Nauk SSSR*, 200, 197 (1971).
4. B. N. Kiselev, *Dokl. Akad. Nauk SSSR*, 200, 197 (1971).
5. B. N. Kiselev, *Dokl. Akad. Nauk SSSR*, 200, 197 (1971).
6. B. N. Kiselev, *Dokl. Akad. Nauk SSSR*, 200, 197 (1971).
7. B. N. Kiselev, *Dokl. Akad. Nauk SSSR*, 200, 197 (1971).
8. B. N. Kiselev, *Dokl. Akad. Nauk SSSR*, 200, 197 (1971).
9. B. N. Kiselev, *Dokl. Akad. Nauk SSSR*, 200, 197 (1971).
10. B. N. Kiselev, *Dokl. Akad. Nauk SSSR*, 200, 197 (1971).

THE DEGREE OF LIGHT POLARIZATION IN NONSTATIONARY PROCESSES



A. Purtseladze

Accepted for publication February, 2002

ABSTRACT. The model consideration of the description of polarization state of light is received when fully polarized light passed through a nonstationary anisotropic device is presented. In this case fully polarized light becomes partially polarized. It is shown that the degree of the polarization of light is immediately connected with the time profile of nonstationary process.

As is known partially polarized radiation is obtained from nonpolarized during reflection or scattering [1]. The reception of partially polarized radiation as a result of passing of originally fully polarized light through the nonstationary device was first investigated in [2,3]. In this work the further development of this approach is made for the nonstationary device, the coefficient of birefringence of which sinusoidally changes in time.

The model polarization device is presented in the form of a medium single thickness (for the simplicity of further discussion) with a birefringent coefficient $\Delta n = n_x - n_y$ (n_x, n_y are the value of n coefficient according to the respective axes) and the orientation of the axis of anisotropy ρ . If Δn and ρ are sufficiently quick functions of time and with this $n_x + n_y$ with sufficient accuracy can be accepted as independent of time, then the model device turns out to be nonstationary. Such a device causes depolarization of the fully polarized wave front and the field of the transmitted wave immediately after the device becomes partially polarized. The degree of light polarization connected with the time profile of the nonstationary process can be presented as [2]:

$$V \approx \left| \frac{\int_{-T'}^{T'} \cos^2 \left[\frac{\alpha_0}{2} \Delta n(t) \right] dt + \int_{-T'}^{T'} \sin^2 \left[\frac{\alpha_0}{2} \Delta n(t) \right] \cos 4\rho(t) dt}{\int_{-T'}^{T'} \cos^2 \left[\frac{\alpha_0}{2} \Delta n(t) \right] dt + \int_{-T'}^{T'} \sin^2 \left[\frac{\alpha_0}{2} \Delta n(t) \right] dt} \right| \quad (1)$$

where $\alpha_0 = \frac{2\pi}{\lambda_0}$ (λ_0 - is the length in a general case of an elliptically polarized wave coming on the device), T' is the time of observation.

As an example of a nonstationary model polarization device let us choose the law of time change in the following form:

$$n_x + n_y \approx 2n_0 \quad (2)$$

$$\Delta n(t) = n_0 \sin \bar{\omega} t, \quad \rho(t) = kt,$$

where $\bar{\omega}$ is a cyclic frequency of the device, n_0 and k are characteristics of the model. Thus we have:

$$V \approx \left| \frac{\int_{-T'}^{T'} \cos^2 \left(\frac{\alpha_0}{2} n_0 \sin \bar{\omega} t \right) dt + \int_{-T'}^{T'} \sin^2 \left(\frac{\alpha_0}{2} n_0 \sin \bar{\omega} t \right) \cos 4ktdt}{\int_{-T'}^{T'} \cos^2 \left(\frac{\alpha_0}{2} n_0 \sin \bar{\omega} t \right) dt + \int_{-T'}^{T'} \sin^2 \left(\frac{\alpha_0}{2} n_0 \sin \bar{\omega} t \right) dt} \right| \quad (3)$$

The transformation of the last expression gives:

$$V \approx \left| \frac{1}{2} + \frac{1}{2T'} \int_0^{T'} \cos(\alpha_0 n_0 \sin \bar{\omega} t) dt + \frac{1}{2T'} \int_0^{T'} \cos 4ktdt - \frac{1}{2T'} \int_0^{T'} \cos(\alpha_0 n_0 \sin \bar{\omega} t) \cos 4ktdt \right| \quad (4)$$

where:

$$\int_0^{T'} (\alpha_0 n_0 \sin \bar{\omega} t) dt = \frac{1}{\bar{\omega}} \int_0^{\bar{\omega} T'} \cos(\alpha_0 n_0 \sin x) dx =$$

$$= \frac{1}{\bar{\omega}} \frac{\bar{\omega} T'}{\pi} \int_0^{\pi} \cos \left[\alpha_0 n_0 \sin \left(\frac{\bar{\omega} T'}{\pi} x \right) \right] d \left(\frac{\bar{\omega} T'}{\pi} x \right) = T' J_0(\alpha_0 n_0), \quad (5)$$

J_0 is the Bessel function of the first kind of zero order [4].

$$\int_0^T \cos(4kt) dt = \frac{1}{4k} [\sin 4kt]_0^T = \frac{\sin 4kT}{4k} \quad (6)$$

$$\int_0^{T'} \cos(\alpha_0 n_0 \sin \bar{\omega} t) \cos 4kt dt = \frac{1}{\bar{\omega}} \int_0^{\bar{\omega} T'} \cos(\alpha_0 n_0 \sin x) \cos \left(\frac{4k}{\bar{\omega}} x \right) dx =$$

$$= \frac{1}{2\bar{\omega}} \int_0^{\bar{\omega} T'} \left[\cos \left(\alpha_0 n_0 \sin x - \frac{4k}{\bar{\omega}} x \right) + \cos \left(\alpha_0 n_0 \sin x + \frac{4k}{\bar{\omega}} x \right) \right] dx =$$

$$= \frac{1}{2\bar{\omega}} \left[\pi \frac{\sin 4kT'}{\sin \left(\frac{4k\pi}{\bar{\omega}} \right)} J_{\frac{4k}{\bar{\omega}}}(\alpha_0 n_0) + \pi \frac{\sin 4kT'}{\sin \left(\frac{4k\pi}{\bar{\omega}} \right)} J_{-\frac{4k}{\bar{\omega}}}(\alpha_0 n_0) \right] =$$

$$= \frac{\pi}{2\bar{\omega}} \frac{\sin 4kT'}{\sin \left(\frac{4k\pi}{\bar{\omega}} \right)} \left[J_{\frac{4k}{\bar{\omega}}}(\alpha_0 n_0) + J_{-\frac{4k}{\bar{\omega}}}(\alpha_0 n_0) \right], \quad (7)$$

J_ν is the function of Anger ν order [4].

Substituting the received integrals into (4) we shall finally receive:



22592

$$V \approx \left| \frac{1}{2} + \frac{1}{2} J_0(x_0 n_0) + \frac{1}{2} \frac{\sin 4kT'}{4kT'} - \frac{1}{4} \frac{\pi}{\omega T'} \frac{\sin 4kT'}{\sin\left(\frac{4k\pi}{\omega}\right)} \left[J_{\frac{4k}{\omega}}(x_0 n_0) + J_{-\frac{4k}{\omega}}(x_0 n_0) \right] \right| \quad (8)$$

We can show according to [5] that

$$J_{\frac{4k}{\omega}}(x_0 n_0) + J_{-\frac{4k}{\omega}}(x_0 n_0) \leq 2 \frac{\sin\left(\frac{4k\pi}{\omega}\right)}{4k\pi/\omega}$$

In this case taking into consideration

$$\begin{aligned} \max\left[\frac{\sin 4kT'}{4kT'}\right] &= 1 & \max[J_0(x_0 n_0)] &= 1 \\ \min\left[\frac{\sin 4kT'}{4kT'}\right] &\approx -0.2 & \min[J_0(x_0 n_0)] &\approx -0.4 \end{aligned} \quad (9)$$

We shall receive from (8)

$$\begin{aligned} \max[V] &= \left| \frac{1}{2} + \frac{1}{2} + \frac{1}{2} - \frac{1}{2} \right| = 1 \\ \min[V] &\approx \left| \frac{1}{2} + \frac{1}{2}(-0.4) + \frac{1}{2}(-0.2) - \frac{1}{2} \cdot 0.2 \right| = 0.3. \end{aligned}$$

Thus for the model:

$$0.3 \leq V \leq 1. \quad (10)$$

The similar results can be received in the approach of geometrical optics, when $\lambda_o \rightarrow 0$. According to [4,5]

$$J_o(x_o n_o) \approx \sqrt{\frac{2}{\pi x_o n_o}} \cos\left(x_o n_o - \frac{\pi}{4}\right) \rightarrow 0,$$

$$J_{\frac{4k}{\omega}}(x_o n_o) \approx \sqrt{\frac{2}{\pi x_o n_o}} \cos\left(x_o n_o - \frac{2k\pi}{\omega} - \frac{\pi}{4}\right) \rightarrow 0,$$

$$J_{-\frac{4k}{\omega}}(x_o n_o) \approx \sqrt{\frac{2}{\pi x_o n_o}} \cos\left(x_o n_o + \frac{2k\pi}{\omega} - \frac{\pi}{4}\right) \rightarrow 0,$$

consequently for the degree of polarization we shall have from (8)

$$V \approx \frac{1}{2} \left(1 + \frac{\sin 4kT'}{4kT'} \right), \quad (11)$$

where using (9) we have:

$$0.4 \leq V \leq 1,$$

which does not contradict (10).

Both in general case (8) and in the approach of geometrical optics (11) in case of final T' the device is stationary when $k = 0$, then it is evident $V = 1$ and the polarization device does not influence the degree of polarization of radiation.

Thus, the described method of the definition of the degree of partial polarization of light can be used for any device if the time profile of its nonstationarity is known. The inverse problem can also be considered – the definition of the kind of device's nonstationarity in case of full depolarization of light, which has passed through the device which is supposed to be carried out in future.

Acknowledgment. The author is grateful to **Sh. Kakichashvili** for the working of the task and helpful discussions.

REFERENCES

1. M. Born, E. Wolf. Principles of Optics. 1973. (Russian).
2. Sh. Kakichashvili. The Journal of Technical Physics, 65, 1995, 200 (Russian).
3. Sh. Kakichashvili, A. Purtseladze. Letter to Journal of Technical Physics, 25, 1999, 74 (Russian).
4. E. Yanke, F. Emde, F. Lesh. Special Functions. 1977, 342 (Russian).
5. Mathematical Encyclopedia. 1, 1977, 1152 (Russian).

Georgian Academy of Sciences
Institute of Cybernetics

ა. ფურცელაძე

სინათლის პოლარიზაციის ხარისხი არასტაციონარულ პროცესებში

დასკენა

წარმოდგენილია არასტაციონარულ ანიზოტროპულ მოწყობილობაში თავდაპირველად სრულად პოლარიზებული სინათლის გავლის შედეგად მიღებული ველის პოლარიზაციის მდგომარეობის აღწერის მოდელური განხილვა. ამ შემთხვევაში სრულად პოლარიზებული სინათლე ხდება ნაწილობრივად პოლარიზებული. ნაჩვენებია, რომ სინათლის პოლარიზაციის ხარისხი უშუალოდ არასტაციონარული პროცესების დროით პროფილთან არის დაკავშირებული.

DYNAMICS OF ATMOSPHERIC PROCESSES AND THEIR ROLE IN ECOLOGICAL PROBLEMS OF GEORGIA

Z. Khvedelidze, I. Aladashvili, T. Shalamberidze,
E. Tagvadze, R. Chakvaia

Accepted for publication March, 2002

ABSTRACT. Any regional microclimate is determined by common atmospheric circulation and Earth "radiative" surface conditions. The microclimate peculiarity considering certain factors is studied in the work and influence of seasonal stability parameter of relief and processes is taken into account. The rate of the air purification from bad admixtures and self purification period for some regions of Georgia are evaluated.

Modern civilization faces urgent problem of today. It includes study and analysis of ecological situations of separate regions of Georgia. It is well-known, that ecological or meteorological phenomena of the given region are caused primarily by the general long-scale circulation of air. This motion forms the background magnitudes of different value variation. Disturbances brought about by the local, thermal and orography reasons are added continuously to it. The events of these types are observed basically in the meso-scale boundary layer of the atmosphere (10-100 km).

Based on the above-mentioned, the dynamics of atmospheric processes should be studied with the consideration of physical and geographical features of a certain region. It is important to determine the leading factors that develop a process and evaluate their roles [1,2,6].

For realization of the stated problem we used a system of hydrothermodynamic equations, which describes the regional atmospheric processes. Because of the small scales of the region, we assume that the effect of the Coriolis force can be omitted, and also $\partial p / \partial t$ is not taken into account as its variation in time is insignificant. After considering the admissions obtained for local processes the indicated system takes the following form [4,5,8]:

$$\frac{du}{dt} = -\frac{1}{\rho} \frac{\partial p}{\partial x} + k' \Delta u + \frac{\partial}{\partial z} \left(k \frac{\partial u}{\partial z} \right), \quad (1)$$

$$\frac{dv}{dt} = -\frac{1}{\rho} \frac{\partial p}{\partial y} + k' \Delta v + \frac{\partial}{\partial z} \left(k \frac{\partial v}{\partial z} \right), \quad (2)$$

$$\frac{dw}{dt} = -\frac{1}{\rho} \frac{\partial p}{\partial z} + \beta' T' + k' \Delta w + \frac{\partial}{\partial z} \left(k \frac{\partial w}{\partial z} \right), \quad (3)$$

$$\frac{\partial u}{\partial x} + \frac{\partial v}{\partial y} + \frac{\partial w}{\partial z} = \sigma w, \quad (4)$$

$$\frac{d\Theta}{dt} = \left(\frac{P}{p} \right)^{\lambda} \frac{\epsilon}{C_p \rho} + k' \Delta \Theta + \frac{\partial}{\partial z} \left(k \frac{\partial \Theta}{\partial z} \right), \quad (5)$$

$$\frac{dq}{dt} = -\frac{m}{\rho} + k' \Delta q + \frac{\partial}{\partial z} \left(k \frac{\partial q}{\partial z} \right), \quad (6)$$

where u, v, w are the components of wind velocity along x, y, z coordinate axis accordingly, t - time, ρ - density, p - pressure, k' - the coefficient of turbulence on the horizontal plane, k - coefficient of turbulence along z axis, β - parameter of buoyancy, T - absolute temperature, Θ - potential temperature, q - specific humidity, λ - parameter of stability, ϵ - heat flux, $\sigma = \frac{g - \bar{\gamma}R}{RT}$, R - gas universal constant, g - free fall acceleration, m - water vapor mass, $\bar{\gamma}$ - vertical gradient of temperature, Δ - Laplace flat transform.

In any meso-meteorological problem the quantities characterizing the main state are considered being already known (so-called background magnitudes). The shape of relief and heterogeneity of the surface temperature have to be given too. By means of solving

equations, the disturbances from the major state are found and then added to the background magnitudes.

The meso-meteorological problems based on the above-pointed (1) – (6) equation system include the studies of air streamlining around the mountain, local wind, the induced convection in the boundary layer. The physical and geographical conditions of the different regions of Georgia give the ability to eliminate the terms with turbulence in (1) – (6) system, and consider air internal friction by bringing in a special term.

While researching the dynamic processes we used the standard method of obtaining well-known equation for the vertical component of vortex velocity from the equations (1) and (2), [2,4]:

$$\frac{\partial \Omega_z}{\partial t} + u \frac{\partial (\Omega_z + f)}{\partial x} + v \frac{\partial (\Omega_z + f)}{\partial y} = -f D, \quad (7)$$

where $\Omega_z = \frac{\partial v}{\partial x} - \frac{\partial u}{\partial y}$, f is Coriolis parameter and D flat divergence of velocity.

Let $\eta = P_z/P_0$ be a parameter that characterizes earth relief, where P_z is the magnitude of atmospheric pressure on the mountain surface, and P_0 standard magnitude of pressure on the sea level. Then the wind velocity components could yield [3,7]:

$$u = -\frac{1}{\eta} \frac{\partial \psi}{\partial y}, \quad v = \frac{1}{\eta} \frac{\partial \psi}{\partial x}. \quad (8)$$

Here ψ is a current function. Then the vertical component of velocity takes the following form [7]:

$$\Omega = \frac{1}{\eta} \Delta \psi - \frac{1}{\eta} \left(\frac{\partial \psi}{\partial x} \frac{\partial \ln \eta}{\partial x} + \frac{\partial \psi}{\partial y} \frac{\partial \ln \eta}{\partial y} \right) = \frac{1}{\eta} \left(\Delta \psi + a \frac{\partial \psi}{\partial x} + b \frac{\partial \psi}{\partial y} \right), \quad (9)$$



where $a = -\frac{\partial \ln \eta}{\partial x}$ and $b = -\frac{\partial \ln \eta}{\partial y}$ are the parameters of the mountain influence along longitude and latitude, accordingly. (9) - (1)

Let us assume, that the friction at the Earth's surface is directly proportional to the vortex velocity, or to the variation of the current function along the latitude or longitude. Thus, after considering all these the above stated equation (7) can be rewritten so:

$$\frac{\partial}{\partial t} (\Delta \psi + a \psi_x + b \psi_y) + \eta k \psi_x = f(\psi, \Delta \psi) - f(\psi, \ln \eta), \quad (10)$$

where the expression (A,B) is a Poisson's parentheses.

Next, we try to get the solution of the equation (10) in the form of wave:

$$\Psi = E_0 e^{i(mx+ny-\sigma t)}, \quad (11)$$

where m and n are wave numbers, E_0 amplitude and σ frequency.

Now, let us discuss the two cases of friction impact and make an attempt to find corresponding phase velocity [5,8]: a) friction is proportional to $\Omega \omega$, so $F_f = k \Omega z$, and then putting (11) into (10) yields the following expression:

$$\sigma = \frac{[f(na - mb) - (am + bn)k] \rho^2 + \rho^2 k(am + bn)}{\rho^4 + (am + bn)^2} + i \frac{[f(na - mb) - (am + bn)k](am + bn) - \rho^4 k}{\rho^4 + (am + bn)^2} = \sigma_1 + i \sigma_2, \quad (12)$$

where

$$\rho^2 = m^2 + n^2.$$

The parameter characterizing relief and the wave numbers must satisfy the condition:

$$am + bn = 0 \quad (13)$$

$$C = \frac{\sigma}{m} = \frac{f}{\rho^2} \left[\left(a \frac{n}{m} - b \right) - i \frac{k}{m^2} \right] \quad (14)$$

Considering it, the real part of the phase velocity depends only on $(am - bn)$ combination and the virtual part of it relies on the friction coefficient and the ratio of the wave number k/m toward leading flux. This dependence is obtained for the first time and gives good opportunity to study dynamics of micro-regional processes. The only thing is to know the magnitudes of a and b parameters and the wave numbers of current region.

b) Friction coefficient is proportional to the derivative of current function along the latitude: $F_{xxx} = k^2 \Psi_x$. Then for the frequency we would have:

$$\sigma = \frac{[f(na - mb) - k_1 m] \rho^2}{\rho^4 + (am + bn)^2} + i \frac{[f(na - mb) - \beta m](am + bn)}{\rho^4 + (am + bn)^2} = \sigma_3 + i\sigma_4 \quad (15)$$

$$C = \frac{f \left(a \frac{n}{m} - b \right) - k_1}{\rho^2} \quad (16)$$

Now consider the waves of the neutral type. Their existence is observed on Transcaucasian territory. [3,5,6]. In this case $C = 0$ and friction coefficient is determined from (16):

$$k_1 = kf = f \left(a \frac{n}{m} - b \right) \quad (17)$$



We have got quite strange, but very important result: air internal friction coefficient is defined by the parameters characterizing the mountain in the given region and with the corresponding wave numbers.

The validity of the obtained results was tested for Mengrelia. Nine meteorological stations were selected and all meteorological quantities were taken for the past 10 years.

The a and b parameters were estimated by consideration of the physical and geographical conditions of the region (Table 1).

Table 1

Locations	Distance between locations, 10 ⁴ m	Altitude from the sea level, m	Pressure, mb	Relief parameters	
				a (10 ⁶) 1/m	b (10 ⁶) 1/m
Zugdidi Gali	1.8	110	989	0.24	0.20
		48	995.2		
Zugdidi Kutaisi	8.0	300	970	0.12	0.12
		5	999.5		
Zugdidi Kobuleti	8.0	5	999.5	0.3	0.11
		28	997.2		
Zugdidi Senaki	3.2	28	997.2	0.08	0.08
		3	999.7		
Zugdidi Poti	4.0	3	999.7	0.10	0.10
		1610	839		
Zugdidi Lebarda	20.0	1610	839	0.10	0.10
		170	983		
Zugdidi Martvili	6.0	170	983	0.10	0.10
		140	986		
Soldhumi Kutaisi	15.0	140	986	0.10	0.10



It appeared that a and b parameters did not change significantly along different directions in the region (center Zugdidi). It confirms the fact that the region is valley with small hills without gorges. The air phase velocity is low, but exists constantly because it is caused by the sea and land thermal radiation [2,6].

According to the definition of wave numbers from (13) it follows:

$$L_x = 1.5 L_y, \tag{18}$$

which means that the air mass along the latitude expands 1.5 times longer than along the longitude. These kinds of processes are observed in operational practice.

Thus, the prolongation along the latitude observed during synoptic processes was proved theoretically. For this region it was done for the first time.

To make phase velocity of synoptic waves $C \neq 0$, it is necessary according to (17) to fulfil the condition $(am - bn) \neq 0$. Actually, this condition fulfils. The expression $(am - bn)$ is not large. It is about (0.005-0.4) m/sec, but never equals to zero. If the length of the wave would be considered being congruent to the sizes of region along the longitude and latitude ($L_x = 500$ km and $L_y = 160$ km correspondingly), then $C = 0.059$ m/sec.

For displaying the microclimatic features caused by dynamics of the mentioned atmospheric processes by applying the data from the selected meteorological stations the correlative relationships between different elements could be determined. The correlation coefficients for the pairs of different meteorological elements on the same stations and the same elements on the different stations were calculated (Table 2,3).

The data from the Table show that the region is characterized by similar magnitudes of the meteorological elements. This conclusion indicates at the ecological alert. Pollution coefficients of air and soil are distributed evenly across the whole region and their alteration in time and space occurs at a low rate.

Indeed, from the equation describing the diffusion of an admixture (stationary case), we have [1,5]:

Table 2. Correlation coefficient for temperature

r coefficient	Zugdidi	Senaki	Kutaisi	Poti	Sokhumi	Gali	Kobuleti
Zugdidi	1	0.77	0.78	0.61	0.71	0.72	0.64
Senaki	0.77	1	0.70	0.55	0.63	0.60	0.71
Kutaisi	0.78	0.70	1	0.87	0.97	0.82	0.92
Poti	0.61	0.55	0.87	1	0.93	0.81	0.46
Sokhumi	0.71	0.63	0.97	0.93	1	0.83	0.96
Gali	0.72	0.60	0.82	0.81	0.83	1	0.78
Kobuleti	0.64	0.71	0.92	0.46	0.96	0.78	1

Table3. Correlation coefficient for temperature according to the seasons

r coefficient	Zugdidi	Kutaisi	Sokhumi	Poti	Gali	Kobuleti
Zugdidi (warm period)	0.93	0.96	0.93	0.93	0.94	0.94
Zugdidi (cold period)	0.99	0.97	0.98	0.88	0.98	0.99

$$u \frac{\partial q}{\partial x} + \left(w - u \frac{dh(x)}{dx} \right) \frac{\partial q}{\partial z'} = \frac{\partial}{\partial z'} \left(k \frac{\partial q}{\partial z'} \right), \quad (19)$$

where q is relative concentration of an admixture, $h(x)$ – shape of relief, $Z' = Z - h(x)$ is a new coordinate.

It follows that for small magnitudes of u and w the stationary regime is retained for a long time. So, the period of self-clarification of air is prolonged significantly.

The seasonal characteristics of atmospheric processes' dynamics was also calculated:

$$A = \frac{t_{\max} - t_{\min}}{t_{\text{base}}} \quad (20)$$

It appeared that A parameter was altered according to the warm and cold seasons. But during the season its magnitude remained stable.

The calculations were done for the several regions of Georgia on the basis of the data for the period of 1990 – 2000 (Table 4). The magnitudes of A parameter given in the Table 4 show clearly the repetition of warm and cold periods with high accuracy. A parameter is new and requires more testing for another periods too.

Table 4. Magnitude of A according to seasons

seasons	1990	1991	1992	1993	1994	1995	1996
(warm period)	1.1	1.1	1.3	1.2	1.2	1.2	1.2
(cold period)	3.2	3.0	3.9	4.8	3.8	3.4	3.1

It is possible to draw a conclusion for the region of Mengrelia: both factors determining microclimate, general circulative processes and physical state of ground surface provide the stability of the atmospheric processes.

REFERENCES

1. P. Demetri, F. Corrado, Ratto. Modeling of Atmospheric Low Fields". World Scientific. 1996, 753.
2. K. Tavartkiladze, I. Shengelia. Current Change of Climate in Georgia, the Variation of Radiation Regime. 1999, 150.
3. T. Salukvadze, Z. Khvedelidze. Radio-location of Convection Khelaia A. Clouds. Georgian Academy of Science, Geophysical Institute Researches. LVIII, 2002, 358.
4. P. Belov. Numerical Methods of Weather Prognosis. 1975. 506.
5. Z. Khvedelidze. Wave Motion in The Lower Layers of



Atmosphere and Pollution Problem. Publication of Tbilisi State University. 1991, 201

6. Z. Khvedelidze. Short course of Synoptic Meteorology. Publications of Tbilisi State University. 1998, 88.
7. Z. Khvedelidze, R. Danelia. Prognosis of Meteorological Elements Considering the Effect of Micro "Polygonal Relief". Bulletin of Georgian Academy of Science, 163, 2, 2001, .273.
8. B. Gaurvits. The Motion of Atmospheric Disturbances, 1958. 317.

Tbilisi State University

ზ. ხვედელიძე, ი. ალადაშვილი, თ. შალამბერიძე,
ე. თაგვაძე, რ. ჩახაია

აგმოსფერული პროცესების დინამიკა და მისი როლი
საქართველოს ეკოლოგიურ პრობლემებში

დასკვნა

დღევანდელი მსოფლიო საზოგადოების წინაშე მდგარი აქტუალური პრობლემის, ცალკეული რეგიონის ეკოლოგიური სიტუაციების შესწავლის მიზნით სტაგიაში ჰიდროთერმოდინამიკის განგოლებათა სისტემის გამოყენების საფუძველზე გათვლილ იქნა საქართველოს გერიტორიაზე გაბატონებული სინოპტიკური მდგომარეობებისათვის ფაზური სიჩქარის მნიშვნელობები. აგრეთვე მცირე გერიტორიის რეგიონებისათვის (10-50 კმ) მიღებულ იქნა ჰაერში მინარევის ვერტიკალური გავრცელების სიჩქარის მნიშვნელობები ადგილის ფიზიკური რელიეფის გავლენის გათვალისწინებით. ეს სიდიდეები გამოიყენება ამა თუ იმ რეგიონის ეკოლოგიური სიტუაციების ანალიზისათვის. გამოთვლილი იქნა აგმოსფეროს დინამიკის სემონური მდგრადობის ახალი პარამეტრი და აღმოჩნდა, რომ იგი სემონების მიხედვით ინარჩუნებს სტაბილურ მდგომარეობას, რაც მიუთითებს მასზე, რომ უახლოეს მომავალში (რამოდენიმე წელი) მეტეოროლოგიური სიდიდეების მკვეთრი სემონური ცვალებადობა არ არის მოსალოდნელი.

PHOTOINDUCED ANISOTROPY IN SELENO-CADMIUM GLASS

L. Tarasashvili, Sh. Kakichashvili

Accepted for publication April, 2002

ABSTRACT. Anisotropic change of the absorption edge of seleno-cadmium glass under the action of linearly polarized monoimpulse of a ruby laser of great power has been investigated. The spectral width of the area of anisotropic bleaching of the sample which is being radiated has been estimated. The dispersion curves of photoinduced birefringence and the anisotropy of the absorption on the absorption edge of the glass of RY-19 type have been obtained in the interval (6500-6700) Å.

The phenomena of photoanisotropy and photogyrotropy in different light-sensitive media have been actively used lately in the tasks of polarization holography and information processing [1-4]. The mechanism of the above-mentioned phenomena can be the most various connected both with photochemical and photophysical transformations of molecules under the action of actinic radiation and with non-linearly optical phenomena. In the latter there are a lot of possibilities for different manifestations of vector effects in photophysical processes [5-8]. Anisotropic non-linear bleaching of seleno-cadmium glass BY-19 under the action of linearly polarised monopulse of a ruby laser of different power on the wavelength of actinic radiation ($\lambda = 6943 \text{ \AA}$) has been discovered and investigated in [9]. On the other hand, it has been estimated that the area of bleaching is not limited to the line width of laser radiation, but it covers a rather broad area of the self-absorption edge of glass RY-19 [10]. On this basis of finding out the nature of non-linear, anisotropic processes, which take place in the seleno-cadmium glass, demands a certain spectral width of the area of anisotropic bleaching of the sample which is being radiated.

In this work the spectral width of the area of anisotropic bleaching of glass RY-19 has been measured for the first time. Besides,



dispersion curves of light-induced birefringence Δn have been received in it and of anisotropy of absorption $\Delta n \tau$ on long-wave edge absorption of the seleno-cadmium glass in spectral range (650 - 750) nm.

The schemes of the experimental installation for defining the spectral area of anisotropic bleaching and measuring light-induced birefringence and anisotropy of absorption on different wave lengths are given in Fig. 1.

A sample of glass RY-191, which was formed into a shape of a cube with optically polished faces was exposed to radiation by a linearly-polarized monopulse of ruby laser 2 with power ~ 6 . The vibration plane of linearly polarized laser light is oriented in the direction perpendicular to the drawing. A quartz haloid lamp KTM 24X300 3 that provided the constance of the light flux in the interval of wave length under investigation was used for probing. The probing beam passes through polarizer 4, gets into the entrance slit of monochromator МДП-45, then through Fresnel's rhomb 6 into polarizer 7, passes through sample 1 and polarizer 8 after which it is detected by device ФЭУ-629. The recording of signals is made on the screen of two-beam storing oscillograph 10. The system of polarizer 7.8 is oriented parallel and was able to rotate as a whole taking the desired position with respect to effective vector of an exciting beam; parallel at an angle of 45° and perpendicularly. The system from polarizer 4 and Fresnel's rhomb 6 was used to exclude polarization distortions of the device on a probing beam. The absorption coefficient of the sample at any stage of bleaching is calculated from the formula $k = k_0 - 1/d \ln I_1 / I_2$, where k_0 is an absorption coefficient for weak light fluxes; k is the same for fluxes of great intensity (the value average by ten measurements); I_1 and I_2 are the intensities of the radiations which passed through the sample, corresponding to values k and k_0 ; d is the thickness of the sample; coefficient k_0 was determined earlier on spectrophotometer СФ-10. The amplitudes of impulses on the screen of the oscillograph were used as I_1 and I_2 while calculating. The dispersion curves of photoinduced birefringence Δn and anisotropy of absorption $\Delta n \tau$ on the edge of the absorption of seleno-cadmium glass RY-19 in spectral range (650 - 750) nm (n is a refractive index, τ is an

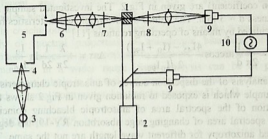


Fig. 1. The principal scheme of the experimental device.

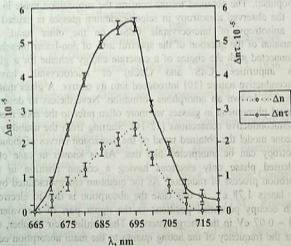


Fig. 2. Dispersion curves of the anisotropic characteristics of the exposed sample

extinction coefficient) are given in Fig.2. The investigated sample had the thickness $d = 3$ mm. The values of anisotropic characteristics have been calculated by means of operating relations [11].

$$\Delta n = \frac{\lambda}{2\pi d} \arccos \frac{4I_{45} - (I_0 + I_{90})}{2\sqrt{I_0 I_{90}}}, \quad \Delta n\tau = -\frac{\lambda}{2\pi} \frac{1}{2d} \ln \frac{I_0}{I_{90}}$$

The analysis of the dispersion curves of anisotropic characteristics of the sample which is exposed to radiation given in Fig.2 shows that the location of the spectral area of anisotropic bleaching coincides with the spectral area of changing edge absorption RY-19; the degree of induced anisotropy for different wave length are not the same. The maximum meaning of anisotropy is observed near an excitation wave length ($\lambda = 694.3$ nm). On the wave length shorter than $\lambda = 694.3$ nm bleaching of the sample hasn't been detected (at the given power of the monopulse). The obtained results confirm the supposition made in [9] that the observed anisotropy in seleno-cadmium glasses is caused by the anisotropy of microcrystals CdSc; on the other hand, the discussion of the question of the spectral area of non-linear bleaching is connected with the choice of a concrete energy scheme for a glass with impurities (CdS and CdCe) of microcrystals having semiconductive nature [10] introduced into its matrix. A glass matrix is as it is known an amorphous formation. Nevertheless to describe physical phenomena in glasses we more often refer to the zone theory of semiconductive connections [12-14]. Starting from the usability of the zone model the obtained trend of the dispersion curves of induced anisotropy can be interpreted like this: As is known in case of a condensed phase only electrons having a certain position in the absorption process of radiation. As the quantum energy radiated by a ruby lasers 1.78 eV, in this case the absorption is due to electrons which occupy permitted positions in the upper part of the valence band ~ 0.07 eV in the energy interval. The smaller their number, the closer the frequency of the acting quanta to the main absorption edge of the substance [12]. As a result of this it can be expected that a noticeable anisotropic change of an absorption coefficient will take place in the spectral region between the absorption edge of the substance and the frequency of incident radiation. While moving away towards big frequencies the amount of the change of the absorption

spectral range (650 - 750 nm) is the same index, r is an

coefficient, and therefore the anisotropy of absorption decreases. Complete bleaching comes only when $\lambda > \lambda_L$.

In conclusion we shall note that in order to make a comprehensive study of spectral properties of anisotropic bleaching of seleno-cadmium glasses it is necessary to measure the energies of actinic illumination in a wider range. Such analysis can be of practical interest particularly in the tasks of creating polarization correctors and speedy reversal polarization holographic memory [13, 14].

REFERENCES

1. F. Weigert. Ann. Physik. **B15**, 1920, 491.
2. S.V. Cherdintzev. Zh. Eksp. Teor. Fiz. **18**, 1948, 352 (Russian).
3. G.M. Gonathen, C. May. App. Opt. **19**, 1980, 624.
4. Sh. Kakichashvili. Vestnik of the Academy of Sciences of the USSR. **7**, 1982, 51 (Russian).
5. A. P. Bucingham. Proc. Phys. Soc. **B69**, 1956, 344.
6. L.A. Ageev, V.K. Miloslavski. Optics and Spectroscopy. **48**, **B5**, 1980, 802 (Russian).
7. S.V. Cherdintzev. Journal of Physical Chemistry. **7**, 1936, 265 (Russian).
8. Sh. Kakichashvili. Optics and Spectroscopy. **52**, **2**, 1982, 317 (Russian).
9. Sh. Kakichashvili, V. Tarasashvili. Optics and Spectroscopy. **60**, **5**, 1986, 1071 (Russian).
10. M.P. Lisitza, N.R. Kulish, I.I. Geetz. Quantum Electronics. **4**, 1969 (Russian).
11. Sh. Kakichashvili. Transactions of the 4 All-Union Conference on Holograph, Erevan, **2**, 1982 (Russian).
12. A.M. Bonch-Bruevich, T.K. Razumova, G.M. Rubanova. Nonlinear Optics. 1968.
13. Sh. Kakichashvili, V. Tarasashvili. Pros. of TSU. Physics. **36**, 2001.
14. Sh. Kakichashvili. Polarization holography. 1989 (Russian).

Georgian Academy of Sciences
Institute of Cybernetics

მ. ყაყიჩაშვილი, ვ. ტარასაშვილი

ფოტოინდუცირებული ანიზოტროპია სელენ-კადმიუმის მინაში

დასკვნა

გამომილია ანიზოტროპული გაუფერულების უბნის სპექტრული სიგანე სელენ-კადმიუმიან მინაში, მასზე ლალის ლაზერის დიდი სიმძლავრის წრფივად პოლარიზებული მონოიმპულსით ზემოქმედებისას. მიღებულია ინდუცირებული ორმაგი სხივგეხის და ანიზოტროპული შთანთქმის დისპერსიის მრუდები KC-19 ტიპის მინების კიდური შთანთქმის სპექტრულ უბანზე (650nm-750nm). ფოტოანიზოტროპიის მოვლენის სპექტრული თვისებების შესწავლა საინტერესოა, როგორც ფერადი მინების აქტიური შთანთქმის ცენტრების სტრუქტურის ანალიზისათვის, ასევე პოლარიზაციული დინამიკური პოლოგრაფიის პრაქტიკულ ამოცანაში.

DIFFRACTION RADIATION OF AN ELECTRON FLOW MOVING ABOVE THE SCREEN WITH SLOTS

I. Sikmashvili, Z. Sikmashvili, O.Tsagareishvili

Accept for publication May,2002

ABSTRACT. The problem of diffraction of an internal field of moving electron flow on a perforated screen of final width is being solved. The quantitative theory of phenomenon of diffraction radiation is constructed and physical interpretation is given on the basis of numerical results.

Let us assume that parallel with surface of a boundless perforated screen (Fig.1) the monochromatic electronic flow with constant speed is moving and instantaneous value of a density of charge is the following:

$$\rho = \rho_0 \delta(z - \zeta) \exp[ih(\alpha_1 x + \alpha_2 y) - \omega t], \quad (1)$$

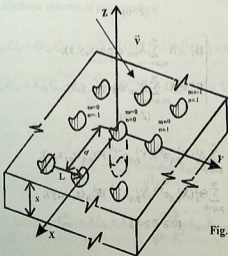


Fig.1

where ρ_0 is amplitude modulation of electronic flow; ω -frequency of modulation; $h = k/\beta$; $k = \omega/c$; $\beta = v/c$ relative velocity of flow; c free space velocity; $\vec{v} = v(\bar{x}_0\alpha_1 + \bar{y}_0\alpha_2)$; $\delta(z-\zeta)$ is Dirace function; α_1, α_2 are direction cosine ($\alpha_1^2 + \alpha_2^2 = 1$); ζ is aiming distance; \bar{x}_0, \bar{y}_0 basis vector of coordinat system.

Field source represented by (1) is a real model for investigation of initiated diffraction radiation [1].

The sought field in a space is represented as a superposition of falling and reflected waves of concrete sectors, as a double Fourier line with certain unknown coefficients (The field over the screen $Z > 0$) is represented as a superposition of internal field of charges and field, scattered on a perforated screen):

$$(1) \quad \begin{cases} H_i^+ = H_i^0 + \Lambda \sum_{m,n=-\infty}^{\infty} A_{mn}^i \exp \psi(x, y, z) \\ E_i^+ = E_i^0 - \Lambda \sum_{m,n=-\infty}^{\infty} B_{mn}^i \exp \psi(x, y, z) \end{cases} \quad (Z > 0) \quad (2)$$

$$\begin{cases} H_i^- = \Lambda \sum_{m,n=-\infty}^{\infty} \tilde{A}_{mn}^i \exp \varphi(x, y, z); \\ E_i^- = \Lambda \sum_{m,n=-\infty}^{\infty} \tilde{B}_{mn}^i \exp \varphi(x, y, z); \end{cases} \quad (Z < -S)$$

$$\begin{cases} H_i^{ins} = \Lambda \sum_{j=1}^2 \sum_{p,q=0}^{\infty} \Delta_i^j (X_{p,q}^j e^{\gamma^j z}, Y_{p,q}^j e^{-\gamma^j z}) \Phi_{p,q}^i(r_0, x, y); \\ E_i^{ins} = \Lambda \sum_{j=1}^2 \sum_{p,q=0}^{\infty} \Theta_i^j (X_{p,q}^j e^{\gamma^j z}, Y_{p,q}^j e^{-\gamma^j z}) F_{p,q}^i(r_0, x, y); \end{cases} \quad (3)$$

(0 ≥ Z ≥ -S).

Here $l = x, y, z$; $\psi_{mn} = i(h_m x + h_n y + h_{mn} z)$; $\varphi_{mn} = i(h_m x + h_n y - h_{mn}(z + s))$; $h_m = h\alpha_1 + 2\pi m/d$; $h_n = h\alpha_2 + 2\pi n/l$; $h_{mn} = \sqrt{k^2 - h_m^2 - h_n^2}$; the constant $\Lambda = (\rho_0 c/2)\sqrt{1-\beta^2} \times \exp[-(k\zeta/\beta)\sqrt{1-\beta^2}]$ entered as a matter of convenience calculations; $\gamma^j = \sqrt{k_{pq}^2 - \varepsilon_r k^2}$; ε_r a relative permittivity of environment inside holes; k_{pq} eigenvalues; and $\bar{\Phi}_{p,q}^j(r_0, x, y)$, $\bar{F}_{p,q}^j(r_0, x, y)$ fundamental functions of wave guides correspond of the configuration r_0 is a geometrical size (the index $j = 1$ corresponds to waves E of a type, and $j = 2$ to waves H of a type); \bar{E}^0 and \bar{H}^0 vectors of an internal field of moving charges; $A_{mn}^i, \tilde{A}_{mn}^i, B_{mn}^i, \tilde{B}_{mn}^i, X_{pq}^j, Y_{pq}^j$ unknown coefficients which are being a subject of definition.

Satisfying boundary conditions on a surface of metal (planes $z = 0$ and $z = -S$), leads to the functional equations, which may be transformed, by means of moment method, to the following infinite linear algebraic systems of pair equations.

$$\begin{cases} \lambda_{\nu\mu} Z_{\nu\mu}^{\pm} + G_{\nu\mu} t_{\nu\mu}^{\pm} - r_{\nu\mu} \sum_{m,n=-\infty}^{\infty} (D_{mn}^{(1)} t_{mn}^{\pm} + D_{mn}^{(2)} Z_{mn}^{\pm}) = V_{\nu\mu}^{(1)} \\ P_{\nu\mu} Z_{\nu\mu}^{\pm} + \lambda_{\nu\mu} t_{\nu\mu}^{\pm} - r_{\nu\mu} \sum_{m,n=-\infty}^{\infty} (D_{mn}^{(3)} t_{mn}^{\pm} + D_{mn}^{(4)} Z_{mn}^{\pm}) = V_{\nu\mu}^{(2)} \end{cases} \quad (4)$$

where

$$Z_{mn}^{\pm} = A_{mn}^x \pm \tilde{A}_{mn}^x + \frac{\alpha_1 \beta}{\sqrt{1-\beta^2}} \delta_{m0} \delta_{n0};$$

$$t_{mn}^{\pm} = A_{mn}^y \pm \tilde{A}_{mn}^y - \frac{\alpha_2 \beta}{\sqrt{1-\beta^2}} \delta_{m0} \delta_{n0};$$

$$V_{\nu\mu}^{(1)} = -\frac{2\alpha_1}{\beta} \sqrt{1-\beta^2} \delta_{\nu 0} \delta_{\mu 0}, \quad V_{\nu\mu}^{(2)} = \frac{2\alpha_2}{\beta} \sqrt{1-\beta^2} \delta_{\nu 0} \delta_{\mu 0},$$

the remaining values are identical to expressions conducted in [2-5].

Having conducted research of matrix elements and free members (4) and having convinced in quadratic convergence in space of Hilbert l^2 we conclude that the equations are Fredholm type and are solved by method of a reduction.

Determining unknown coefficients of a problem, we build relation of a flow of power of a spatial harmonic from a single site of a screen (Π_{mn}) from miscellaneous geometrical and electrical parameters.

$$\Pi_{mn} = \frac{J_0^2 (1-\beta^2)}{4\beta^2} \exp\left[-\frac{4\pi\zeta\sqrt{1-\beta^2}}{\beta\lambda}\right] \cdot Z_0 \Omega_{mn} = \frac{J_0^2}{2} R_{\Sigma}, \quad (5)$$

where J_0 is a line density of a current; Z_0 an environmental wave resistance;

$$\Omega_{mn} = \left(1 + \frac{h_m^2}{h_{mn}^2}\right) \cdot |A_{mn}^x|^2 + \left(1 + \frac{h_n^2}{h_{mn}^2}\right) \cdot |A_{mn}^y|^2 + \\ + 2 \frac{h_m h_n}{h_{mn}^2} \operatorname{Re}\left(A_{mn}^x A_{mn}^{y*}\right);$$

(* - complex conjugate value).

Numerical computation was carried out for rectangular slots. On the basis of these numerical data the analysis of physical features of diffraction radiation is conducted.

The Fig.2 illustrates exponential decrease of a radiation energy with increase of the distance between electronic stream and lattice. As it is visible from a figure, starting from the value $\zeta = \zeta_0/\lambda = 0.1$ the radiation becomes practically unobservable.

In Fig.3 the dependence of R_{Σ} on the speed of the beam $\beta=v/c$ is presented. The continuous line defines areas of meaning, where the

condition of radiation is carried out for the data m, n, χ . The dotted line defines areas, where this condition is not carried out. In all cases

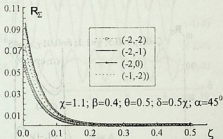


Fig.2

the diffraction radiation disappears, when the speed of a flow approaches to the speed of light. As is known [1] currents inducing radiation undergo Lorentz reduction and aspires to zero at $\beta \rightarrow 1$.

From Figs. 4-5 where the dependence of factor R_Σ as a function of geometrical parameters of a lattice δ and θ is presented obvious, that the radiating power is periodic function of the depth of lattice. The characteristic resonance takes place, when the depth of lattice is approximately multiple $k/2\gamma^2$.

In Fig.6 the dependence R_Σ on parameter χ (frequency of fluctuation) at the fixed depth of the screen and various meanings of factor of filling is given. The substantial growth of capacity of radiation as a result of a choice of appropriate depth of lattice is appreciable only at width of slots, smaller than half-cycle of structure. The sharp change of intensity of radiation in a neighborhood of meanings is observed

$$\chi^+ = \frac{|m\beta|}{\sqrt{\beta^2 - (\alpha_2 + n\beta/\chi_2)^2 - \alpha_1}}; \chi^- = \frac{|m\beta|}{\sqrt{\beta^2 - (\alpha_2 + n\beta/\chi_2)^2 + \alpha_1}}; \quad (6)$$

($m = -1, -2, \dots$; $n = \pm 1, \pm 2, \dots$) which is connected to the resonant phenomena similar to Wood anomalies. The formula (6) precisely predicts conditions, at which the Wood anomalies in diffraction radiation take place.

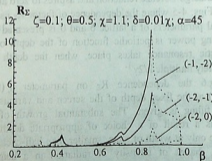
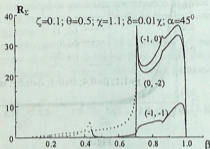


Fig.3

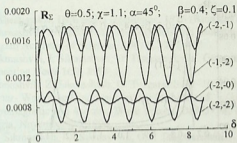


Fig.4

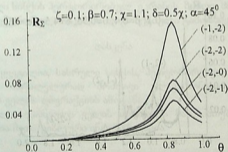


Fig.5

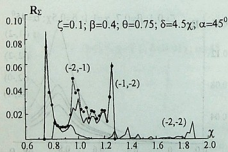
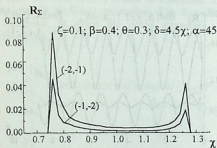


Fig.6

REFERENCES

1. V.P.Shestopalov. Diffraction electronics. 1976 (Russian).
2. Z. Sikmashvili, I. Sikmashvili, O. Tsagareishvili. Bulletin of the Georgian Academy of Sciences, 156, 3, 1997, 403.
3. Z. Sikmashvili, I. Sikmashvili, O. Tsagareishvili.. Georgian Engineering News 1(5), 1998, 5.
4. I. Sikmashvili, Z. Sikmashvili, O. Tsagareishvili. III International Seminar- Workshop Direct and Inverse Problems of Electromagnetic and Acoustic Wave Theory, DIPED'98, Tbilisi, Georgia, November 2-5 1998.
5. Z.I. Sikmashvili, I.Z. Sikmashvili, O.P. Tsagareishvili. Radiophysics and Quantum Electronics, 44, 2001.

Tbilisi State University

ი. სიყმაშვილი, ზ. სიყმაშვილი, ო. ცაგარეიშვილი

სასრული სისქის პერფორირებულ ეკრანის ზემოთ მოძრავი ელექტრონული ნაკადის დიფრაქციული გამოსხივება

ლასკენა

გადაწყვეტილია, სასრული სისქის, პერფორირებული ეკრანის სიბრტყის პარალელურად მოძრავი ელექტრონული ნაკადის საკუთარი ველის დიფრაქციის ამოცანა.

აგებულია გაბნეული ველის ძირითადი მახასიათებლები და მოცემულია მათი ფიზიკური ინტერპრეტაცია.



ON MODELING OF THE DIURNAL VARIATION OF THE
COEFFICIENT OF COMPUTATION OF TILT SOUNDING
FROM VERTICAL SOUNDING OF IONOSPHERE

K. Tukhashvili, V. Kandashvili, J. Mdinradze

Accepted for publication May, 2002

ABSTRACT. A method of modeling of the diurnal variation of parameter M (3000) F2 has been developed. The method has been tested by the use of the data of Ionospheric Digital Database of the National Geophysical Data Center (NGDC), Boulder, Colorado, USA, namely, the data of Juliusruh - ($\varphi = 54.5^{\circ} N$). The type of the parameter dependence on solar activity has been studied and a model of diurnal variation of the median values in January has been made. The model is uniquely dependent on F10.7 allowing prediction of M (3000) F2. The method permits to make models for any point of the Earth (where the measurements are carried out during several cycles of solar activity) for every month.

INTRODUCTION.

Due to peculiarities of propagation of short waves the problem of computation and projection of radio-communication line is different for short waves compared to the problem posed for long and medium waves. For computations within the diapason of long and medium waves the problem is to define the length of the most advantageous wave, necessary transmitting power and necessary type of transmitting antenna. In many cases the sought values are found by means of solution of one mathematical problem as the above-said values are in a certain relation with one another.

Working within the diapason of short waves, first of all, it should be taken into consideration that it is necessary to use several waves for diurnal communication. Besides, due to absorption of radio waves independently of the transmitter power there exists the most advantageous wave for any diurnal period. On the one hand this factor makes computations easier, since the most advantageous wave is

defined independently from the transmitting power, and on the other hand, it is necessary to choose several waves while only one operating wave is enough to work on long and medium waves. Besides, it is necessary to know the time of change from one wave to another. Situation is complicated as annual minimal number of total waves is necessary to be taken into consideration. Besides, the reserve waves are necessary because of variation of solar activity.

Thus, for designing the short-wave radio-communication line it is necessary to define the most advantageous annual number of total waves and the time of change from one wave to another to have a diurnal communication [1].

Ionosphere layers E and F2 have special functions in propagation of spatial short waves in normal conditions: in such a case layer E is an absorber, and layer F2 – the reflector. The diagram of propagation of radio waves is given in Fig. 1.

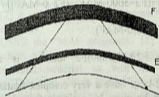


Fig. 1. The trajectory of radio waves while propagation of short radio waves in normal conditions

Analysis of Fig. 1 gives ground to conclude that in normal conditions concentration of electrons in the E layer is not enough to reflect the short waves. Besides, absorption of short waves while reflection from the F2 is less than while penetration E layer: on the ground of a well-known experimental fact daytime concentration of electrons in F2 is about 10-times more than in E layer [1].

It should be noted that while propagation in real conditions short waves are absorbed not only in E layer but also in lower part of the ionosphere - in D area. In such conditions the absorption coefficient

does not change inversely proportional of frequency square but frequency increase causes reduction of absorption coefficient.

Absorption of radio waves in ionosphere must be taken into account to choose the working frequency. The more the frequency the less the absorption, but we are limited from above by critical frequency of the reflective layer. For prognosis (while reflection from F2 layer) of maximum applicable frequency (MAF) it is necessary to predict two parameters: critical frequency of F2-layer - f_0F_2 and the coefficient of computation of tilt sounding M (3000) F2 = M3.

It is necessary to know two values to compute MAF in reflection from F2-layer: MAF of F2-0 and MAF of F2-4000 defining MAF on routes 0 and 4000, respectively (4000 km – maximum distance of one reflection).

$$F2-0-MAF = f_0 F_2 + 1/2 f_H \quad (1)$$

$$F2-4\ 000\ MAF = 17.8 [(F2-3000-MAF) - (F2-0-MAF)] / 14.75 + (F2-0-MAF), \quad (2)$$

where $(F2-3000-MAF) = f_0 F_2 * M(3000)F_2$ and f_H is a Larmor frequency [2].

The parameters of F2-layer have a very complex spatial and time distribution, which cannot be given by a simple formula. Therefore, until the recent time the prognosis of F2 and M3 was done by means of handwork of numerous graphical materials. Development of the methods of computational mathematics and wide use of computers allows automation of this labor-consuming work. On this purpose it has become necessary to develop a method of analytical description of complex spatial variations allowing computation of the values of parameters of F2-layer for any point of the Earth for any period of time. One of such methods was developed in USA in 1962 [3]. In 1973 Chernishev and Vasileva in the USSR developed an analogous method. This method of analytical description of planetary distribution of ionosphere parameters is based on the spherical harmonics method of analysis, where solar activity is considered as follows: in the first

volume the prognosis is made for solar activity, when Wolf's number $W=10$, in the next three volumes $W=50, 100$ and 150 , respectively [2].

The main goal of the study of the structure of upper atmosphere is to define variation of atmosphere parameters according to height and time. To find the causes of variation of the upper atmosphere it is necessary to describe it by model. Therefore, one of the main directions of investigations by means of rockets and satellites is to make its model [4].

An empirical and statistical planetary model of monthly median values used at present for long-term prognosis of radio communication conditions (e.g. CCIR [5] and "MAF prognosis" [2]) is based on the dependence of 12-month smoothed value (R_{12}) of sunspots and f_0F_2 . But some works [6-8] show that application of ionospheres permits to obtain more exact approximation of f_0F_2 dependence on solar activity. In [9] it is shown that application of GSSN (global sunspot number) instead of R_{12} permits to increase the exactness of prognosis: six month earlier - by 11%, a year earlier - by 18%. According to the authors of [7] it is quite prospective to turn to ionosphere indices for long-term prognosis.

In the USSR the "MAF prognosis" [2] was used for long-term prognosis, which differs from the international CCIR in the volume of used experimental material as well as in the method of its construction. Therefore, direct application of a "strange" ionosphere index for the model might be ineffective, though in [10] it is partially shown, that the change of R by GSSN permits to increase the precision of modeled description of median values of f_0F_2 . Standard method of R prognostication is given in [11]. Besides, deviation of f_0F_2 prognosis in daytime is $\sim 20\%$ [12].

The method of modeling of the diurnal variation of f_0F_2 described in [13] is quite different from the previous methods. It is uniquely dependent on the solar activity parameter ($F10.7$). By means of this method the dependence of the values of f_0F_2 on $F10.7$ changes according to zenith angle of the Sun and it is necessary to solve an equation for every hour, but computer can do it easily. As shown in [13], precision of f_0F_2 prognostication a few years earlier is lesser than 10% for any hour of the day.



In the present work a model of M3 diurnal variation has been made in analogous method. These two models allow the prediction of f_0F_2 and M3, which is necessary for MAF prognosis.

EXPERIMENTAL RESULTS

Data obtained by German station (Julruh, $\phi = 54.38^\circ$ N) in 1958-1986 have been used as in [13].

Table 1.

Monthly median values of M(3 000)F2 and F10.7
Julruh. January.

Year	Hour						F10.7		
	0	1	2	*	*	*	22	23	
1958	235	235	230				248	240	243
1959	250	245	245				260	258	266
*									
*									
*									
1986	295	300	305				310	300	71

Parameter M3 in a fixed point of current month depends on the solar activity as well as on the Sun's zenith angle i.e. on local time $T - M3(F10.7; T)$. To study the M3 dependence on F10.7 it is necessary to fix T in current month. On this purpose all the data should be arranged as given in Table 1. The terminal column of the Table represents the relevant value of F10.7. Each line of the Table shows diurnal variation of median values of M3 in January of the given year. The Sun's zenith angle for each column of the Table is constant permitting to study mutual relation between M3 and solar activity. This relation is given by the function

$$M3 = A + B * F10.7 \quad (3)$$

Fig. 2 shows the graph of M3 dependence on F10.7 for 12^hUT. Linear analysis is carried out in the program of "Origin 6.1".

Correlation parameter R appears to be rather high. Fig.2 shows that increasing the solar activity, M3 decreases, which maybe caused by encrease of the height of reflected layer [14]. Only two points are at $F10.7 > 200$ and at low activity there are comparatively more points. Therefore, deviation in M3 prognostication will be more for the year of high solar activity. Using the data of the period as longer as possible for modeling provides more precise prognosis. Dependence for each hour is linear but the parameters of the line are different. Fig. 3 shows diurnal variation of R (coefficient correlation between (3) line and experimental points). Great changes in that variation coincide with the moments of sunrise and sunset in that latitude. Collection of statistical data will allow in-depth study of this effect.

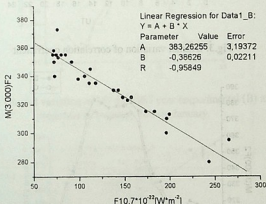


Fig. 2. Dependence between M3 and F10.7 for January, 12th. Julruh.

For modeling it is necessary to compute M3 for every i-th hour by means of the following formula:

$$M3_i = A_i + B_i * F10.7$$

Fig.4 shows the model of diurnal variation of M3 for quiet (B, $F10.7=70$) and active (C, $F10.7=250$) Sun.

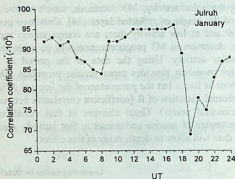


Fig.3. Diurnal variation of correlation coefficient

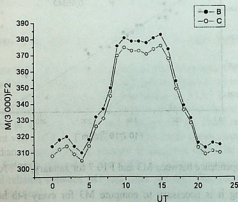


Fig. 4 Diurnal variation M3 for quiet (F10.7=70; (B)) and active (F10.7=250; (C)) sun. Juluh, January.



As noted above, the material collected up to 1986 have been used to make a model. Prognosis can be done for 1987(i.e. a year earlier). Deviation of predicted values of M3 from the real one does not exceed 5% for any hour.

Fig.5 shows real (B) and predicted (C) diurnal variation of M3 for January 1987. The variations are found to be rather similar and Fig.6 shows how precise they are.

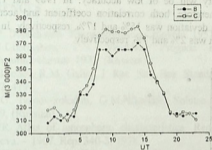


Fig. 5. Diurnal variation of M3 for 1987 year (experimental (B) and prognosis (C) values). Julruh, January.

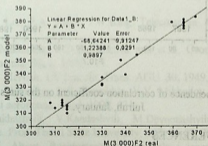


Fig. 6. Comparison of prognosis (model) and experimental (real) values of M3.



The coefficient of correlation between the real and predicted M3 is over 0.98 indicating rather high accuracy.

Fig.7 shows variation of the coefficient of correlation between experimental and predicted values of M3 according to solar activity. The increase of activity causes the decrease of R. As noted above, it is mainly due to insufficient data on high activity while modeling. Only two points are $F10.7 > 200$, therefore, it is expectable that the prognosis of high activity will be of low accuracy. In 1989 and 1990 years $F10.7 > 200$, therefore, both correlation coefficient and accuracy was low – average deviation was 15% and 17%, respectively. In 1987 and 1988 deviation was 2% and 7%, respectively.

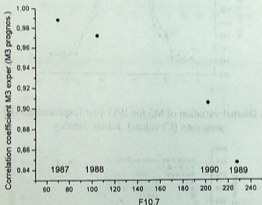



Fig. 7. Dependence of correlation coefficient on the sun's activity. Julruh, January.

THE INFERENCES

A method of modeling of the diurnal variation of parameter $M(3000)F2$ has been developed. The $M(3000)F2$ dependence on $F10.7$ has been studied. It has been established that the increase of $F10.7$ linearly decreases $M(3000)F2$, which might be caused by



increase of $h_m F2$. Coefficients of the line change according to the Sun's zenith angle. Coefficients of correlation between the line and experimental monthly median data are high in daytime. Deviation of the prognosis for high activity is 15-17%. It is mainly due to insufficient data on high activity while modeling.

REFERENCES

1. M.P. Dolukhanov. Rasprostranenie radiovoln. 1951, (Russian).
2. O.V. Chernishov, T.N. Vasileva. Prognoz maksimalnix primcnimix chastot. 1973, (Russian).
3. W.B. Jones, R.M. Gallet. J. Res. Nat. Bur. Standarts, 66d, 4, 1962, 419.
4. A. G. Ivanov-xolodnii, G.M. Nikolskii. Solntse i ionosfera. 1969, (Russian).
5. CCIR Atlas of ionospheric characteristics. Rep. 340. ITU Geneva. - 1967. Rep. 340-3. 1978.
6. P.J. Wilkinson. Solar-Terrrestrial prediction. 1984.
7. A.B. Mikhailov, I. L. Teriokhin, V.V. Mikhailov. Geomagnetizm i aeronomia. 30, 4, 1990, 624.
8. C.M. Minnis, G.H. Bazzard. J. Atmos. Terr. Phys. 18, 1972, 297.
9. R.Y. Liu, P.A. Smith, J.W. King. Telecommun. J. 50, 1983, 408.
10. A.B. Mikhailov, C.D. Buldenkova and et.al. Geomagnetizm i aeronomia. 30, 1, 1990, 113.
11. A.G. McNish, J.V. Lincoln. Trans. AGU. 30, 1949, 408.
12. A.B. Mikhailov, I. L. Teriokhin, V.V. Mikhailov. Geomagnetizm i aeronomia, 30, 4, 1990, 631.
13. K. Tukhashvili, V. Kandashvili, M. Devnozashvili, J. Mdinaradze. Proc. Tbilisi State University, 345, 36-37, 2001, 142.
14. Ja. L. Alpert. Rasprostranenie radiovoln i ionosfera. 1960, (Russian).

Tbilisi State University

იონოსფეროს ვერტიკალური ზონდირებიდან დახრილ ზონდირებაზე გადასაანგარიშებელი კოეფიციენტის დღელამური ცვლილების მოდელირების შესახებ

დასკვნა

შემუშავებულია M(3000)F2 პარამეტრის დღელამური ცვლილების მოდელის შედგენის მეთოდი. მეთოდის შემოწმებისთვის გამოყენებულია Ionospheric Digital Database of the National Geophysical Data Center (NGDC), Boulder, Colorado, USA, კერძოდ, Juliusruh - ($\varphi = 54,5^{\circ} \text{N}$)-ის მონაცემები. გამოკვლეულია პარამეტრის მზის აქტივობაზე დამოკიდებულების სახე და შედგენილია იანვრის თვის მედიანური მნიშვნელობების დღელამური ცვლილების მოდელი. მოდელი ცალსახადაა დამოკიდებული F10.7-ზე, რაც საშუალებას იძლევა M(3000)F2-ის წინასწარმეტყველების. ამ მეთოდით შეიძლება მოდელის შედგენა დღელამიწის ნებისმიერი პუნქტისათვის (სადაც ჩატარებულია გამოკვებები მზის აქტივობის რამდენიმე ციკლის განმავლობაში) ყოველი თვისთვის.

ANTHROPOGENIC EFFECT ON NATURAL PROCESSES AND ITS STUDY USING RADIOCARBON METHOD

S.Tsereteli, V.Bochorishvili, M.Makhviladze, M.Samkharadze

Accepted for publication April, 2002

ABSTRACT. On the basis of radiocarbon concentration measurement data in the Earth's atmosphere we have determined the value of Suess effect using three different methods. The obtained results within the admissible error are in good agreement with each other.

From the end of the 19th century parallel with the development of the Industrial Revolution the decrease (illusory decrease) of atmospheric radiocarbon concentration is noted, which is the result of nonradioactive fossils combustion. The anthropogenic effect on the natural processes and the decrease of the atmospheric radiocarbon concentration were experimentally studied for the first time by Suess [1] and therefore this phenomenon is known as Suess effect.

For today there have been already existed numerous factors which allow to account in detail all these phenomena which make an action on Suess effect:

- Radiocarbon concentration for 1850-1940 has been determined with great preciseness (0.2 -0.3)% in wood rings [2] which makes easy the study of radiocarbon fluctuations unlike other works [3] where only averaged values of radiocarbon concentration are considered.
- As a result of many-years stratospheric observations [4] half empiric dependence between cosmic rays and the parameters of solar activity is obtained

$$I(t) = I_0 \exp \left[-A\eta^{0.8} \varphi^{-1.2} \right] \quad (1)$$

where $I(t)$ is the intensity of galactic cosmic rays for t time moment; I_0 denotes the intensity of unmodulated flux of cosmic rays; η is the number of the groups of the Sun's spots and φ is their heliographic

latitude; A is the constant multiplier. Thus there appeared the possibility to study more thoroughly the dependence of radiocarbon concentration on time in the mentioned period. While investigating Suess effect with the help of experimental data of radiocarbon concentration for the first time it becomes possible to exclude from them such significant factor as solar activity.

The Suess effect makes possible to study more thoroughly the geochemical processes proceeding with the participation of radiocarbon which helps the geochronologists to date more accurately this or that sample using radiocarbon method, etc.

The study of Suess effect is of particular significance for climatology because the raise of anthropogenic carbon dioxide action on climate becomes more and more noticeable [5].

The present paper aims to determine the value of Suess effect using different known methods on the basis of experimental data obtained at the laboratory of nuclear researches of the Tbilisi State University.

1. Radiocarbon method. Historically using this very method there was found the dilution of atmospheric radiocarbon with industrial CO_2 . The difficulty of this approach is that it is impossible to determine just with the measurements the ^{14}C concentration existed before the industrialization. Therefore the Suess effect is calculated as the difference between the measured series of the ^{14}C concentration and the level of radiocarbon concentration of 1850. Then the data are approximated by the least-square method.

2. Cosmophysical method. This method gives the possibility to determine the value of Suess effect more accurately using annual measurements of radiocarbon. As was mentioned above the dependence of cosmic rays intensity on the parameter of solar activity is given by half empiric formula (1).

If we consider that (1) equality took place in the past too we can exclude modulated influence of solar activity from experimental radiocarbon series and obtain 'pure' image of Suess effect. For this it is necessary to calculate the velocity of ^{14}C formation in the Earth's atmosphere from formula

$$I(0.2 - 50 \text{ gv}) = 385 Q^{2.45} \quad (2)$$

and variation ($\delta^{14}\text{C}$) of its concentration, which is calculated using five reservoir model of ^{14}C "redistribution" [4]. If we subtract the calculated value from radiocarbon experimental series we get the value of Suess effect.

3. Industrial method. This method is based on the evaluation of the injected industrial carbon content. For this there are used statistical data on the production amount of various fuels determined by the United Nations Organization. In this model it is also necessary to take into consideration the effect of carbonic gas flux in other spheres (ocean, biosphere, etc.) on its concentration in the atmosphere [3].

We have determined the value of Suess effect by radiocarbon method based on the data from [2] (Fig.1 fine dashed line).

At the same time we have modified radiocarbon method in order to exclude modulated action of solar activity: linear approximation of data from earlier period of Suess effect by the least-square method (Fig.1, firm dashed line). We assume that in the period of Suess effect action modulated solar effect was denoted by the same line and from the obtained result we subtract approximated line in the period of Suess effect (Fig.1, continuous line).

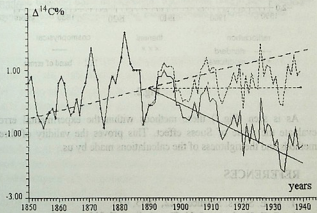


Fig.1.

The results were compared with the lines obtained by the above mentioned methods. It should be noted that according to our research the value of Suess effect made $\sim (2.4 \pm 0.35) \%$ for 1940.

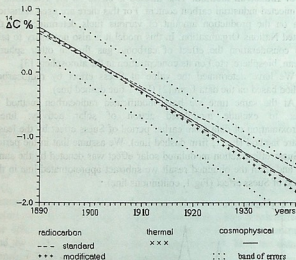


Fig.2.

As is seen (Fig.2) these methods within the experimental error evaluate the value of Suess effect. This proves the validity of three methods and the rightness of the calculations made by us.

REFERENCES

1. H. E. Suess. Science. 122, 1955, 415.
2. G. E. Kocharov, I. V. Zhorzholiani, Z. V. Lomtadidze, R. Y. Metskvarishvili, S. L. Tsereteli. Radiocarbon, 34, 2, 1992, 231.



3. M. S. Baxter, A. Walton, Proc. Royal Soc., London, A **318**, 1970, 213.
4. A. N. Charakhchian, G. A. Bazilevskaia, Y. I. Stojkov, T. N. Charakhchian, Trudi FIAN, **88**, 3, 1976, 3
5. Astrofizicheskie iavlenia I radiouglerod. Pod redakcii G. E. Kocharova, 1985 (Russian).

Tbilisi State University

ს. წერეთელი, ე. ბოჭორიშვილი, მ. მახვილაძე, მ. სამხარაძე

ანიონოპოგენური ზემოქმედება ბუნებრივ პროცესებზე და მისი შესწავლა რადიონახშირბადული მეთოდით

დასკვნა

დედამიწის აგმოსფეროში გამოშვებული რადიონახშირბადის კონცენტრაციის მონაცემების საფუძველზე განსაზღვრულია ზიუსის ეფექტის სიდიდე სამი სხვადასხვა მეთოდით. მიღებული შედეგები ელომელების ფარგლებში კარგ თანხვედრაშია ერთმანეთთან.

EQUATIONS OF MOTION FOR SUPERFLUID $\text{He}^3 - \text{He}^4$ SOLUTIONS FILLED POROUS MEDIA

Sh. Kekutia, N. Chkhaidze, Sh. Ben-Ezra

Accepted for publication April, 2002

ABSTRACT. The theory of the deformation of porous elastic solid containing a compressible superfluid He^4 has been considered in earlier publication. In the present paper, hypothetic experiments of measurement are described for the determination of the elastic coefficients of the theory. We aim at extending classical theory for the case when the porous media is saturated with superfluid $\text{He}^3 - \text{He}^4$ mixture. Finally, derived equations are applied to the most important particular case when the normal fluid component is locked inside a highly porous media by viscous forces. It is shown, that in highly porous media there exist two longitudinal sound modes: one is the intermediate mode between the first and fourth sound and another is the second sound like mode.

1. INTRODUCTION

We consider the case, when impurities participate only in normal fluid flow [1]. Sound propagation in a superfluid $\text{He}^3 - \text{He}^4$ solution has a number of peculiarities connected with the oscillation of the He^3 concentration in the acoustic wave. Whereas in pure helium II only the pressure oscillates in the first sound wave, and only the temperature oscillates in the second sound wave (neglecting the coefficient of thermal expansion, which is enormously small for helium), in a solution there are pressure, temperature, and concentration oscillations in both waves. In the first sound wave the oscillation of the temperature is proportional to the coefficient $\beta = (c/\rho) \frac{\partial \rho}{\partial c}$ and in the second sound wave the same coefficient is proportional to the pressure oscillation (c-maximum He^3 concentration, ρ - density of the solution), and at low



He^3 concentration the quantities proportional to β cannot be neglected ($\beta = -0.3-0.4$ for highly concentrated solutions). Unlike pure He^4 , the first sound wave in solutions contains a relative oscillation of the normal and superfluid liquids, the magnitude of which is proportional to β . In pure He^4 , there are no oscillations of the total flux $\vec{J} = \rho^n \vec{V}^n + \rho^s \vec{V}^s$ in the second sound wave, whereas in the solution the deviation from the equilibrium value of \vec{J} is also proportional to β [1]. On the other hand when aerogel is saturated even with pure He II new phenomena are caused by the presence of aerogel: namely, the coupling between two sound modes is provided by $\sigma \rho^s \rho^n$ (ρ^n - is the aerogel density, σ - He^3 - He^4 solution entropy) [2]. So, in this paper we have considered the peculiarities of sound propagation for impure homogeneous superfluids, where these phenomena are caused by both impurities (including He^3 in He II) and by the presence of aerogel. The task of the article represents the derivation of hydrodynamic equations for consolidated porous media filled with superfluid $He^3 - He^4$ solution and determination of all input elastic coefficients of the theory by physically measured quantities without any additional adjustable parameters.

EXPRESSION OF GENERALIZED COEFFICIENTS BY PHYSICALLY MEASURED QUANTITIES

The elastic properties of a system containing a superfluid helium completely filling the pores were considered in [3], where methods for measurement of generalized elastic coefficients are described with jacketed and unjacketed compressibility tests in the case of a homogeneous and isotropic porous matrix. In our case according to [3, 4,5] the stress-strain relations are

$$\sigma_x = 2N\epsilon_x + A\epsilon + Q^s \epsilon^s + Q^n \epsilon^n,$$

$$\sigma_y = 2N\epsilon_y + A\epsilon + Q^s \epsilon^s + Q^n \epsilon^n,$$

$$\sigma_z = 2N\epsilon_z + A\epsilon + Q^s \epsilon^s + Q^n \epsilon^n,$$

$$\tau_x = N\gamma_x, \quad \tau_y = N\gamma_y, \quad \tau_z = N\gamma_z. \quad (1)$$

$$s' = Q^s e + R^s \epsilon^s + R^n \epsilon^n,$$

$$s'' = Q^n e + R^n \epsilon^n + R^m \epsilon^s,$$

where $\sigma_x, \sigma_y, \sigma_z$ and τ_x, τ_y, τ_z are normal and tangential forces acting on the solid parts of each face of the cube with the following orientation, s' and s'' are forces acting on the solution part of each face of the cube corresponding to superfluid and normal components of superfluid solution. Scalars s' and s'' are expressed in the following form

$$s' = -\Phi p^s, \quad s'' = -\Phi p^n. \quad (2)$$

Here $p^s = \rho^s \mu$, $p^s + p^n = p$ [6], where μ is chemical potential, p - liquid pressure and Φ - porosity. Thus, we have taken into consideration the circumstance that the existence of pressure gradient is not enough for acceleration of superfluid and normal components of superfluid liquid unlike usual fluid.

The average displacement vector of the solid has the components u_x, u_y, u_z and that of the mixture $U_x^s, U_y^s, U_z^s, U_x^n, U_y^n, U_z^n$. The solid strain components are then given by

$$e_x = \frac{\partial u_x}{\partial x}, \quad e_y = \frac{\partial u_y}{\partial y}, \quad e_z = \frac{\partial u_z}{\partial z}, \quad (3)$$

$$\gamma_x = \frac{\partial u_y}{\partial z} + \frac{\partial u_x}{\partial y}, \quad \gamma_y = \frac{\partial u_x}{\partial z} + \frac{\partial u_z}{\partial x}, \quad \gamma_z = \frac{\partial u_x}{\partial y} + \frac{\partial u_y}{\partial x}.$$

Due to two possible types of motion in He II \vec{U} breaks down into the sum of two parts

$$\vec{U} = \frac{\rho^s}{\rho} \vec{U}^s + \frac{\rho^n}{\rho} \vec{U}^n \quad (4)$$

corresponding to displacement of superfluid and normal components. Thus the strain in fluid is defined by the dilatation

$$\varepsilon = \frac{\rho^s}{\rho} \nabla \vec{U}^s + \frac{\rho^n}{\rho} \nabla \vec{U}^n \quad (5)$$

Because of the fact that superfluid and normal part of He II cannot be divided physically and there is no sense to speak about belonging of some atoms to superfluid or normal components, the following relation is to be fulfilled

$$Q^s \varepsilon^s + Q^n \varepsilon^n = Q \varepsilon \quad (6)$$

The coefficients A and N correspond to the well-known Lamé coefficients in the theory of elasticity and are positive. The coefficients Q and R are the familiar Biot's coefficients [7]. The physical interpretation of the coefficients R^s , R^n , R^m is given in [1,5].

To illustrate the above mentioned let us discuss some cases of experiments which may be used to relate generalized elastic coefficients of the theory to the directly measurable coefficients: the bulk modulus of fluid K_f , the bulk modulus of solid K_{sol} , the bulk modulus of the skeletal frame K_b and N.

For clear determination we note, that in the unjacketed compressibility experiment, a sample of the porous solid is immersed in a superfluid $He^3 - He^4$ solution to which a pressure p' is applied. Under the action of pressure the solution penetrates the pores completely and the dilations of the porous solid ε and solutions ε' are measured. Unjacketed elastic coefficients of solid and fluid are determined by

$$(A) \quad \frac{1}{K_{sol}} = -\frac{e}{p'}; \quad \frac{1}{K_f} = -\frac{\varepsilon}{p'}$$

Also we note, that from expression of the solution chemical potential we have the form of the force acting on the superfluid component and normal component portions:

$$\begin{aligned} \sigma^s &= -\Phi \frac{\rho^s}{\rho} (1 + \beta) p'; \\ \sigma^n &= -\Phi \frac{\rho^n}{\rho} \left(1 - \frac{\rho^s}{\rho^n} \beta \right) p'. \end{aligned} \quad (8)$$

After considering these conditions $\varepsilon^s = \varepsilon^n = \varepsilon$ we have:

$$\begin{aligned} \left(\frac{2}{3} N + A \right) \frac{1}{K_{sol}} + (Q^s + Q^n) \frac{1}{K_f} &= (1 - \Phi), \\ Q^s \frac{1}{K_{sol}} + (R^s + R^n) \frac{1}{K_f} &= \Phi \frac{\rho^s}{\rho} (1 + \beta), \\ Q^n \frac{1}{K_{sol}} + (R^n + R^m) \frac{1}{K_f} &= \Phi \frac{\rho^n}{\rho} \left(1 - \frac{\rho^s}{\rho^n} \beta \right). \end{aligned} \quad (9)$$

The following test corresponds to the jacketed compressibility test, when a specimen of the material is enclosed in a thin impermeable jacket and then subjected to an external fluid pressure p' . The dilatation of the specimen is measured and coefficient of jacketed compressibility K_b is determined by

$$\frac{1}{K_b} = -\frac{e}{p'} \quad (10)$$

and also we have relations

$$\sigma_x = \sigma_y = \sigma_z = -p'; \quad \varepsilon^s = \varepsilon^n = \varepsilon; \quad s' = s'' = 0. \quad (11)$$

Therefore we have the three relations

$$\left(\frac{2}{3}N + A\right)e + (Q^s + Q^n)\varepsilon = -p', \quad (12)$$

$$Q^s e + (R^s + R^{sn})\varepsilon = 0, \quad (12)$$

$$Q^n e + (R^n + R^{sn})\varepsilon = 0.$$

From (9) and (12) it follows

$$Q = \frac{\Phi K_{sol} \left(1 - \Phi - \frac{K_b}{K_{sol}}\right)}{1 - \Phi + \Phi \frac{K_{sol}}{K_f} - \frac{K_b}{K_{sol}}}, \quad (13)$$

$$\frac{2}{3}N + A = K_{sol} \frac{(1 - \Phi) \left(1 - \Phi - \frac{K_b}{K_{sol}}\right) + \Phi \frac{K_{sol}}{K_f}}{1 - \Phi + \Phi \frac{K_{sol}}{K_f} - \frac{K_b}{K_{sol}}}, \quad (14)$$

$$R^n + R^{sn} = K_f \frac{\rho^n}{\rho} \left(\Phi - \frac{Q}{K_{sol}}\right) \left(1 - \frac{\rho^s}{\rho^n} \beta\right), \quad (15)$$

$$R^s + R^{sn} = K_f \frac{\rho^s}{\rho} \left(\Phi - \frac{Q}{K_{sol}}\right) (1 + \beta). \quad (16)$$

Let us consider the situation when the jacket is communicated with reservoir by the superleak. Therefore only superfluid component pours into reservoir and we can write the following relations:

$$\left(\frac{2}{3}N + A\right)c + Q^s \varepsilon^s + Q^n \varepsilon^n = -(1 - \Phi)p',$$

$$Q^s c + R^s \varepsilon^s + R^n \varepsilon^n = 0, \quad (17)$$

$$Q^n c + R^n \varepsilon^n + R^s \varepsilon^s = -\Phi p'.$$

In this compressibility test we have not the relation between ε^s and ε^n . For its determination we should utilize the conservation laws of mass and entropy. Then we have

$$\left(\varepsilon^s - \varepsilon^n\right) \frac{\bar{\sigma}^2}{\partial \sigma} \frac{\rho^s}{\rho} = \frac{1 + \beta}{\rho} p', \quad (18)$$

where

$$\bar{\sigma}^2 = \bar{\sigma}^2 + c^2 \frac{\partial}{\partial c} \left(\frac{Z}{\rho} \right) \frac{\partial \sigma}{\partial T}; \quad \bar{\sigma} = \sigma - c \frac{\partial \sigma}{\partial c}.$$

The quantity $Z = \rho(\mu_3 - \mu_4)$ is defined in terms of the chemical potentials μ_3, μ_4 for He^3 and He^4 in the solution.

These equations (17-18) together with (13-16) give:

$$R^n = \frac{\rho^s \rho^n}{\rho^2} (1 + \beta) \left(1 - \frac{\rho^s}{\rho^n} \beta \right) R - \frac{(\rho^s)^2 \bar{\sigma}^2 T \Phi}{\rho C_{\text{He}}}, \quad (19)$$

$$R^n = \frac{(\rho^n)^2}{\rho^2} \left(1 - \frac{\rho^s}{\rho^n} \beta \right)^2 R + \frac{(\rho^s)^2 \bar{\sigma}^2 T \Phi}{\rho C_{He}}, \quad (20)$$

$$R^s = \frac{(\rho^s)^2}{\rho^2} (1 + \beta)^2 R + \frac{(\rho^s)^2 \bar{\sigma}^2 T \Phi}{\rho C_{He}}. \quad (21)$$

Where Biot-Willis coefficient R is equal to [7]

$$R = \frac{\Phi^2 K_{sol}}{1 - \Phi + \Phi \frac{K_{sol}}{K_f} - \frac{K_b}{K_{sol}}}, \quad (22)$$

and C_{He} is the specific heat of the solution.

Equations for elastic waves are received by analogy with articles [1,5], expressing stress tensor through strain tensor. For three-dimensional cases we can write:

$$\nabla^2 \vec{u} + (A + N) \text{grad } e + Q^s \text{grad } \varepsilon^s + Q^n \text{grad } \varepsilon^n =$$

$$= \frac{\partial^2}{\partial t^2} \left(\rho_{11} \vec{u} + \rho_{12}^s \vec{U}^s + \rho_{12}^n \vec{U}^n \right) + bF(w) \frac{\partial}{\partial t} \left(\vec{u} - \vec{U}^n \right),$$

$$Q^s \text{grad } e + R^s \text{grad } \varepsilon^s + R^n \text{grad } \varepsilon^n = \frac{\partial^2}{\partial t^2} \left(\rho_{12}^s \vec{u} + \rho_{22}^s \vec{U}^s \right),$$

$$Q^n \text{grad } e + R^n \text{grad } \varepsilon^n + R^m \text{grad } \varepsilon^s =$$

$$= \frac{\partial^2}{\partial t^2} \left(\rho_{12}^n \vec{u} + \rho_{22}^n \vec{U}^n \right) - bF(w) \frac{\partial}{\partial t} \left(\vec{u} - \vec{U}^n \right), \quad (23)$$

where ρ_{11} is total effective density of the solid moving in the He³-He⁴ solution. Coefficients ρ_{12}^s and ρ_{12}^n are mass parameters of "coupling" between a solid and correspondingly, superfluid and normal components of solution or mass coefficient $\rho_{12}^{s(n)}$ describes the inertial (as opposed to viscous) drag that the fluid exerts on the solid as the latter is accelerated relative to the former and vice-versa.

It is well known, that the He³-He⁴ solution densities have the following form [1,5]:

$$\rho_{22}^s = \Phi \rho^s - \rho_{12}^s - \rho_{12}^n; \quad \rho_{22}^n = \Phi \rho^n - \rho_{12}^n - \rho_{12}^s$$

$$- \rho_{12}^s > 0, \quad - \rho_{12}^n > 0.$$

Complex quantity $F(w)$ describes the deviation from Poiseuille flow at finite frequencies. The coefficient $b = \eta \Phi^2 / k_0$ is the ratio of total friction force to the average normal fluid velocity, where η is the fluid viscosity and k_0 is the permeability.

SOUND PROPAGATION IN UNRESTRICTED GEOMETRY AND AEROGEL.

Now it will be interesting to ignore dissipative process in equations (20) and consider the case of unrestricted geometry. Then from equations (23) we have

$$R^s \text{grad} \epsilon^s + R^{sn} \text{grad} \epsilon^n = \rho^s \frac{\partial^2 \vec{U}^s}{\partial t^2},$$

$$R^n \text{grad} \epsilon^n + R^{ns} \text{grad} \epsilon^s = \rho^n \frac{\partial^2 \vec{U}^n}{\partial t^2}. \quad (24)$$

Here we take into account that in the limit interest to us purely geometrical quantity α_r , which is independently of solid or fluid densities, and porosity Φ are equal to one. Because the induced mass tensor per unit volume $\rho_{12}^{(n)} = -(\alpha_n - 1)\Phi\rho^{(n)}$ and

$$\begin{aligned}
 R^s &= \frac{(\rho^s)^2}{\rho^2} (1 + \beta)^2 K_f + \frac{(\rho^s)^2 \bar{\sigma}^2 T}{\rho C_{He}} \\
 R^n &= \frac{(\rho^n)^2}{\rho^2} \left(1 - \frac{\rho^s}{\rho^n} \beta \right)^2 K_f + \frac{(\rho^s)^2 \bar{\sigma}^2 T}{\rho C_{He}} \\
 R^m &= \frac{\rho^s \rho^n}{\rho^2} (1 + \beta) \left(1 - \frac{\rho^s}{\rho^n} \beta \right) K_f - \frac{(\rho^s)^2}{\rho C_{He}} \bar{\sigma}^2 T
 \end{aligned} \quad (25)$$

So, for pure $He^3 - He^4$ solution solving the system (24) in the usual manner we obtain the dispersion equation for the bulk waves propagating in free $He^3 - He^4$ solution:

$$C^4 \rho^s \rho^n - C^2 (\rho^s R^n + \rho^n R^s) + R^s R^n - (R^m)^2 = 0 \quad (26)$$

Equation (26) has two roots

$$C_1^2 = \frac{K_f}{\rho} \left(1 + \frac{\rho^s}{\rho^n} \beta^2 \right); \quad C_2^2 = \frac{\rho^s}{\rho^n} \frac{\bar{\sigma}^2 T}{C_{He} \left(1 + \frac{\rho^s}{\rho^n} \beta^2 \right)} \quad (27)$$

which conform to the velocity of the first and the second sounds correspondingly [8].

From (24) equations it follows the well known results for the fourth sound in free $He^3 - He^4$ solutions [3]. If we assume $\bar{U}^n = 0$ in (21), we derive [9,10]

$$C_4^2 = \frac{\rho^n}{\rho} C_1^2 \frac{(1 + \beta)^2}{1 + \frac{\rho^s}{\rho^n} \beta^2} + \frac{\rho^n}{\rho} C_2^2 \left(1 + \frac{\rho^s}{\rho^n} \beta^2 \right) \quad (28)$$

Propagation of the fourth sound in a He^3 - He^4 solution was studied in [9, 10] from the hydrodynamic equations.

A great deal of effort has recently been dedicated to the investigation of superfluid solution in porous materials. We cite here recent articles describing the specific features of superfluid liquid in various porous structures [11]. The sound velocity in porous media can provide information about the superfluidity property as well as elastic properties of the solid matrix. McKenna et al [12] developed a theory explaining the behavior of sound modes in aerogel filled with He II, taking into account coupling between the normal component and the aerogel and its elasticity. Here the normal component is locked in a very compliant solid matrix so that the liquid and aerogel fibers move together under mechanical and thermal gradients. It takes place at low sound frequencies, when the viscous penetration depth is bigger than the pore size so the entire normal component is viscously locked to the solid matrix. In this case from (23) for longitudinal waves we have the following dispersion equation:

$$\rho^s [\rho^o + \rho^n] C^4 - C^2 [R^s (\rho^o + \rho) + \rho^s (A + 2N + 2Q + R) - 2\rho^s \times (Q^s + R^s + R^{sn})] + R^s (A + 2N + 2Q + R) - (Q^s + R^s + R^{sn})^2 = 0 \quad (29)$$

The bulk velocities can express this dispersion equation:

$$\left(1 + \frac{\rho^o}{\rho^n}\right) C^4 - C^2 \left\{ C_1^2 + \left(1 + \frac{\rho^s}{\rho^n} \beta^2\right) C_2^2 + \frac{\rho^o}{\rho^n} (C_3^2 + C_4^2) \right\} + C_1^2 C_2^2 + \frac{\rho^o}{\rho^n} C_3^2 C_4^2 = 0 \quad (30)$$

here $C_3^2 = \frac{K_b + (4/3)N}{\rho^a}$.

The first solution is intermediate between the first and fourth sound

$$C_{14}^2 = \frac{C_1^2 + \frac{\rho^o}{\rho} C_3^2}{1 + \frac{\rho^o}{\rho^n}} \quad (31)$$

and it resembles the fast mode.

Another solution corresponds to the slow mode, which is an oscillation of a deformation of the aerogel combined with a simultaneous out-of-phase motion of the superfluid component:

$$C_{2a}^2 = \frac{C_2^2 + \frac{\rho^* \rho^s}{\rho^n \rho} C_4^2 C_0^2}{1 + \frac{\rho^* \rho^s}{\rho^n \rho}} \quad (32)$$

In this wave the main oscillated quantity is temperature. From experiment data for silica aerogel $C_{2a}^2 \gg C_2^2$ [12], so from the above mentioned formula it follows that $C_{2a}^2 \gg C_2^2$. Therefore, the velocity of slow wave is much bigger than that of temperature sound in free solutions.

From (31) and (32) it follows that an aerogel filled with superfluid He^3 - He^4 solution simultaneously possesses the properties of elastic solid and superfluid liquid. Also, in this paper we have considered the peculiarities of sound propagation for impure homogeneous superfluids, where these phenomena are caused both by impurities (including He^3 in He^4) and by the presence of aerogel.

REFERENCES

1. I.M. Khalatnikov. Zh. Eksp. Teor. Fiz. **23**, 1952, 263.
2. P. Brusov, J.M. Parpia, P. Brusov, G. Lawes. Phys. Rev. B. **63**, 2002, 140.
3. Sh. Kekutia, N. Chkhaidze. Proc. Tbilisi State University, "Physics", **345**, 36-37, 2001, 49.
4. Sh. Kekutia, N. Chkhaidze. Fiz. Niz. Temp. **28**, 11, 2002, 1115.
5. M.A. Biot, J. Acoust. Soc. Am. **28**, 1956, 168.
6. S. Patterman. Hidrodinamika sverxtekuchei zhidkosti. 1978 (Russian).
7. M.A. Biot, D.G. Willis. J. Appl. Mech. **24**, 1957, 594.
8. I.M. Khalatnikov. Teoria sverkhtekuchesti. M., 1971 (Russian).
9. D.G. Sanikidze, D.M. Chernikova. Zh. Eksp. Teor. Fiz. **46**, 1964, 1123.



10. B.N. Eelson, N.E. Dyumin, E. Ya. Rudavski, I.A. Serbin. Zh Eksp. Teor. Fiz. 51, 1966, 1065.
11. J.D. Reppy. J. Low Temp. Phys. 87, 1992, 205.
12. M.J. McKenna, T. Slawewski, J.D. Maynard. Phys. Rev. Lett. 66, 1991, 878.

Georgian Academy of Sciences
Institute of Cybernetics
Hebrew University of Jerusalem

შ. კეკუტია, ნ. ჩხაიძე, შ. ბუნეზრა

$He^3 - He^4$ ხსნარით შევსებულ ფოროვან გარემოს მოძრაობის განგოლებები

დასკვნა

სტაგიაში მიღებულია $He^3 - He^4$ ხსნარით შევსებული ფოროვან გარემოს მოძრაობის გაწრფივებული განგოლებები. მათში შემავალი განზოგადებული დრეკადობის კოეფიციენტები გამოსახულია ექსპერიმენტულად გამოძვადი ფიზიკური შინაარსის მქონე სიდიდეებით. მიღებული განგოლებების გამოყენებით განსამღვრულია მაღალი ფოროვნების მქონე გარემოში - აეროგელში გავრცელებადი გრძივი ბგერების სიჩქარეები. ნაჩვენებია, რომ სწრაფი ბგერის სიჩქარე წარმოადგენს პირველი და მეოთხე ბგერების სიჩქარეების კომბინაციას, ხოლო ნელი ბგერა ეთანადება გემპერატურულ ბგერას, რომლის სიჩქარე სილიკა აეროგელებში მეტია თავისუფალ ხსნარებში გემპერატურულ ბგერის სიჩქარესთან შედარებით.

(Russian)

7 M.A. Bior, D.G. Willis, J. Appl. Phys. 54, 1957, 294

8 I.M. Khalaturkov, Teora svyazaniy, No. 1921 (Russian)

9 D.G. Saninidze, D.M. Chikolava, Zh. Eksp. Teor. Fiz. 46,

1964, 1123

THE DISSOCIATIVE EXCITATION PROCESSES IN COLLISIONS OF ELECTRONS AND HELIUM IONS WITH OXYGEN MOLECULES.

M. Gochitashvili, B. Kikiani, R. Kvizhinadze, R. Lomsadze

Accepted for publication May, 2002

ABSTRACT. Absolute cross sections for dissociative excitation processes of oxygen atomic and ionic lines in the collisions of e^- -O₂ and He⁺-O₂ are determined. The high intense oxygen ionic line OII (83.4 nm) has been observed. In case of electrons impact a doubly charged oxygen ionic line OIII (70.5 nm) has been observed too. For He⁺-O₂ collisions the experimental results are interpreted qualitatively in terms of quasidiatomic approximation.

In the present work, the values for absolute cross sections of dissociative excitation processes at collisions of electrons and helium ions with oxygen molecules in 200-500 eV and 2-11 keV energy range are given respectively. The measurements were carried out by optical spectroscopy method. The experimental set-up and calibration procedure for the determination of absolute value of cross sections of excitation processes has been described in details [1,2]. An estimation of uncertainties of the absolute value of all cross sections given here did not exceed 20-25% and the accuracy of relative measurements was 4-5%.

The ion beam extracted from the discharge ion source is focused, accelerated and mass selected in a 60° magnetic sector field. The formed He⁺ ion beam was passed through collimating slits and finally entered into the collision chamber. To ensure single collision condition a working gas pressure was an order of $1-2 \times 10^{-3}$ Torr.

The radiation emitted in the collision was observed at angle 90° with respect to the direction of the primary ion beam. The spectral analysis of this radiation was performed in the vacuum ultraviolet (VUV) spectral region by a Sava-Namioka monochromator incorporating a toroidal diffraction grating. The intensity of the radiation was detected by secondary electron multipliers under integrating or pulse-counting conditions.

Particular attention was devoted to the reliable determination and control of the relative and absolute spectral sensitivity of the light recording system. This was done by measuring the signal due to the emission of the molecular bands and atomic lines excited by electrons in collisions with H_2 , N_2 , O_2 molecules and Ar atoms. For this an electron gun was located directly in front of the entrance slit of the collision chamber. The relative spectral sensitivity and the values of the absolute cross sections were obtained by comparison with cross sections for the same lines and molecular bands reported in [3-8].

RESULTS

In Figs. 1 and 2 the review spectrum for $He^+ - O_2$ pair in the 80 - 150 nm spectral region at a fixed helium ion energy ($E = 10$ keV) and for $e - O_2$ in the 55 - 90 nm spectral region at a fixed energy ($E = 0.44$ keV) are presented accordingly. In Fig. 3 the dependencies of absolute cross sections from the collision energy for the dissociative excitation of oxygen atomic OI (97.4, 99.0 nm, 102.6 nm, 115.2 nm) and ionic OII (83.4 nm) lines at $He^+ - O_2$ collision are presented. Here for the sake of comparison the excitation cross-section of helium resonance atomic lines HeI (53.7 nm, 58.4 nm) are presented as well. As it seems main inelastic channel responsible for the dissociative excitation processes is an oxygen ionic line OII (83.4 nm), due to its intensity. At the collision of electron with oxygen molecules the most intense ionic line OII (83.4 nm) is observed. The emission spectrum (in an area of 83.4 nm) includes also relatively intensive ionic line OIII (83.3 nm, $2p^2\ ^3P - 2p^3\ ^3D^0$) (not shown in Fig.). Besides, it is interesting to mention that the weak ionic line of doubly charged ion OIII (70.6 nm) is observed too. The absolute value of excitation cross section of OIII (70.6 nm, $2p^2\ ^3P - 2p^3\ ^3P^0$) line at an electron energy $E=200$ eV is equal to the $3.4 \times 10^{-20} \text{ cm}^2$ and at an energy $E = 440$ eV to the $3.8 \times 10^{-20} \text{ cm}^2$.

DISCUSSION

The dissociation of molecules and hence the formation of excited atomic or ionic products proceed via decay of intermediate core-excited oxygen molecular ions.

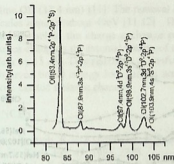


Fig.1. Spectrum of O₂ at 10 keV helium ion impact energy from 80 to 105 nm

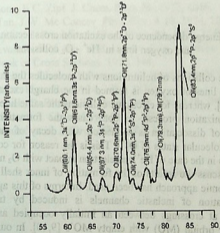


Fig.2. Spectrum of O₂ at 440 eV electron impact energy from 55 to 90 nm

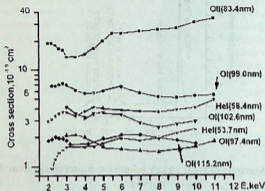


Fig.3. Energy dependence of the excitation cross section of helium and oxygen lines in $\text{He}^+ - \text{O}_2$ collisions

At the collisions of helium ions with molecules the intense atomic and ionic lines of oxygen is formed in the charge exchange process mainly [9], whereas for electronic collisions the same lines are formed in the ionization process. In both cases the formation of excited products of dissociation is connected with decay of the same high excited molecular states of O_2^{+*} . This is the reason for comparison of the results in the case of He^+ and electron impact with O_2 molecule.

To discuss the results of the formation of inner shell vacancy the quasidiatomic approach has been used. In terms of this approximation the excitation of inelastic channels is induced by transitions of electrons at crossings between an initially occupied and promoted molecular orbital (MO) with empty MO's [9,10]. In our case initial vacancy in He (1s) orbital becomes an inner vacancy of the quasimolecule, hence core-excited, one-hole molecular states can be formed. In particular, the decay of one-hole $2\sigma_g^{-1}$ high excited molecular states $^2\Sigma_g^-$ or $^4\Sigma_g^-$ of oxygen cause the excitation of intense



oxygen ionic line OII (83.4 nm) [11]. The removal of a $2s\sigma_g$ electron from O_2 molecules requires about 40eV [11,12]. Therefore excitation of the inelastic channel in the charge exchange process $He(1s^3) + O_2^+(2\sigma_g^{-1})$ requires changing the internal energy of the quasimolecular $(He, O_2)^+$ system by 15 eV. This statement is confirmed from [9] too. In fact, the observed broad energy loss spectra around 22 eV might contain the above excited inelastic channel.

REFERENCES

1. M.R. Gochitashvili, R.V. Kvizhinadze, N.R. Jaliashvili, B.I. Kikiani. Zh. Tech. Fiz. **49**, 1993, 2338.
2. M.R. Gochitashvili, N.R. Jaliashvili, R.V. Kvizhinadze, B.I. Kikiani. J. Phys. **B28**, 1995, 2453.
3. M.J. Mumma, E.C. Zipf J. Chem. Phys. **55**, 1971, 1661.
4. K.H. Tan, F.G. Donaldson, J.W. Mc Concey. Can. J. Phys. **52**, 1974, 786.
5. E.J. Stone, E.C. Zipf J. Chem. Phys. **56**, 1972, 4646.
6. K.H. Tan, J.W. Mc Concey. Phys. Rev. A **10**, 1974, 1212.
7. J.M. Ajello, B. Franklin. J. Chem. Phys. **82**, 1985, 2519.
8. S.V. Avakian, R.N. Ilin, V.M. Lavrov, G.N. Ogurtsov. A Handbook of Cross Sections. 1998, 344.
9. D. Doweck, D. Dhuicq, J. Pommier, Vu Ngoe Tuan, V. Sidis, M. Barat. Phys. Rev. **A24**, 1981, 2425.
10. D. Doweck, D. Dhuicq, M. Barat, Phys. Rev. **A28**, 1983, 2838.
11. R.S. Freund. J. Chem. Phys. **54**, 7, 1971, 3125.
12. F.B. Yousif, et al. J. Phys. **B20**, 1987, 5079.

Tbilisi State University

During the derivation of the formula of critical velocity of the first vortex generation V_{cr1} [3] obtained the following expression of the angular momentum of the vortex, which is directed along the axis of a cylinder

$$L = \frac{1}{2} \rho \Omega R^2 H, \quad (1)$$

დისოციაციის პროდუქტების აღგზნების გამოკვლევა
ელექტრონებისა და He^+ იონების ენგბადის მოლეკულებთან
დაჯახების პროცესში

დასკვნა

$e-O_2$ და He^+-O_2 წყვილებისათვის დისოციატიური აღგზნების პროცესებში გამოიყენება ენგბადის იონური და ატომური სპექტრალური ხაზების გამოსხივების აბსოლუტური კვანძი. დაკვირვებულ იქნა მაღალი ინტენსიობის იონური ხაზი OII (83.4 ნმ). ელექტრონებით დაჯახების პროცესში გამოიყენებოდა იქნა ორჯერად იონიზირებული ენგბადის იონის ოპტიკური ხაზის -OIII (70.5 ნმ) აღგზნების კვანძი. He^+-O_2 წყვილისათვის ექსპერიმენტული მონაცემები თვითნებურად აღწერილია კვაზიდიამეტრული მიხედვებით.

ANGULAR MOMENTUM CAUSED BY ANY SHAPE VORTEX LINE



L.Kiknadze, Yu.Mamaladze

Accepted for publication July 2002

ABSTRACT The contribution of any shape vortex line to the angular momentum of the liquid confined to the axially symmetric vessel is considered. The general formulae, which do not require the knowledge of the velocity distribution of the liquid, are received (only the shape and disposition of vortex and wall are enough).

1. INTRODUCTION

The contribution $\vec{r} \times \vec{v} \rho dV$ of each element ρdV is to be integrated over the volume V of a liquid to determine its angular momentum \vec{L} (ρ is the density, and v is the velocity). The existence of a vortex line causes the inversely proportional dependence of the velocity on the distance from this line. Because of it the contribution of the remote part of a liquid to angular momentum is more sufficient than the contribution of the vortex core though in its vicinity the velocity tends to infinity (the product rv is finite as well as in far areas, where the velocity tends to zero). That is why the angular momentum cannot be determined by rough but simple and effective estimations with a weak dependence on the form of wall and of the distance to it (such estimations are possible and widely used for energy of the vortex in hydrodynamics of superfluid He II [1], see also [2]).

During the derivation of the formula of critical velocity of the first vortex generation Vinen [3] obtained the following expression of the angular momentum of the vortex, which is disposed along the axis of a cylinder:

$$L = \frac{1}{2} \rho \Gamma R^2 H, \quad (1)$$

where H is the height of the cylinder, R is its radius, and Γ is a circulation, which was quantized in Vinen's paper, as well as in [4-7] mentioned below, in the units of $2\pi\hbar/m$ (m is the mass of helium atom). But the structure of the vortex core (the size of this formation is of order of 3 \AA) is neglected as if the incompressible liquid was considered. The same approximation is exploited in this paper (if one has in mind the superfluid component of He II denotations ρ and Γ must be substituted by ρ_s and $2\pi\hbar/m$).

The interaction in the incompressible liquid spreads in a moment. Because of this three following expressions of angular momentum are received also in the hydrodynamics of superfluid liquid. Namely, if a vortex is disposed parallel to the axis of a cylinder on the distance r_v from this axis being parallel to it then [4,5]:

$$\bar{L} = \frac{1}{2}\rho\Gamma(R^2 - r_v^2)H. \quad (2)$$

If a vortex is disposed along the axis of rotation of a sphere (its diameter), then [6]:

$$L = \frac{2}{3}\rho\Gamma R^3, \quad (3)$$

where R is the radius of the sphere. If a vortex is disposed along the axis of rotation of two concentric spheres with radii R_1, R_2 , then [7]:

$$L = \frac{2}{3}\rho\Gamma(R_2^3 - R_1^3). \quad (4)$$

Eqs. (1,3,4) were received by the direct integration of $\rho v 2\pi r dr$ with $v = \Gamma/2\pi r$. In the case of a displaced vortex its image must be taken into account, and the integration is complicated.

We would not be surprised if in classical hydrodynamics the formulae exist, which determine the angular momentum of a vortex in

some other geometry, but we had not seen them in the textbooks. May be the point is that in the classical physics the ideal liquid is treated as the excessive idealization of the properties of real liquid. In the real liquid the core of a vortex diffuses. Unlike this situation the vortex filaments in He II are stable and attract more attention.

In several works are calculated the angular moments of many vortex arrays formed in rotating He II (both in cylindrical and spherical geometry). But in this paper we are interested only in the angular momentum of a single vortex. Just this problem is connected with some aspects of vortex dynamics including the ones connected with pulsar quakes.

2. THE ANGULAR MOMENTUM OF ANY SHAPE VORTEX LINE CONFINED TO THE AXIALLY SYMMETRIC VESSEL

The main restrictions in the following derivation of Eq. (6) is that the vessel has an axially symmetry (its wall is the surface of revolution), and the vortex is supposed to be on one plane with the z -axis of liquid rotation (Fig.1). The equation of the wall is $r = r_w(z)$, the equation of the vortex line is $r = r_v(z)$ (the cylindrical coordinates r, α, z are used), and both these dependencies are supposed to be single-valued. The possible generalizations see in Sec.5.

In such conditions the integral mentioned above in the beginning of Sec.1 may be written down as:

$$L_z = L = \rho \int_{z_{\min}}^{z_{\max}} dz \int_0^{r_w(z)} dr \int_0^{2\pi} v_\alpha r d\alpha, \quad (5)$$

$L_r = L_\alpha = 0$ under the supposed conditions.

The last integral in Eq. (5) is the circulation around the z -axis. It is zero if there is no vortex in the circle with the radius r on the height z , and it is equal to $\Gamma = \text{const}$ if there is a vortex in such circle. Therefore

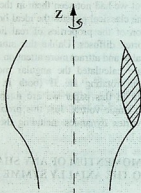


Fig.1. The section of the axially symmetric vessel with a vortex on it. The surface outlined by the vortex and the wall is shaded.

$$L = \frac{1}{2} \rho \Gamma \int_{z_{\min}}^{z_{\max}} (r_w^2 - r_v^2) dz, \quad (6)$$

where z_{\min} and z_{\max} are the limits of the vortex disposition. One can exploit this equation without necessity to determine the velocity distribution in the vessel.

The known formulae (Eqs. (1-4)) may be received from Eq. (6). Using this equation it is easy to get the result for the case where the vortex is disposed on the distance r_v from the axis of rotation of the sphere, being parallel to this axis:

$$L = \frac{2}{3} \rho \Gamma (R^2 - r_v^2)^{3/2} \quad (7)$$

3. IMPULSE IN THE SENSE OF KELVIN AND THE ANGULAR MOMENTUM

The impulse in the Kelvin's sense differs on principle from the momentum [8-10]. It is so because the transfer of the momentum which is necessary to set unmoving liquid in the state of given motion (just this is the impulse in the sense of Kelvin) is accompanied by the action of walls which can sufficiently change the momentum of a liquid. In the case of angular momentum the similar situation is less necessary because the action of walls to change the direction of the rotating liquid flow is centripetal and does not change the angular momentum. E.g. let us consider the cases shown in Fig.2. A liquid is rotating around the vortex disposed along the axis of cylinder or parallel to it. To create such a motion one must do a push on the shaded surface in the direction perpendicular to this figure plane. The following centripetal action of walls is oriented radial, and the angular momentum oriented along z -axis remains unchanged.

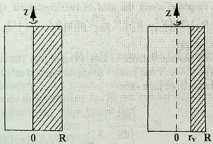


Fig.2. The section of a cylinder with a vortex disposed along its axis and parallel to it. The surface which must be pushed to create the considered motion of liquid is shaded.

In general case shown in Fig.1 the Kelvin's impulse is also expressed by the shaded surface [4]:

$$p_K = \rho \Gamma S,$$

where S is the magnitude of the surface limited by the vortex and walls. It is reasonable to think that the angular momentum can be calculated as the product of the Kelvin's impulse on the radius vector R_c of the center of this surface:

$$L = R_c p_K. \quad (9)$$

All preceding formulae for L confirm our proposition. Namely, if the vortex is disposed along the axis of a cylinder then $R_c = R/2$, and $p_K = \rho \Gamma R H$. Their product gives Eq. (1). If a vortex is disposed parallel to the axis of rotation of the cylinder then $R_c = r_v + (R - r_v)/2 = (R + r_v)/2$, $p_K = \rho \Gamma (R - r_v) H$, and their product gives Eq. (2). If the vortex is disposed along the axis of sphere then $R_c = 4R/3\pi$, $p_K = \rho \Gamma \pi R^2/2$, and their product gives Eq. (3). If the vortex is disposed along the axis of two concentric spheres then $R_c = 4(R_2^3 - R_1^3)/3\pi(R_2^2 - R_1^2)$, $p_K = \rho \Gamma \pi(R_2^2 - R_1^2)/2$, and their product gives Eq. (4).

Let us prove the equivalence of Eqs. (9) and (6). The center of the imaginary surface which one pushes to create a given motion is on the following distance from the z -axis:

$$R_c = \frac{\int r dS}{\int dS} = \frac{1}{S} \int_{r_{\min}}^{r_{\max}} z r dr$$

(r_{\min} , r_{\max} are the minimal and the maximal distances of the surface S from the axis of rotation).

According to Eqs. (8,9) we obtain:

$$L = \rho \Gamma \int_{r_{\min}}^{r_{\max}} z r dr. \quad (10)$$

On the other hand

$$\int_{r_{\min}}^{r_{\max}} z r dr = -\frac{1}{2} \phi z dr^2.$$

The last integral must be taken along the boundary of the surface S in the positive direction of revolution. Substituting Eqs. (8,10) in Eq. (9) we obtain:

$$L = -\frac{1}{2} \rho \Gamma \phi z dr^2. \quad (11)$$

Eq. (6) may be also transformed in the integral about the same path that gives another expression of L :

$$\int_{z_{\min}}^{z_{\max}} (r_w^2 - r_v^2) dz = \phi r^2 dz, \quad (12)$$

$$L = \frac{1}{2} \rho \Gamma \phi r^2 dz. \quad (13)$$

The equivalence of Eqs. (11,13) means the equivalence of Eqs. (6,9,10). We have obtained these formulae for conditions determined in Sec.2. However some generalizations, described in the following section, provide the possibility to use our general equations (Eqs. (6,9-11,13)) for actually any shape vortex line.

4. GENERALIZATIONS

The simplest generalization, which can be made as compared with Fig.1, is the case where a vortex is placed between the wall and another (also axially symmetric) body. Our general formulae (Eqs. (6,9-11,13)) may be directly exploited in this case. E.g. so may be received Eq. (4) and the following expression for the case where a vortex is disposed between two coaxial cylinders parallel to the axis of their rotation. In this doubly connected area the existence of a circulation Γ_1 is possible on the surface of inner cylinder which gives

the additional contribution to the angular momentum. Together with the contribution of a vortex it implies:

$$L = \rho \Gamma_1 (R_2^2 - R_1^2) + \rho \Gamma (R_2^2 - r_v^2). \quad (14)$$

If a vortex is disposed between two concentric spheres parallel to the axis of their rotation, and the edges of a vortex are placed on the surfaces of both spheres ($r_v < R_1$) then:

$$L = \frac{2}{3} \rho \Gamma \left[(R_2^2 - r_v^2)^{3/2} - (R_1^2 - r_v^2)^{3/2} \right], \quad (15)$$

and if the edges of a vortex are placed on the surface only of the outer sphere $r_v > R_1$ then (cf. Eq. (7)):

$$L = \frac{2}{3} \rho \Gamma (R_2^2 - r_v^2)^{3/2}. \quad (16)$$

We would like to note that in doubly connected area between two cylinders a circulation Γ_1 on the surface of inner cylinder is possible independently from the fact if a vortex exists or not. In the simply connected area between two spheres a circulation on the surface of the inner sphere is possible only if it is caused, according the Stokes theorem, by a vortex that pierces the sphere.

If the functions $r(z)$ which describe walls or a vortex are not single-valued then one must divide the curves r_v, r_w into several single-valued parts and Eq. (6) would be replaced by the sum of several integrals with the own z_{\min}, z_{\max} and r_{\min}, r_{\max} . The values of these integrals depend on the absence or existence of a circulation and its sign in the interval considered. In similar way one must deal with Eq. (10) if the dependence $z(r)$ is not single valued. Eqs. (9, 11, 13) may be used without any changes.

If z -axis divides the shaded area into two parts, then their p_K have opposite signs. But corresponding R_e also have opposite signs.

Therefore the sum of two products $\rho_K R_c$ will appear in Eq. (9). Eqs. (6,11,13) may be used without any changes.

Now let us consider the closed vortex, which has no contact with walls. If we increase the radius of circumference around the axis of rotation, then the part of the vortex, which is on the distance $r_{\min}(z)$ from the axis, enters in this circumference earlier than the other ones. This part contributes in Eq. (6) nonzero Γ until the part of vortex with $r_{\max}(z)$ and with circulation $-\Gamma$ enters. The contribution of circulation in Eq. (5) for $r_{\max} < r < r_w$ is zero. Eq. (6) is valid but r_v, r_w must be substituted by r_{\min}, r_{\max} . Eqs. (9,11,13) may be used without any changes. It is right also in the case where the axis divides the closed vortex in two parts. But, in this case, in Eq. (9) the product $\rho_K R_c$ must be substituted by the sum of such products.

5. SUMMARY

The momentary shape and disposition of a vortex and walls completely determine the angular momentum of a liquid at the same moment (let us remind that the interaction in the incompressible liquid spreads in a moment). The motion of a vortex and its stability is not considered in this paper. Eqs. (6,9-11,13) only imply the angular momentum corresponding to definite configuration of a vortex and walls.

ACKNOWLEDGMENTS. This work is partly supported by Grant 2.17.02 of Georgian Academy of Sciences.

REFERENCES

1. R.P.Feynman. In Prog. in Low Temp.Phys., ed. C.J.Gorter. N.-H. Publ.Co.,Amsterdam, 1, 1955, ch.II.
2. L.Kiknadze, Yu. Mamaladze. Proc. Tbilisi State University, Physics, 36-37, 96, 2001.
3. W.F.Vinc. Nature 181, 1958,1524.
4. E.L.Andronikashvili,Yu.G.Mamaladze. Rev.Mod.Phys. 38, 1966, 567.

5. A.L.Fetter. Phys.Rev. 153, 1967, 285.
6. L.Kiknadze, Yu.Mamaladze. Fiz.Nizk.Temp. 6, 1980, 413.
7. L.Kiknadze, Yu.Mamaladze. Low Temp.Phys. 127, 2002, 271.
8. G.Lamb. Hidrodinamika. 1947 (Russian).
9. Yu.G.Mamaladze. Sb. Fizika Nizkix Temperatur, 1965 (Russian).
10. L.V.Laperashvili, Yu.G.Mamaladze. Sb. Fizika Nizkix Temperatur, 1965 (Russian).

Georgian Academy of Sciences
Institute of Physics
Tbilisi State University

ლ. კიკნაძე, ი. მამალაძე


**ნებისმიერი ფორმის გრიგალით განპირობებული
მოძრაობის რაოლენობის მომენტი**

დასკვნა

გრიგალით განპირობებული მოძრაობის რაოლენობის მომენტი-სათვის ცნობილია მხოლოდ რამდენიმე ფორმულა (ამ სტატიის (1-4)). ეს ფორმულები (გარდა (2)-ისა), გამოიყენება იმ შემთხვევებისათვის, როდესაც გრიგალი მბრუნავი ჭურჭლის ლერძზეა განლაგებული. ამის მიზეზი, ალბათ, არის ის, რომ, თუ გრიგალი ლერძზე არაა მოთავსებული, ძნელდება სიჩქარეთა განაწილების განსაზღვრა და ინტეგრება. ამ სტატიაში მიღებულია მოძრაობის რაოლენობის მომენტის გამოსათვლელი ფორმულები (6) და (10), რომლებიც არ მოითხოვს სიჩქარეთა განაწილების ცოდნას. საჭიროა ვიცოდეთ მხოლოდ გრიგალისა და კედლის ფორმა (გრიგალის ფორმა ნებისმიერია, კედლისა კი - ბრუნვის ნებისმიერი ზედაპირი). მიღებულია, აგრეთვე, ამავე პირობებში სამართლიანი ფორმულა (9), რომელშიაც გამოყენებულია კელვინის აზრით იმპულსის ცნება. ცნობილია, რომ ეს იმპულსი შეიძლება ძალიან არსებითად განსხვავებოდეს მოძრაობის რაოლენობისაგან, მაგრამ აქ ნაჩვენებია, რომ აღწერილ პირობებში იგი იძლევა მოძრაობის რაოლენობის მომენტის სწორ მნიშვნელობას. კიდევ ორი ზოგადი ფორმულა



(11,13) წარმოგვიდგენს საბიბეულ სიდილეს წირითი ინტეგრალუბის სახით, რომლებიყ გამოითულება შეკრული გრიგალის მიერ ან გრიგალისა და კელის მიერ შემოწერილ კონტურებზე. ხუთივე ზოგალი ფორმულა მოიცავს ღლემდე ცნობილ ფორმულუბს (1-4) და იძლევა სხვა კერძო შემთხვევების განსხილის საშუალუბას (ფორმულუბი (7,14-16)).



ELECTRON IMPACT DOUBLE IONIZATION OF HELIUM-LIKE IONS IN THE METASTABLE STATES

P. Defrance, T. Kereselidze, I. Noselidze, M. Tzulukidze

Accepted for publication May, 2002

ABSTRACT. For the first time total cross sections for double ionization of two-electron atomic systems He, Li⁺, Be²⁺, B³⁺ and C⁴⁺ being in the 2¹S and 2³S metastable states are calculated within the framework of the shake-off model. Only radial correlation between the target electrons is taken into account and repulsion between the ejected electrons is ignored.

1. INTRODUCTION

Double ionization of helium and helium-like ions has been a subject of intensive theoretical and experimental studies for recent years. The reason is that the consideration of the simplest atomic systems — the members of the helium isoelectronic sequence — is the most effective tool for exploring the dynamics of double ionization and, in this way, to study the role of electron-electron correlation in atoms and ions.

In the experimental studies of ionization processes, the crossing beam technique is generally used [1]. For helium, the target beam is formed at room or even lower temperatures [2]. Therefore, one may suppose that all the helium atoms of the parent beam are kept in the ground state. However, for ion beams, the situation is quite different: depending on the method of formation of the parent beam, the population of long-lived excited states in it can be significant. Ions formed in metastable states are frequently observed in various plasmas and, in particular, in ion sources [3,4]. Due to their large lifetime, such particles can easily survive along the path from the source to the collision region and contribute to the ionization signal. As a consequence, it is easily understood that the population of the excited metastable states may play an important role in many collision experiments. This role was observed in single ionization experiments, in particular for electron energies below the ground state ionization

threshold [5]. These observations were confirmed by the theory [6]. It was also found that ions being in the metastable states might play a remarkable role in double ionization experiments [7].

It is worth noting that the same situation arises when an He^+ ion beam passes through a gas target in order to form an He atom beam by charge exchange [8,9]. Consequently, in order to interpret the experimental results correctly one needs to take into account all the states (ground and excited) presented in the parent beam. In order to estimate the respective role of these states in the double ionization (DI) process, it is necessary to know the corresponding cross sections.

In a series of three recent papers, within the framework of shake-off mechanism the first order contribution was analyzed in the case of electron impact DI of two-electron atomic systems, assuming that these systems are in their ground state. In the first paper [10] the fully (eightfold) differential cross section was calculated using plane waves for the incident and scattered electrons, the Hylleraas-type wavefunction (with radial correlation only) for the bound electrons and the Coulomb double-continuum wavefunction for the ejected electrons. The use of relatively simple wavefunctions allowed us to calculate the eightfold and fourfold differential cross sections analytically. The further integration of the fourfold differential cross section has been performed numerically and the total cross sections (TCS) were obtained for the members of helium isoelectronic sequence from $\text{H}^-(Z = 1)$ to $\text{N}^{5+}(Z = 7)$ [11]. The calculated values of TCS are found to be in fair agreement with the available experimental data for He and Li^+ . In the third paper [12] the coefficients of the asymptotic formula for the TCS in the Bethe-Born approximation are determined.

In the present paper the scheme developed for the ground state two-electron systems is extended to both the 2^1S and 2^3S excited metastable states. To the best of the author's knowledge, the Born approximation has not been applied to the calculation of total DI cross section for any atom or ion in excited states. (In their recent paper Muktavat and Srivastava [13] calculated the fully differential cross sections for DI of helium being in the 2^1S and 2^3S metastable states.) Again, only radial correlation between the bound electrons is taken into account in the present calculation. The fully differential cross

section is obtained in an analytical form and it is integrated numerically in order to obtain the TCS.

The paper is organized as follows. After determining the goal of the present study (section 1), we give briefly the theory of double ionization process for helium-like ions in the metastable states (section 2). In section 3 we present the result of calculations and discuss the obtained cross sections. Atomic units ($e = m = \hbar = 1$) will be used throughout this paper.

2. THEORY

The eightfold differential cross section (8DCS) for double ionization of helium-like ions is given as

$$\frac{d^8\sigma^{(\pm)}}{d\Omega_3 d\Omega_1 d\Omega_2 d(k_1^2/2) d(k_2^2/2)} = \frac{(2\pi)^4 k_s k_1 k_2}{k_i} |T_{fi}^{(\pm)}|^2 \quad (1)$$

Here $\vec{k}_i, \vec{k}_s, \vec{k}_1, \vec{k}_2$ are the wavevectors of the incident, scattered and ejected electrons respectively, $d\Omega$ denotes the element of solid angle surrounding the corresponding wavevector, $T_{fi}^{(\pm)}$ represents the matrix element given by

$$T_{fi}^{(\pm)} = \int \Psi_f^{(\pm)*} V_i \Psi_i^{(\pm)} d\vec{r} d\vec{r}_1 d\vec{r}_2, \quad (2)$$

where $\Psi_i^{(\pm)}$ and $\Psi_f^{(\pm)}$ are the wavefunctions of the colliding system in the initial and final states, respectively; V_i describes the interaction between the incident electron and a target

$$V_i = -\frac{Z}{r} + \frac{1}{|\vec{r} - \vec{r}_1|} + \frac{1}{|\vec{r} - \vec{r}_2|} \quad (3)$$

In (1) and (2) the unlike signs (\pm) indicate that the total spin of the two bound electrons is zero or one, i.e. the target is in the 2^1S or 2^3S metastable states, respectively.

As noted above our scheme is based on an analytical calculation of the 8DCS. For this we employ the relatively simple wavefunctions. Namely, we describe the initial and final states of the colliding system by the following wavefunctions:

$$\Psi_i^{(\pm)}(\vec{r}, \vec{r}_1, \vec{r}_2) = \varphi_{\vec{k}_i}(\vec{r})\Phi_i^{(\pm)}(\vec{r}_1, \vec{r}_2) \quad (4)$$

$$\Psi_f^{(\pm)}(\vec{r}, \vec{r}_1, \vec{r}_2) = \varphi_{\vec{k}_f}(\vec{r})\left[\Phi_f^{(\pm)}(\vec{r}_1, \vec{r}_2) - S^{(\pm)}\Phi_i^{(\pm)}(\vec{r}_1, \vec{r}_2)\right] \quad (5)$$

Here $\varphi_{\vec{k}_i} = e^{i\vec{k}_i\vec{r}}/(2\pi)^{3/2}$ and $\varphi_{\vec{k}_f} = e^{i\vec{k}_f\vec{r}}/(2\pi)^{3/2}$ are the plane waves describing the incident and scattered electrons, respectively, $\Phi_i^{(\pm)}(\vec{r}_1, \vec{r}_2)$ is the wavefunction of the bound electrons in the target, $\Phi_f^{(\pm)}$ is the wavefunction of the ejected electrons and $S^{(\pm)} = \langle \Phi_i^{(\pm)} | \Phi_f^{(\pm)} \rangle$ is the overlap integral, which provides the orthogonalization of the double-continuum wavefunction $\Phi_f^{(\pm)}$ with respect to the target wavefunction $\Phi_i^{(\pm)}$.

The bound state wavefunctions $\Phi_i^{(+)}(\vec{r}_1, \vec{r}_2)$ and $\Phi_i^{(-)}(\vec{r}_1, \vec{r}_2)$ representing the initial target states and describing the metastable singlet state 2^1S and the metastable triplet state 2^3S , respectively, are chosen in the form:

$$\Phi_i^{(\pm)}(\vec{r}_1, \vec{r}_2) = C_i^{(\pm)}\left[e^{-\alpha r_1}e^{-\beta r_2}(1-\gamma r_2) \pm e^{-\alpha r_2}e^{-\beta r_1}(1-\gamma r_1)\right] \quad (6)$$

Here $C_i^{(\pm)}$ is a normalization constant; α, β, γ are the variational parameters, which have been calculated following the procedure suggested by Hylleraas and Undheim [14]. For the 2^1S and 2^3S metastable states of He, Li⁺, Be²⁺, B³⁺ and C⁴⁺ the obtained values of α, β, γ parameters together with the corresponding DI energies are presented in Table 1.

Table 1. Variational parameters and DI energies for 2^1S and 2^3S metastable and 1^1S ground states of He, Li^+ , Be^{2+} , B^{3+} and C^{4+}

		α	β	γ	I_{theor}	I_{exp}
He ($Z=2$)	2^1S	1.997	0.558	0.682	2.1429	2.1460
	2^3S	2.003	0.633	1.429	2.1742	2.1752
	1^1S	2.214	1.442	-0.396	2.8762	2.9036
Li^+ ($Z=3$)	2^1S	2.985	1.061	1.192	5.0347	5.0408
	2^3S	3.005	1.142	1.881	5.1094	5.1104
	1^1S	3.332	2.399	-0.454	7.2492	7.2798
Be^{2+} ($Z=4$)	2^1S	3.977	1.566	1.698	9.1768	9.1842
	2^3S	4.006	1.645	2.370	9.2956	9.2965
	1^1S	4.429	3.351	-0.492	13.6233	13.6560
B^{3+} ($Z=5$)	2^1S	4.971	2.070	2.203	14.5691	14.5777
	2^3S	5.007	2.146	2.866	14.7322	14.7350
	1^1S	5.515	4.305	-0.524	21.9978	22.0325
C^{4+} ($Z=6$)	2^1S	5.967	2.573	2.705	21.2117	21.2211
	2^3S	6.007	2.647	3.364	21.4128	21.4203
	1^1S	6.591	5.260	-0.549	32.3725	32.4089

The wavefunction $\Phi_f^{(\pm)}$ describing the ejected electrons in the final state is taken in the following form:

$$\Phi_f^{(\pm)}(\vec{r}_1, \vec{r}_2) = \frac{1}{\sqrt{2}} \left[f_{k_1}^{(\pm)}(\vec{r}_1) f_{k_2}^{(\pm)}(\vec{r}_2) \pm f_{k_1}^{(\pm)}(\vec{r}_2) f_{k_2}^{(\pm)}(\vec{r}_1) \right], \quad (7)$$

where $f_{\vec{k}}(\vec{r})$ is the Coulomb continuum wavefunction normalized to a delta function in momentum space,

Substituting wavefunctions of the initial and final states (4-7) into (2) and performing the integration over \vec{r}_1, \vec{r}_2 the matrix element can be written as

$$T_{fi}^{(\pm)} = \frac{C_i^{(\pm)}}{\sqrt{2\pi^2 q^2}} \left\{ T_{\alpha}^{(0)}(\vec{k}_1) \left[J_{\beta}^{(0)}(k_2) - \gamma J_{\beta}^{(1)}(k_2) \right] \pm \right.$$

$$\pm \left[I_{\beta}^{(0)}(\vec{k}_1) - \gamma I_{\beta}^{(1)}(\vec{k}_1) \right] J_{\alpha}^{(0)}(k_2) \} \pm \vec{k}_1 \Leftrightarrow \vec{k}_2, \quad (8)$$

where

$$I_{\mu}^{(n)}(\vec{k}_j) = \int f_{\vec{k}_j}^*(\vec{r}) \left(e^{i\vec{q}\vec{r}} - \frac{1}{2} G^{(\pm)} \right) e^{-i\mu r} r^n d\vec{r} = \\ = \frac{1}{(2\pi)^{3/2}} \Gamma(1 - iZ/k_j) e^{\pi Z/2k_j} A_{\mu}^{(n)}(\vec{k}_j) \quad (9)$$

$$J_{\nu}^{(n)}(k_j) = \int f_{\vec{k}_j}^*(\vec{r}) e^{-i\nu r} r^n d\vec{r} = \frac{1}{(2\pi)^{3/2}} \Gamma(1 - iZ/k_j) e^{\pi Z/2k_j} B_{\nu}^{(n)}(\vec{k}_j)$$

$$G^{(\pm)} = \int \Phi_i^{(\pm)*}(\vec{r}_1, \vec{r}_2) (e^{i\vec{q}\vec{r}_1} + e^{i\vec{q}\vec{r}_2}) \Phi_i^{(\pm)}(\vec{r}_1, \vec{r}_2) d\vec{r}_1 d\vec{r}_2$$

and $\vec{q} = \vec{k}_i - \vec{k}_s$ is the momentum transfer. The explicit expressions for $A_{\mu}^{(n)}(\vec{k}_j), B_{\nu}^{(n)}(\vec{k}_j)$ ($n = 0, 1$) and $G^{(\pm)}, C_i^{(\pm)}$ are given in appendix.

Formula (8) shows that, when only radial correlation between target electrons is taken into account, the matrix element $T_{ii}^{(\pm)}$ may be represented as a sum of four terms, each of them being the product of two factors $I_{\mu}(\vec{k}_j)$ and $J_{\nu}(k_j)$. Here $I_{\mu}(\vec{k}_j)$ describes the direct ejection of a bound electron by the incident electron and $J_{\nu}(k_j)$ describes ionization of the second target electron due to the sudden change in potential. Now substituting (8) into (1) and taking into consideration (9) we obtain for the 8DCS corresponding to DI of helium-like ions in the 2^1S and 2^3S metastable states

$$\frac{d^8\sigma^{(\pm)}}{d\Omega_3 d\Omega_1 d\Omega_2 d(k_1^2/2) d(k_2^2/2)} =$$

$$(8) \quad = \frac{Z^2 [C_i^{(\pm)}]^2 N(k_1, k_2) k_z}{2\pi^4 q^4 k_i} \left[M_I^{(\pm)} + M_{II}^{(\pm)} + M_{int}^{(\pm)} \right], \quad (10)$$

where

$$N(k_1, k_2) = \left[\left(1 - e^{-2\pi Z/k_1} \right) \left(1 - e^{-2\pi Z/k_2} \right) \right]^{-1} \quad (11)$$

$$M_I^{(\pm)} = \left| A_\alpha^{(0)}(\bar{k}_1) \right|^2 \left(B_\beta^{(0)}(k_2) - \gamma B_\beta^{(1)}(k_2) \right)^2 \pm \text{Re} \left[A_\alpha^{(0)}(\bar{k}_1) A_\alpha^{(0)*}(\bar{k}_2) \right] \times \\ \times \left(B_\beta^{(0)}(k_1) - \gamma B_\beta^{(1)}(k_1) \right) \left(B_\beta^{(0)}(k_2) - \gamma B_\beta^{(1)}(k_2) \right) + \bar{k}_1 \leftrightarrow \bar{k}_2$$

$$M_{II}^{(\pm)} = \left| A_\beta^{(0)}(\bar{k}_1) - \gamma A_\beta^{(1)}(\bar{k}_1) \right|^2 \left(B_\alpha^{(0)}(k_2) \right)^2 \pm \\ \pm \text{Re} \left[\left(A_\beta^{(0)}(\bar{k}_1) - \gamma A_\beta^{(1)}(\bar{k}_1) \right) \left(A_\beta^{(0)}(\bar{k}_2) - \gamma A_\beta^{(1)}(\bar{k}_2) \right)^* \right] \times \\ \times B_\alpha^{(0)}(k_1) B_\alpha^{(0)}(k_2) + \bar{k}_1 \leftrightarrow \bar{k}_2 \quad (12)$$

$$M_{int}^{(\pm)} = 2 \text{Re} \left[A_\alpha^{(0)}(\bar{k}_1) \left(A_\beta^{(0)}(\bar{k}_2) - \gamma A_\beta^{(1)}(\bar{k}_2) \right)^* \right] \times \\ \times B_\alpha^{(0)}(k_1) \left(B_\beta^{(0)}(k_2) - \gamma B_\beta^{(1)}(k_2) \right) \pm \\ \pm 2 \text{Re} \left[A_\alpha^{(0)}(\bar{k}_1) \left(A_\beta^{(0)}(\bar{k}_1) - \gamma A_\beta^{(1)}(\bar{k}_1) \right)^* \right] \times \\ \times B_\alpha^{(0)}(k_2) \left(B_\beta^{(0)}(k_2) - \gamma B_\beta^{(1)}(k_2) \right) + \bar{k}_1 \leftrightarrow \bar{k}_2$$

In (10) the first term corresponds to direct ejection of an electron from inner-shell (1s) and the subsequent ejection of outer-shell (2s) electron due to the sudden change in potential (process I). The second term corresponds to direct ejection of an electron from outer-shell (2s) followed by ejection of the electron from inner-shell (1s) (process II). The third term in (10) describes the interference between these two processes.

The total DI cross section can be obtained by integrating the 8DCS over the solid angles $\Omega_1, \Omega_2, \Omega_3$ and the ejection energies $\varepsilon_1 = k_1^2/2$ and $\varepsilon_2 = k_2^2/2$

$$\sigma^{(\pm)}(E_i) = \frac{Z^2 [C_i^{(\pm)}]^2}{2\pi^4 k_i} \int_0^{\varepsilon_{1\max}} \int_0^{\varepsilon_{2\max}} N(k_1 k_2) k_3 \times \\ \times \iiint [M_i^{(\pm)} + M_{II}^{(\pm)} + M_{int}^{(\pm)}] d\Omega_1 d\Omega_2 \frac{d\Omega_3}{q^4} d\varepsilon_1 d\varepsilon_2 \quad (13)$$

Here $\varepsilon_{1\max} = (E_i - I^{(\pm)})/2$ and $\varepsilon_{2\max} = (E_i - I^{(\pm)})/2 - \varepsilon_1$, where $E_i = k_i^2/2$ and $I^{(\pm)}$ is the DI potential of electrons in helium-like ions. About the choice of the upper limits of integration in (full curves) see comment in [11].

3. RESULTS AND DISCUSSION

Using formulae (11-13) we have calculated the total DI cross section for two-electron atomic systems from He ($Z = 2$) to C^{4+} ($Z = 6$) being in the 2^1S and 2^3S metastable states. The calculations have been carried out for incident energies extending up to a maximum 150 times the DI threshold. The results for He, Li^+ and C^{4+} are presented in Figures 1, 2 and 3 (full curves).

Before analysing the obtained cross section let us estimate the contributions of process I and process II to double-electron ejection. From the explicit expressions for the matrix elements (formulae {A1} and {A2} in appendix) it is clear that

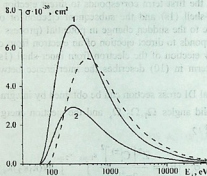


Fig.1. The total cross sections for DI of helium atoms by electrons. Curves 1 and 2 correspond to 2^1S and 2^3S metastable states, respectively. The dashed curve corresponds to the ground state.

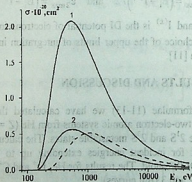


Fig.2. The total cross sections for DI of Li^+ ions by electrons. Curves 1 and 2 correspond to 2^1S and 2^3S metastable states, respectively. The dashed curve corresponds to the ground state.

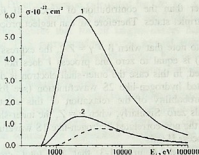


Fig.3. The total cross sections for DI of C^{4+} ions by electrons. Curves 1 and 2 correspond to 2^1S and 2^3S metastable states, respectively. The dashed curve corresponds to the ground state.

$$B_{\alpha}^{(0)}(k_j) \sim (Z - \alpha) \quad (14)$$

$$B_{\beta}^{(0)}(k_j) - \gamma B_{\beta}^{(1)}(k_j) \sim \left\{ \frac{Z - \beta - \gamma}{Z - \beta} + 2\gamma \frac{(Z - 2\beta)}{\beta^2 + k_j^2} \right\} \quad (15)$$

It means that after direct ejection of one of the bound electron the probability of a second ionization is proportional to $(Z - \alpha)^2$ for the inner-shell electron and to the square of expression in curly brackets in (15) for the outer-shell electron. Taking into consideration that $\alpha \cong Z$ (see Table 1) one can easily determine that the probability of relaxation to continuum is much less for the inner-shell electron than for the outer-shell one. This fact allows us to draw the conclusion that though direct ejection is more probable for the outer-shell electron than for the inner-shell one, nevertheless process I plays dominant role. The numerical calculations confirm this conclusion. For instance, in the case of He the contribution of process I is nearly three order of

magnitude larger than the contribution of process II for both the singlet and the triplet states. Therefore we can neglect process II in the further analysis.

It is worth to note that when $\beta = \gamma = Z/2$, the expression in curly brackets in (15) is equal to zero and process I does not occur as it should be. Indeed, in this case the outer-shell electron is described by the non-correlated hydrogen-like 2S wavefunction (see formula (6)), therefore the probability of the relaxation of this electron to the continuum equals zero. Similarly, when $\alpha = Z$, the inner-shell electron is described by the non-correlated hydrogen-like 1S wavefunction and, accordingly, process II fails.

It is clear from Figures 1-3 that the total cross section corresponding to the singlet state is larger in magnitude than the TCS corresponding to the triplet state. The difference between the maximum values of TCS increases from 2.5 for He to 4.5 for C^{4+} . Because the values of α parameters for the singlet and triplet states are close the probabilities of direct ejection of the inner-shell electron are almost the same for the both states. It means that the difference between the TCS is completely determined by the difference between the probabilities of relaxation of the outer-shell electron to the continuum. The latter is less for the triplet states than for the singlet state. This statement can be easily shown by analyzing the expression in curly brackets in (15). Indeed, in (15) the second term is of the order of one for the both states. As for the first term it is of the order of one for the singlet state, while owing to the closeness of the sum $\beta + \gamma$ to Z (see Table 1) it is very small for the triplet state.

The method suggested by Hylleraas and Undheim [14] allows us to calculate simultaneously the wavefunction of the 1^1S ground state and the wavefunction of the 2^1S metastable states. (The lowest root of the equation for energy gives the variational parameters for the ground state, while the next root corresponds to the metastable state.) Results obtained for α , β , γ and DI energies are presented in Table 1 for He, Li^+ , C^{4+} . As it can be seen in Table 1 parameter γ is negative for all the targets being in the ground state. Accordingly the relevant wavefunctions are nodeless as it should be. We emphasize that such a procedure for constructing the wavefunctions ensures the mutual orthogonality of the wavefunctions corresponding to the ground and 2^1S metastable states.



The total DI cross section calculated for He, Li⁺, C⁴⁺ being in the ground state are also shown in Figures 1,2 and 3 (dashed curves). It is clear from the figures that for all targets except helium maximum values of the TCS corresponding to the ground state are less than those corresponding to the metastable states. For helium the ground state maximum is between the two maxima corresponding to the singlet and triplet metastable states.

Recently the total DI cross section has been measured for C⁴⁺ ions in the keV energy region [7]. The experiment has been carried out at an electron-ion crossed-beam set-up using an electron-cyclotron-resonance ion source. An appreciable fraction of the ion beam was found to be in the 2³S metastable state (about 8%) owing to the small lifetime of the 2¹S metastable state.

Assuming that the population of the ground state and of the 2³S metastable state are 0.92 and 0.08, respectively, and using the calculated values for the cross sections corresponding to each component in the ion beam we obtain for the apparent cross section $\sigma_{app} = 0.6 \times 10^{-23} \text{cm}^2$ at 1000 eV incident electron energy. The experimentally measured value at that energy is $\sigma_{app} = 2.6 \times 10^{-23} \text{cm}^2$. Taking in the view that the region of validity of the first Born approximation is far away from the above mentioned energy (which only a little exceeds the DI potential for the ground state) one can conclude that there is satisfactory agreement between theory and experiment.

Thus, in order to check the reliability of results obtained in the present study it is necessary to carry out the systematic measurements of total DI cross sections for helium-like ions in the medium and especially in the high energy region.

ACKNOWLEDGMENTS

The authors would like to thank Professor L. Kurdadze for fruitful discussion.

APPENDIX

The explicit analytical expressions for $B_{\mu}^{(n)}(k_j)$ and $A_{\mu}^{(n)}(\bar{k}_j)$ ($n = 0, 1$) are

$$B_{\mu}^{(0)}(k_j) = -8\pi \frac{Z - v}{(\mu^2 + k_j^2)^2} e^{\frac{Z}{k_j} \arctg \frac{2\mu k_j}{\mu^2 - k_j^2}}, \quad (\text{A.1})$$

$$B_{\mu}^{(1)}(k_j) = \left[\frac{1}{Z - \mu} - \frac{2(Z - 2\mu)}{\mu^2 + k_j^2} \right] B_{\mu}^{(0)}(k_j), \quad (\text{A.2})$$

$$A_{\mu}^{(n)}(\bar{k}_j) = \left[\frac{a_{\mu}(q, k_j)}{(\mu^2 + q^2 + k_j^2 - 2qk_j x_j)^2} d_{\mu}^{(n)}(x_j) - \frac{1}{2} G^{(\pm)}(q) B_{\mu}^{(n)}(k_j) + i \left[\frac{a_{\mu}(q, k_j)}{(\mu^2 + q^2 + k_j^2 - 2qk_j x_j)^2} h_{\mu}^{(n)}(x_j) \right] \right] \quad (\text{A.3})$$

In the formulae given above $x_j = \cos \vartheta_j$, where ϑ_j is the angle between \bar{q} and the wavevector \bar{k}_j .

The functions $a_{\mu}(q, k_j)$, and $d_{\mu}^{(n)}(x_j)$, $h_{\mu}^{(n)}(x_j)$ in (A.3) are determined as follows:

$$a_{\mu}(q, k_j) = -\frac{8\pi}{\left[\mu^2 + (q + k_j)^2 \right] \left[\mu^2 + (q - k_j)^2 \right]} e^{\frac{Z}{k_j} \arctg \frac{2\mu k_j}{\mu^2 + q^2 - k_j^2}}, \quad (\text{A.4})$$

$$d_{\mu}^{(0)}(x_j) = \left[(\mu^2 + q^2 - k_j^2) w_{\mu}^{(1)}(x_j) - 4\mu^2 k_j w_{\mu}^{(2)}(x_j) \right] \cos \chi_{\mu}(x_j) -$$

$$-2\mu \left[(\mu^2 + q^2 - k_j^2) w_\mu^{(2)}(x_j) + k_j w_\mu^{(1)}(x_j) \right] \sin \chi_\mu(x_j), \quad (\text{A.5})$$

$$h_\mu^{(0)}(x_j) = \left[(\mu^2 + q^2 - k_j^2) w_\mu^{(1)}(x_j) - 4\mu^2 k_j w_\mu^{(2)}(x_j) \right] \sin \chi_\mu(x_j) + \\ + 2\mu \left[(\mu^2 + q^2 - k_j^2) w_\mu^{(2)}(x_j) + k_j w_\mu^{(1)}(x_j) \right] \cos \chi_\mu(x_j), \quad (\text{A.6})$$

where

$$w_\mu^{(1)}(x_j) = 2Zqk_j x_j - q^2(Z + \mu) + (Z - \mu)(\mu^2 - k_j^2),$$

$$w_\mu^{(2)}(x_j) = Zq x_j - (Z - \mu)k_j,$$

$$\chi_\mu(x_j) = \frac{Z}{k_j} \ln \frac{\mu^2 + q^2 + k_j^2 - 2qk_j x_j}{\sqrt{(\mu^2 + q^2 - k_j^2)^2 + (2\mu k_j)^2}},$$

and

$$d_\mu^{(1)}(x_j) = \left[\frac{2Z(q^2 - k_j^2 - \mu^2) + 4\mu(\mu^2 + q^2 + k_j^2)}{(\mu^2 + (q + k_j)^2)(\mu^2 + (q - k_j)^2)} + \right.$$

$$\left. + \frac{4\mu}{\mu^2 + q^2 + k_j^2 - 2qk_j x_j} \right] d_\mu^{(0)}(x_j) +$$

$$+ \frac{2\mu Z}{k_j} \left[\frac{1}{\mu^2 + q^2 + k_j^2 - 2qk_j x_j} - \frac{\mu^2 + q^2 + k_j^2}{(\mu^2 + (q + k_j)^2)(\mu^2 + (q - k_j)^2)} \right] \times$$

$$\times h_{\mu}^{(0)}(x_j) + Q_{\mu}(x_j) \sin \chi_{\mu}(x_j) - R_{\mu}(x_j) \cos \chi_{\mu}(x_j), \quad (\text{A.7})$$

$$h_{\mu}^{(0)}(x_j) = \left[\frac{2Z(q^2 - k_j^2 - \mu^2) + 4\mu(\mu^2 + q^2 + k_j^2)}{(\mu^2 + (q + k_j)^2)(\mu^2 + (q - k_j)^2)} + \frac{4\mu}{\mu^2 + q^2 + k_j^2 - 2qk_jx_j} \right] h_{\mu}^{(0)}(x_j) - \frac{2\mu Z}{k_j} \times$$

$$\times \left[\frac{1}{\mu^2 + q^2 + k_j^2 - 2qk_jx_j} - \frac{\mu^2 + q^2 + k_j^2}{(\mu^2 + (q + k_j)^2)(\mu^2 + (q - k_j)^2)} \right] d_{\mu}^{(0)}(x_j)$$

$$- R_{\mu}(x_j) \sin \chi_{\mu}(x_j) - Q_{\mu}(x_j) \cos \chi_{\mu}(x_j), \quad (\text{A.8})$$

$$Q_{\mu}(x_j) = 2Zqx_j(3\mu^2 + q^2 + k_j^2) - 4Zk_jq^2,$$

$$R_{\mu}(x_j) = -4Zq\mu k_j x_j + 4\mu Z(\mu^2 + k_j^2) - 4\mu^2(\mu^2 + k_j^2 + q^2) -$$

$$-(\mu^2 + (q + k_j)^2)(\mu^2 + (q - k_j)^2). \quad (\text{A.9})$$

The expressions for $C_i^{(\pm)}$ and $G^{(\pm)}$ are:

$$C_i^{(\pm)} = \frac{1}{4\pi} \left[\frac{\beta^2 - 3\gamma\beta + 3\gamma^2}{8\alpha^3\beta^5} \pm \frac{8(\alpha + \beta - 3\gamma)^2}{(\alpha + \beta)^8} \right]^{\frac{1}{2}} \quad (\text{A.10})$$

$$\begin{aligned}
 G^{(\pm)}(q) = & 32\pi^2 (C_i^{(\pm)})^2 \left\{ \frac{\alpha(\beta^2 - 3\gamma\beta + 3\gamma^2)}{\beta^5(4\alpha^2 + q^2)^2} + \right. \\
 & + \frac{1}{\alpha^3(4\beta^2 + q^2)^2} \left[\beta - \frac{\gamma(12\beta^2 - q^2)}{4\beta^2 + q^2} + \frac{12\beta\gamma^2(4\beta^2 - q^2)}{(4\beta^2 + q^2)^2} \right] \pm \\
 & \left. \pm \frac{8(\alpha + \beta - 3\gamma)}{(\alpha + \beta)^4((\alpha + \beta)^2 + q^2)^2} \left[\alpha + \beta - \frac{2\gamma(3(\alpha + \beta)^2 - q^2)}{(\alpha + \beta)^2 + q^2} \right] \right\} \quad (A.11)
 \end{aligned}$$

REFERENCES

1. K. Dolder. In: Atomic Processes in Electron-Ion and Ion-Ion Collisions. 1986.
2. M. B. Shah, D. S. Elliott, P. McCallion, H. B. Gilbody. *J. Phys. B: At. Mol. Phys.* **21**, 1988, 2751.
3. M. Zamkov, M. Benis, P. Richard, H. Tawara, T. J. M. Zouros. 2001 Proc. 22th Int. Conf. on Photonic, Electronic and Atomic Collisions (Santa Fe, 18-24 July 2001) ed: S. Datz, M.E. Bannister, H. F. Krause, L. H. Saddiq, D. Schultz, C. R. Vane. Abstracts of contributed papers, 356.
4. A. Müller, C. Boehme, J. Jacobi, H. Knopp, S. Schippers. 2001a Proc. 22th Int. Conf. on Photonic, Electronic and Atomic Collisions (Santa Fe, 18-24 July 2001) ed: S. Datz, M.E. Bannister, H. F. Krause, L. H. Saddiq, D. Schultz, C. R. Vane. Abstracts of contributed papers, 322.
5. S. Rachafi, M. Zambra, Hui Zhang, M. Duponchelle, J. Jureta, P. Defrance. *Physica Scripta*, **28**, 1989, 12.
6. Y. Attaourti, P. Defrance, A. Makhoute, C. J. Joachain. *Physica Scripta*, **43**, 1991, 578.
7. A. Müller, C. Boehme, J. Jacobi, H. Knopp, K. Ariki, S. Schippers. 2001b Proc. 22th Int. Conf. on Photonic, Electronic and Atomic Collisions (Santa Fe, 18-24 July 2001) ed: S. Datz, M.E. Bannister, H. F. Krause, L. H. Saddiq, D. Schultz, C. R. Vane. Abstracts of contributed papers, 321.

8. A. J. Dixon, M. F. A. Harrison, A. C. H. Smith. J. Phys. B: At.Mol. Phys. 9, 1976, 2617.
9. E. Brook, M. F. A. Harrison, A. C. H. Smith. J. Phys. B: At.Mol. Phys. 17, 1978, 3115.
10. P. Defrance, T. M. Kereselidze, Z. S. Machavariani, J.V. Mebonia. J. Phys. B: At.Mol.Opt. Phys. 32, 1999, 2227.
11. P. Defrance, T. M. Kereselidze, Z. S. Machavariani, I. L. Noselidze. J. Phys. B: At.Mol.Opt. Phys. 33, 2000, 4323
12. P. Defrance, T. M. Kereselidze, Z. S. Machavariani, I. L. Noselidze. J. Phys. B: At.Mol.Opt. Phys. 34, 2001, 4957.
13. K. Muktavat, M. K. Srivastava. Pramana J. Phys. 58, 2002, 39.
14. E. A. Hylleraas, B.Undheim. Zs. f. Phys. 65, 1930, 759.

**Universite' Catholique de Louvain,
De'partment de Physique,
Louvain-la-Neuve, Belgium
Tbilisi State University**

კ. ლეფრანსი, თ. კერესელიძე, ი. ნოსელიძე, მ. წულუკიძე

**მეტასტაბილურ მდგომარეობაში მყოფი პელიუმისმაგვარი
იონების ორჯერადი იონიზაცია ელექტრონებით**

დასკვნა

გამოთვლილია მეტასტაბილურ 2^1S და 2^3S მდგომარეობაში მყოფი ორელექტრონიანი ატომური სისტემების He, Li⁺, Be²⁺, B³⁺ და C⁴⁺ ორჯერადი იონიზაციის სრული განივკვეთები, რისთვისაც გამოყენებულია ე.წ. შენჯღრევის მექანიზმი. სამიზნის ტალღურ ფუნქციაში მხოლოდ რადიალური კორელაციის შესაბამისი წევრია გათვალისწინებული.

ABSTRACT. The problem of nonlinear resonance is reduced to the research of motion corresponding to the universal Hamiltonian, quantum mechanical investigation of which leads to the study of the eigenfunctions and eigenvalues of the Mathieu – Schrodinger equation. The eigenstates of the Mathieu – Schrodinger equation in the area of the classical separatrix are nondegenerate. Going out from this area by the variation of pumping amplitude both for the least and largest values of pumping amplitudes, the system passes in the area of degenerate energy terms. The degeneration occurs in the form of energy terms branching from both of the nondegenerate areas. At multiple passage through the branching points, which can be achieved by slow modulation of the pumping amplitude, the “creeping” of the system with respect to energy terms takes place. This phenomenon of “creeping” of the level population, foreordained by the presence of branching points of the energy terms, is a peculiar property of the equation of Mathieu – Schrodinger and can be considered as quantum analog of the classical stochastic layer originating near the separatrix at the classical investigation of the same problem.

§ 1. INTRODUCTION. STATEMENT OF THE PROBLEM

It is known [1], that in the approximation of moderate nonlinearity, Hamiltonian, describing the phenomenon of the nonlinear resonance can be represented in the form of universal Hamiltonian coinciding by the form to the Hamiltonian of the mathematical pendulum. The universal Hamiltonian circumscribes those small deviations of the action from its resonance value (i.e. the value of the action followed from a resonance condition), which arise in this approximation.

At the classical reviewing the motion generated by the universal Hamiltonian on the phase space, consists of two types of topologically distinguished curves divided by the separatrix [1]. In consequence of

perturbation of trajectories near to the separatrix by the periodic perturbation arises stochastic layer, i.e. the area of stochastic motion near to the separatrix. At quantum reviewing Schrodinger equation for the universal Hamiltonian is represented in the form of the equation of Mathieu, solutions of which (wave functions) are the periodic functions of Mathieu.

Many physical problems can be reduced to the solution of the equation of Mathieu. For example, in view of research the phenomenon of parametrical resonance, the analysis of the equations of Mathieu leading to the origin of zones of unstable motion [2]. At study of motion of electron in the periodic potential field, the analysis of the Schrodinger equation, which is reduced to the equation of the Mathieu, explains the presence of forbidden energy zones in semiconductors [3]. It is possible to cite other similar examples, however equation of the Mathieu-Schrodinger for the universal Hamiltonian differs from them, because in the case, considered by us, the motion is finite and, hence, energy spectrum without fail is discrete. Depending on the values of parameters of the problem, energy spectrum can become degenerate. In the present work the quantum mechanical research of the equation of the Mathieu-Schrodinger for the universal Hamiltonian will be carried out. The condition of degeneration of the energy spectrum and the reasons of their emerging will be investigated. An attempt is made to find quantum analog of the classical stochastic layer.

§ 2. UNIVERSAL HAMILTONIAN

Let us present atom as a nonlinear oscillator under the action of the variable monochromatic field. Then Hamiltonian of the system atom + field is of the following form:

$$H(x, p, t) = H_0(x, p) + H_{NL}(x) + \varepsilon V(x, t), \quad (1)$$

where $H_0 = \frac{1}{2} \left(\frac{p^2}{m} + \omega_0^2 m x^2 \right)$, $H_{NL} = \beta x^3 + \gamma x^4 + \dots$

At the classical reviewing the motion generated by the universal Hamiltonian H_0 consists of trajectories which are distinguished by the universal Hamiltonian H_0 and H_{NL} are the nonlinear terms. $V(x, t) = V_0 x \cos \Omega t$, $V_0 = \frac{e}{m} f_0$, $\varepsilon \ll 1$,

e , m are the charge and mass of the electron, x , p the coordinate and impulse of the electron, ω_0 the eigenfrequency, γ and β are the coefficients at the nonlinear terms, f_0 and Ω the amplitude and frequency of a variable field, interaction $V(x, t)$ of the electron with the variable field we shall consider as small perturbation.

Having made passage to the variables of action-angle (I, θ) with the help of transformations $x = (2I/m\omega_0)^{1/2} \cos \theta$, $p = -(2I \cdot m\omega_0)^{1/2} \times \sin \theta$, assuming that resonance condition $\dot{\theta} \approx \Omega$ is fulfilled and averaging the equation with respect of fast phase θ from the Hamiltonian (1) we get

$$H(I, \varphi, t) = H_0^{NL} + \varepsilon \cdot V(I) \cos \varphi,$$

$$H_0^{NL} = \omega_0 I + \overline{H_{NL}}, \quad \overline{H_{NL}} = \frac{3}{2} \left(\frac{I}{m\omega_0} \right)^2 \cdot \gamma, \quad (2)$$

$$V(I) = V_0 (I/2m\omega_0)^{1/2}.$$

The anharmonicity of electronic oscillation $\overline{H_{NL}}$ plays an essential role in the generation of the third harmonics in solids like isotropic crystals (Li, NaCl), and also in anisotropic ones with the birefringence (CaCO₃).

Here we have introduced the slow phase $\varphi = \theta - \Omega t$, which in time $\approx 2\pi/\Omega$ varies insignificantly. The resonance condition is fulfilled for the particular value of the action I_0 , value of which can be find from the same resonance condition

$$\dot{\varphi} \approx \omega(I_0) = 0, \quad (3)$$

where

$$\omega(I) = \left(\frac{\partial H_0^{NL}}{\partial I} \right) - \Omega.$$

Introducing the dimensionless parameter of nonlinearity [1]

$$\epsilon_1 = \left| \frac{d\omega}{dI} \right| \cdot \frac{I}{\omega}, \quad (4)$$

and expanding Hamiltonian (2) in the series with respect of small deviations of the action $\Delta I = I - I_0$, in the approximation of the moderate nonlinearity

$$\epsilon \ll \epsilon_1 \ll 1/\epsilon, \quad \Delta I/I_0 \ll 1, \quad (5)$$

we obtain Hamiltonian in the form of

$$H = \frac{\omega'}{2} (\Delta I)^2 + V \cos \varphi, \quad (6)$$

where

$$V = \epsilon \cdot V(I_0), \quad \omega' = \left. \frac{d\omega}{dI} \right|_{I=I_0}$$

Hamiltonian (6), called universal, as it is easy to note, is similar to the Hamiltonian of the pendulum with "mass" $1/\omega'$ in the "gravity" field with acceleration of gravity $g \sim V$. If in (6) ΔI is substituted by the appropriate operator $\Delta I \rightarrow -i\hbar \partial / \partial \varphi$, one can obtain the universal Hamiltonian in the quantum form

$$H = -\frac{\hbar^2 \omega'}{2} \frac{\partial^2}{\partial \varphi^2} + V \cos \varphi. \quad (7)$$

With the help of (7) it is possible to explore quantum properties of motion for the nonlinear resonance in the quasi-classical area ($I_0 \gg \hbar$).

§ 3. SYMMETRIES OF THE EQUATIONS OF MATHIEU-SCHRODINGER

(*) Having written the stationary Schrodinger equations

$$\hat{H} \psi_n = E_n \psi_n, \quad (8)$$

for the Hamiltonian (7), we get

$$\frac{\partial^2 \psi_n}{\partial \varphi^2} + (E_n - V(I, \varphi)) \cdot \psi_n = 0, \quad (9)$$

$$V(l, \varphi) = l \cos 2\varphi,$$

where the dimensionless quantities are introduced

$$E_n \rightarrow \frac{8E_n}{\hbar^2 \omega'}, \quad l \rightarrow \frac{8V}{\hbar^2 \omega'} \quad (10)$$

and the replacement $\varphi \rightarrow 2\varphi$ is done.

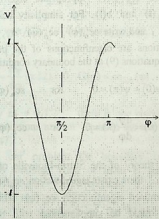


Fig.1. The dependence of the energy of interaction V from the phase φ

The interaction has the following properties of the symmetry:

1. $V(\varphi) = V(-\varphi)$, 2. $V(\varphi) = V(\pi + \varphi)$, 3. $V\left(\frac{\pi}{2} + \varphi\right) = V\left(\frac{\pi}{2} - \varphi\right)$.

G.M.Zaslavsky and G.P.Berman [4] were the first who considered the equation of the Mathieu-Schrodinger for the quantum description of the nonlinear resonance in the approximation of moderate nonlinearity. They studied the case of quasiclassical approximation

$\Delta I \gg \hbar$ for both variables I_0 and ΔI . In this work we shall not apply quasiclassical approximation with respect to ΔI . We investigate the equation of the Mathieu - Schrodinger in essentially quantum area.

We content ourselves with only even and odd solutions with respect to φ of equation of the Mathieu - Schrodinger (9). Those solutions have n zeroes in the interval $0 \leq \varphi \leq \pi$. Eigenfunctions ψ_n can be recorded with the help of the Mathieu functions [4]: even $ce_n(\varphi, l)$ and odd $se_n(\varphi, l)$. Appropriate eigenvalues are usually designated by $a_n(l)$ and $b(l)$. For simplicity below sometimes we omit the argument l and write $ce_n(\varphi)$, $se_n(\varphi)$, a_n , b_n .

Mathieu functions are eigenfunctions of the problem of Sturm-Liouville for the equations (9) at the boundary conditions

$$\begin{aligned} \psi(0) = \psi(\pi) = 0 & \quad \text{for} \quad se_n(\varphi), \\ \frac{d\psi}{d\varphi}(0) = \frac{d\psi}{d\varphi}(\pi) = 0 & \quad \text{for} \quad ce_n(\varphi). \end{aligned} \quad (11)$$

From the general theory of the Sturm-Liouville it follows, that for arbitrary $n=1,2, \dots$ there exists eigenfunction $se_n(\varphi)$ and for each $n=0,1,2, \dots$ determined eigenfunction $ce_n(\varphi)$. The definition of the Mathieu function must be supplemented with the choice of the arbitrary constant so that the conditions were fulfilled:

$$\begin{aligned} ce_n(0, l) > 0, \quad \frac{1}{\pi} \int_0^{2\pi} ce_n^2(\varphi, l) d\varphi = 1, \\ \frac{dse_n}{d\varphi}(0, l) > 0, \quad \frac{1}{\pi} \int_0^{2\pi} se_n^2(\varphi, l) d\varphi = 1. \end{aligned} \quad (12)$$

If $\psi(\varphi) = G(\varphi)$ means either $ce_n(\varphi)$, or $se_n(\varphi)$, then $G(\varphi)$ and $G(\pi - \varphi)$ satisfy the same equation (9) and the same boundary conditions (11). Therefore these functions differ from each other only

by the constants. Hence, $G(\varphi)$ is even or odd function with respect to $\pi/2 - \varphi$. Taking this into account, two functions (11) break up into four Mathieu functions:

$$\psi(0) = \psi(\pi/2) = 0, \quad G(\varphi) = se_{2m+2}(\varphi), \quad \text{phase } \pi,$$

$$\psi(0) = \frac{d\psi}{d\varphi}(\pi/2) = 0, \quad G(\varphi) = se_{2m+1}(\varphi), \quad \text{phase } 2\pi, \quad (13)$$

$$\frac{d\psi}{d\varphi}(0) = \psi(\pi/2) = 0, \quad G(\varphi) = ce_{2m+1}(\varphi), \quad \text{phase } 2\pi,$$

$$\frac{d\psi}{d\varphi}(0) = \frac{d\psi}{d\varphi}(\pi/2) = 0, \quad G(\varphi) = ce_{2m}(\varphi), \quad \text{phase } \pi.$$

For arbitrary $m = 0, 1, 2, \dots$ there is one eigenfunction for each of four boundary conditions and m equal to the number of zeroes in the interval $0 < \varphi < \pi/2$.

In case of our problem the boundary conditions (13) are predetermined by nothing; each of them is feasible in the equal measure. The functions (13) represent a complete system of eigenfunctions of the equation (9).

The properties of symmetry of the Mathieu function can be presented in Table 1 [5].

Let us remark, that as $\cos 2\varphi$ is the invariant concerning all of the four transformations of the Table 1, the interaction $V(l, \varphi)$, entering in the equation of Mathieu-Schrodinger (9) is a scalar value in configurational space of the Mathieu function.

By immediate check it is easy to convince, that four elements of transformation

$$\begin{aligned} G(\varphi \rightarrow -\varphi) &= a, & G(\varphi \rightarrow \pi - \varphi) &= b, \\ G(\varphi \rightarrow \pi + \varphi) &= c, & G(\varphi \rightarrow \varphi) &= e, \end{aligned}$$

Table 1. Relations of a symmetry for the Mathieu function

$G(\varphi)$	$G(-\varphi)$	$G(\pi - \varphi)$	$G(\pi + \varphi)$
$ce_{2m}(\varphi)$	$ce_{2m}(\varphi)$	$ce_{2m}(\varphi)$	$ce_{2m}(\varphi)$
$ce_{2m+1}(\varphi)$	$ce_{2m+1}(\varphi)$	$-ce_{2m+1}(\varphi)$	$-ce_{2m+1}(\varphi)$
$se_{2m+1}(\varphi)$	$-se_{2m+1}(\varphi)$	$se_{2m+1}(\varphi)$	$-se_{2m+1}(\varphi)$
$se_{2m+2}(\varphi)$	$-se_{2m+2}(\varphi)$	$-se_{2m+2}(\varphi)$	$se_{2m+2}(\varphi)$

are forming a group. For this it is enough to test the realization of the following relations:

$$a^2 = b^2 = c^2 = e,$$

$$ab = c, \quad ac = b, \quad bc = a. \quad (14)$$

The group contains three elements a, b, c , of the second order and unity element e . The group G is isomorphic to the well-known group of the Klein [6]. This group is known in the group theory by the applications to the quantum mechanics (designated as V). All the elements of the group commute. This assertion can be easily checked taking into account group operations (14). So, the symmetry group of the Mathieu function G is the Abelian group and consequently has only one-dimensional indecomposable representations. This last statement can be examined in the other way. If in the base of four functions (13) with the help of Table 1 we construct the representation for the four elements of the symmetry group G , such four-dimensional representation will be reducible and break up on four one-dimensional representations. It will be a direct sum of the four one-dimensional representations. Each of three elements a, b, c in combination with unit e forms a subgroup

$$G \begin{cases} \supset G_+ : e, b \\ \supset G_- : e, c \\ \supset G_0 : e, a \end{cases} \quad (15)$$



Each of subgroups G_0, G_+, G_- is the invariant subgroup in-group G . The characters of representation of quadruple group (and also its subgroups) are well investigated and we do not reduce them.

The presence of the symmetry in a group, describing the considered problem of only one-dimensional representations means the absence of degeneration in the energy spectrum. So, we conclude, that the eigenvalues of the equation of the Mathieu - Schrodinger (9) are nondegenerated, and the eigenfunctions are the Mathieu functions (13). However we shall remind, that both the energy terms a_n, b_n , and the Mathieu functions depend on the parameter l . At the variation of l in the system can appear symmetry higher, than assigned in Table 1, that might lead to the degeneration of levels.

§ 4. DEGENERATE CONDITION OF THE EQUATION OF THE MATHIEU - SCHRODINGER

The condition $E_n \approx 1$ at the classical reviewing of motion of the mathematical pendulum corresponds to the case, when the initial kinetic energy of the pendulum is close to the maximum potential, i.e. to the condition of motion near to the separatrix. Therefore it is possible to announce, that the results of the previous paragraph (absence of degeneration and determination of eigenfunctions) concern to the appointed restricted area (sizes of which will be established below) from two sides of the separatrix $E = 1$, on the phase plane with the coordinates E and l . In this paragraph we shall try to find out what happens outside of this area in case of small and big values of l .

(01) *a) Degeneration of states at small l (area from the left of the separatrix line)*

In the limit $l \rightarrow 0$ the equation of the Mathieu - Schrodinger (9) takes the form:

$$\frac{d^2 \psi_n}{d\varphi^2} + E_n \psi_n = 0 \tag{16}$$

The orthonormalized system of solutions of the equation (16) consists of even and odd solutions

$$\psi_g = \cos n\varphi, \quad \psi_u = \sin n\varphi. \quad (17)$$

They both correspond to the one eigenvalue of the energy $E_n = n^2$. Let us remark, that the functions (17) are in correspondence with the well-known limiting values ($l \rightarrow 0$) of Mathieu functions [8]:

$$cc_n(\varphi) \rightarrow \cos n\varphi, \quad se_n(\varphi) \rightarrow \sin n\varphi, \quad (18)$$

i.e. at $l=0$ double degeneration of the levels $E_n = n^2$ takes place. This means, that at the diminution of l the approximation of the energy terms with the identical n takes place and for $l=0$ they are merged together. It is necessary to find out that this confluence happens in the point $l=0$ or earlier at $l \neq 0$. By that we shall establish the boundaries of the variation of the parameter l , where energy spectrum is nondegenerated.

Let us find out, how the eigenfunctions of the degenerated states corresponding to the level $E_n = n^2$ look like. The functions (17) for this purpose are unsuitable as they form base of reduced representation of the symmetry group of the equation (16). Really, the equation (16) is the Schrodinger equation for free rotation in the phase plane φ . The receptivity symmetry group is named as a symmetry group of two-dimensional rotations $O^*(2)$. The group $O^*(2)$ is continuous and Abelian [6] with the infinitesimal operator

$$J = \frac{\partial}{\partial \varphi}. \quad (19)$$

In the base of functions (17) operators J forms two-dimensional representation

$$e \rightarrow \begin{vmatrix} 1 & 0 \\ 0 & 1 \end{vmatrix}, \quad J \rightarrow \frac{1}{n} \begin{vmatrix} 0 & 1 \\ -1 & 0 \end{vmatrix}. \quad (20)$$

As the Abelian group can have only one-dimensional indecomposable representations, the two-dimensional representation (20) is reducible. To surmount this problem we shall recollect, that the eigenfunctions for degenerate condition can be also complex.

Usually, as base of the nondecomposable representation of the group $O^*(2)$ complex functions are taken [6]

$$\psi_n(\varphi) = e^{-in\varphi} \quad (21)$$

In this base the operator J forms one-dimensional representation. However, it is necessary to take into account that due to the symmetry with respect to the change of sign of time in the quantum mechanics complex conjugate wave functions correspond to one energy eigenvalue. Therefore two complex conjugate representations $\psi_n(\varphi)$ and $\psi_n^*(\varphi)$ should be considered together, as one representation with doubled dimension [6,7]. So in degenerate area in view of conditions of normalization (see (12)), for eigenfunctions it is necessary to take complex conjugate functions

$$\psi_n(\varphi) = \frac{\sqrt{2}}{2} e^{-in\varphi}, \quad \psi_n^*(\varphi) = \frac{\sqrt{2}}{2} e^{in\varphi} \quad (22)$$

Let us remark, that the infinitesimal operator of the axial symmetry group J (19) forms a transformation group, which is isomorphic to the subgroup G_- (15). The element of the symmetry $c = G(\varphi \rightarrow \pi + \varphi)$ of the subgroup G_- provides recurrence of the phase variation after each period and consequently the symmetry G_- characterizes the condition of motion similar to the classical rotary motion.

So, at $l=0$ we are having double degenerate state with the wave functions (22). Let us find out, if the perturbation

$$V(l, \varphi) = l \cos 2\varphi, \quad l \ll 1 \quad (23)$$

can take off the existing degeneration.

It is known, first order terms of the perturbation theory for the energy eigenvalues and the exact functions of zero approximation for double degenerate levels look like [7]

$$E_{0\pm}^{(1)} = \frac{1}{2} \left[(V_{11} + V_{22}) \pm \sqrt{(V_{11} + V_{22})^2 + 4 \cdot |V_{12}|^2} \right],$$

$$\psi_n^{\pm} = \psi^{(0)} = C_1 \cdot \psi_1^0 + C_2 \cdot \psi_2^0,$$

$$C_1^{(0)} = \left\{ \frac{V_{12}}{2|V_{12}|} \left[1 \pm \frac{V_{11} - V_{22}}{\sqrt{(V_{11} - V_{22})^2 + 4|V_{12}|^2}} \right] \right\}^{1/2}, \quad (24)$$

$$C_2^{(0)} = \pm \left\{ \frac{V_{21}}{2|V_{12}|} \left[1 \mp \frac{V_{11} - V_{22}}{\sqrt{(V_{11} - V_{22})^2 + 4|V_{12}|^2}} \right] \right\}^{1/2},$$

where the index in brackets corresponds to the order of the perturbation theory, matrix elements of the perturbation (23) V_{ik} ($i, k=1, 2$) are calculated by using of functions (22) of the degenerate state of the nonperturbed Hamiltonian. Taking into account expressions (22) we shall calculate the matrix elements:

$$V_{11} = \int_0^{\pi} \psi_n^*(\varphi) \cdot \psi_n(\varphi) \cdot \cos 2\varphi d\varphi = 0, \quad V_{22} = 0$$

$$V_{12} = \int_0^{\pi} \psi_n^2(\varphi) \cdot \cos 2\varphi d\varphi = \begin{cases} 0 & \text{if } n \neq 1 \\ \frac{l\pi}{4} & \text{if } (n=1) \end{cases}$$

After substitution of those matrix elements in the expressions (24) for the eigenvalues and exact eigenfunctions we shall obtain:

$$E_{\pm}^{(1)} = \pm \frac{l\pi}{4}, \quad \Psi_{n=1}^{+} = \cos \varphi, \quad \Psi_{n=1}^{-} = -i \sin \varphi. \quad (25)$$

Thus, the exact wave functions (25) of the nondegenerate state only for $n = 1$ coincide with the Mathieu function in the limit ($l \rightarrow 0$) (18). It is possible to expect, in the state $n \neq 1$ the degeneration disappears at $l \neq 0$, where the eigenfunctions of the nondegenerate states are expressed by the functions of Mathieu. For example, for wave functions with odd n , with increasing l function (22) takes the form

$$\Psi_{+}^{2m+1} = \Psi_n(l, \varphi) = \frac{\sqrt{2}}{2} (cc_n \varphi + isc_n \varphi)$$

$$\Psi_{-}^{2m+1} = \Psi_n^{*}(l, \varphi) = \frac{\sqrt{2}}{2} (cc_n \varphi - isc_n \varphi) \quad n \neq 1, \quad l \neq 0 \quad (26)$$

The singularity of the problem solved by us is that the Hamiltonian (7) and therefore eigenvalues and the eigenfunctions depend on the parameter l . This dependence leads to the degeneration of the energy levels for some values of the parameter l while for other values of l energy levels are not degenerated. From well-known problems of the quantum mechanics similar dependence from the parameter arises for example at the research of electronic terms of diatomic molecules, where the role of the parameter plays a distance between the kernels of the atoms [7].

Let us assume, that at $l = l_n$ the removal of degeneration for the n -th energy term happens. Then, accordingly on the left and right from l_n the equation of the Mathieu-Schrodinger (8-10) is possible to rewrite as

$$\hat{H}(l_{-}^n) \psi = E(l_{-}^n) \psi \quad l_{-}^n \leq l^n,$$

$$\hat{H}(l_{+}^n) \psi = E(l_{+}^n) \psi \quad l_{+}^n \geq l^n, \quad (27)$$

$$\left| l_{+}^n - l_{-}^n \right| = \delta l_n.$$

As H depends on l continuously, then in immediate proximity to the point l_n it is possible to write (9)

$$\hat{H}(l_n^+) \approx \hat{H}(l_n^-) + \frac{\partial \hat{H}}{\partial l_n} \delta l_n, \quad (28)$$

where with account of (9)

$$\frac{\partial \hat{H}}{\partial l_n} \delta l_n = -\delta l_n \cos 2\varphi. \quad (29)$$

Substituting in (28) $\hat{H}(l_+) \rightarrow \hat{H}$ and $\hat{H}(l_-) \rightarrow \hat{H}_0$, the Hamiltonian in nearby of the point $l = l_n$ we shall present in the form of

$$H = H_0 + V(\delta l, \varphi), \quad (30)$$

where

$$H_0 = \frac{\partial^2}{\partial \varphi^2} - l_0 \cos 2\varphi, \quad (31)$$

$$V(\delta l, \varphi) = -\delta l \cos 2\varphi, \quad \delta l > 0 \quad (32)$$

Let us ascertain if the degenerate states situated to the left of l_n , correspond to the accidental degenerate conditions. Let us remind, that usual removal of the degeneration is connected to the lowering of the Hamiltonian symmetry caused by the perturbation, while in case of casual degeneration the total Hamiltonian and the perturbation have the identical symmetry [6]. On the first sight the nonperturbed Hamiltonian (31) and perturbation (32) have the identical dependence from the phase φ and, hence, have the identical symmetry. However, as a matter of fact it is not so. The special role of the point l_n is that on the right from l_n the system is characterized by the wave functions with the quadruple symmetry of the group G (Table 1) while on the left - by the symmetry of subgroup G_- .

Making transformation for the odd wave functions $n \rightarrow 2m + 1$ and for the even wave functions $n \rightarrow 2m$ (see (11)-(13)) for the odd matrix elements we get:

$$V_{\pm\mp}^{2m+1} = \frac{1}{\pi} \int_0^{\pi} \Psi_{\pm}^{2m+1} V(\delta l, \varphi) (\Psi_{\mp}^{2m+1})^* d\varphi =$$

$$= \frac{\delta l}{\pi} \int_0^{\pi} (cc_{2m+1}^2 - se_{2m+1}^2 \pm i2ce_{2m+1} \cdot se_{2m+1}) \cos 2\varphi d\varphi, \quad (33)$$

$$V_{\pm\pm}^{2m+1} = \frac{1}{\pi} \int_0^{\pi} \Psi_{\pm}^{2m+1} V(\delta l, \varphi) (\Psi_{\pm}^{2m+1})^* d\varphi =$$

$$= \frac{\delta l}{\pi} \int_0^{\pi} (ce_{2m+1}^2 + se_{2m+1}^2) \cos 2\varphi d\varphi. \quad (34)$$

Here for the brevity of Mathieu function we write without argument φ . Moreover as the Mathieu functions for the small δl as a result of continually depending from the parameter l changes slightly (see Fig.2) at the calculation of matrix elements we neglect this dependence.

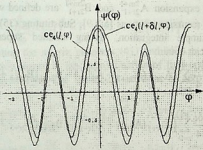


Fig.2. Plots of the Mathieu function $cc_4(1 + \delta l, \varphi)$ $cc_4(l, \varphi)$, at values of parameters near the point of branching $l = 2$, $\delta l = 1$ plotted by the use of numerical methods. It is obvious that small variation of the parameter l leads to the small variation of the Mathieu functions.



Let us remark the matrix elements (33), (34) refer to the same indecomposable representations (superscripts of wave functions are identical). The perturbation $V(\delta l, \varphi)$, as was already mentioned, is scalar in space of these wave functions. The group theory gives a simple method for the determination of selection rules for the matrix elements [6,7]. Not to go into details, we want to accentuate, according to this method, for scalar value only matrix elements for the transition between states of identical type are distinct from zero [7] (i.e. referring to the same indecomposable representation). Thus, matrix elements can be distinct from zero and we shall initiate with their calculation.

Let us take advantage of expansion formulas in the Fourier series for Mathieu functions [5].

$$ce_{2m+1} = \sum_{r=0}^{\infty} A_{2r+1}^{2m+1} \cos(2r+1)\varphi, \quad (35)$$

$$se_{2m+1} = \sum_{r=0}^{\infty} B_{2r+1}^{2m+1} \sin(2r+1)\varphi. \quad (36)$$

The factors of expansion A_{2r+1}^{2m+1} and B_{2r+1}^{2m+1} are defined with the help of well-known recursion relations [5,8,9]. Substituting (35) in (33) and (34), after simple integration, having omitted superscripts for simplicity one can obtain:

$$V_{+-} = V_{-+} = \frac{\delta l}{4} \sum_{r=0}^{\infty} \{A_{2r+1}(A_{2r+3} + A_{2r-1}) - B_{2r+1}(B_{2r+3} + B_{2r-1})\}, \quad (37)$$

$$V_{++} = V_{--} = \frac{\delta l}{4} \sum_{r=0}^{\infty} \{A_{2r+1}(A_{2r+3} + A_{2r-1}) + B_{2r+1}(B_{2r+3} + B_{2r-1})\}. \quad (38)$$

These expressions can be simplified with the help of the recursion relations [5] for A_{2r+1}

$$2[a_{2m+1} - (2r+1)^2]A_{2r+1}^{2m+1} - l_{-}^{2m+1}(A_{2r-1}^{2m+1} + A_{2r+3}^{2m+1}) = 0, \quad (39)$$

$$2[b_{2m+1} - (2r+1)^2]B_{2r+1}^{2m+1} - l_{-}^{2m+1}(B_{2r-1}^{2m+1} + B_{2r+3}^{2m+1}) = 0, \quad (40)$$

where $a_{2m+1} = a_{2m+1}(l)$ and $b_{2m+1} = b_{2m+1}(l)$ are energy terms (Mathieu characteristics [8]) in nondegenerate area for the states ce_{2m+1} and se_{2m+1} accordingly. In degenerate area the terms a_{2m+1} and b_{2m+1} converge together. Determining from the (39), (40) $A_{2r-1} + A_{2r+3}$ and $B_{2r+1} + B_{2r+3}$ and substituting in the (37), (38) we obtain

$$V_{++}^{2m+1} = V_{--}^{2m+1} = \frac{\delta l}{l_{-}^{2m+1}} \left[\frac{a_{2m+1} + b_{2m+1}}{2} - \frac{1}{2} (\bar{A}^{2m+1} + \bar{B}^{2m+1}) \right], \quad (41)$$

$$V_{-+}^{2m+1} = V_{+-}^{2m+1} = \frac{\delta l}{l_{-}^{2m+1}} \left[\frac{a_{2m+1} - b_{2m+1}}{2} - \frac{1}{2} (\bar{A}^{2m+1} - \bar{B}^{2m+1}) \right], \quad (42)$$

where

$$\bar{A}^{2m+1} = \sum_{r=0}^{\infty} (2r+1)^2 [A_{2r+1}^{2m+1}], \quad \bar{B}^{2m+1} = \sum_{r=0}^{\infty} (2r+1)^2 [B_{2r+1}^{2m+1}].$$

For the deriving of the formulas (41) and (42) we used the relations [5,8]

$$\sum_{r=0}^{\infty} [A_{2r+1}^{2m+1}]^2 = 1 \quad \text{and} \quad \sum_{r=0}^{\infty} [B_{2r+1}^{2m+1}]^2 = 1.$$

Substituting the matrix elements (41) and (42) in the expressions of perturbation theory in the approximation of first order with respect to energy eigenvalues and for exact functions of zero approximation (24) we get

$$E_{+}^{2m+1} = \frac{\delta l}{l_{-}^{2m+1}} \left[a_{2m+1}(l_{-}^{2m+1}) - \bar{A}^{2m+1}(l_{-}^{2m+1}) \right],$$

$$E_{-}^{2m+1} = \frac{\delta l}{l_{-}^{2m+1}} \left[b_{2m+1}(l_{-}^{2m+1}) - \bar{B}^{2m+1}(l_{-}^{2m+1}) \right], \quad (43)$$

$$\psi_{+}^{2m+1}(l_{-}^{2m+1}, \varphi) = ce_{2m+1}(l_{-}^{2m+1}, \varphi),$$

$$\psi_{-}^{2m+1}(l_{-}^{2m+1}, \varphi) = se_{2m+1}(l_{-}^{2m+1}, \varphi), \quad (44)$$

where l_{-}^{2m+1} is the value of l at which the removal of degeneration with $2m+1$ -th term happens in the area on the left from the line of the separatrix. Therefore in this point it is possible to write

$$E^{2m+1}(l_-^{2m+1}) = a_{2m+1}(l_-^{2m+1}) = b_{2m+1}(l_-^{2m+1}). \quad (45)$$

The second part of this relation to all intents and purposes is the equation for the definition of l_-^{2m+1} . However, analytical solution of this relation is not possible to derive and therefore for determination of l_-^{2m+1} might be realized only using numerical methods (see Table 2). The exact functions of the zero order (44) within insignificant phase multiplier coincide with the appropriate pair of wave functions (13) from the states of nondegenerate area. So in points l_-^{2m+1} the wave functions of the degenerate states turn into the wave functions of the nondegenerate states. Similarly it is possible to calculate the matrix elements for even states $V_{\pm\pm}^{2m}$ and $V_{\pm\mp}^{2m}$, taking into account expansion formulas of functions $ce_{2m}(l, \varphi)$ and $se_{2m}(l, \varphi)$, in the Fourier series [5,8] and also by use of the similar to (39), (40) relations of recursion. Omitting mathematical details of these calculations, we present final results for approximation of first order with respect to energy eigenvalues and for exact wave functions of zero approximation:

$$\begin{aligned} E_+^{2m} &= \frac{\delta l}{l_-^{2m}} \left[a_{2m}(l_-^{2m}) - \bar{A}^{2m}(l_-^{2m}) \right], \\ E_-^{2m} &= \frac{\delta l}{l_-^{2m}} \left[b_{2m}(l_-^{2m}) - \bar{B}^{2m}(l_-^{2m}) \right], \end{aligned} \quad (46)$$

$$\begin{aligned} \psi_+^{2m}(l_-^{2m}, \varphi) &= ce_{2m}(l_-^{2m}, \varphi), \\ \psi_-^{2m}(l_-^{2m}, \varphi) &= ise_{2m}(l_-^{2m}, \varphi). \end{aligned} \quad (47)$$

The points of a branching l_-^{2m} of energy terms are obtained (using numerical methods, see Table 2) with the help of equations

$$a_{2m}(l_-^{2m}) = b_{2m}(l_-^{2m}). \quad (48)$$

Table 2. Results of numerical calculations for the coordinates of left branching points

n	Left points of branching	
	l^{2n+2} (48)	l^{2n+1} (45)
0	0.30	0
1	2.0	1.2
2	8.0	4.5
3	28.0	13.0

Exact wave functions of the zero order (47), in case of disdain non-stationary phase factor coincide with the appropriate pair of functions from (13), describing the nondegenerate state. In other words, in the point l^{2m} the removal of degeneration happens. On the basis of the obtained results it is possible to present a qualitative picture of the variation of energy terms on the plane (E, l) in left-hand area from the line of the separatrix (Fig.3).

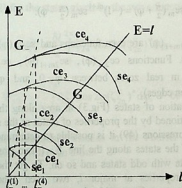


Fig.3. Energy levels as function of parameter l on the plane (E, l) in left-hand area from the line of the separatrix. The points of the branching of curves represent the boundaries between degenerate and nondegenerate states.

Similar picture is usually obtained when investigating stability areas in the parametrical resonance [2].

At the end of this paragraph we shall remark that degenerate state, located at the left of separatrix line, can be considered, as analog of classical rotary motion.

b) Degenerate state at major l . The area on the right of the separatrix line.

With magnification of l the particle can be thrilled in deep "hole" of the potential energy ($V = l \cos 2\varphi$, $0 < \varphi < \pi$ a Fig.1), making oscillatory motion. Properties of wave functions of quantum oscillator near to the bottom of the hole are well known. This is even and odd wave functions relative to the center of the hole $\pi/2$ of and presence of zeros in wave functions. With the help of the third column of Table I it is possible to write symmetry conditions close to $\pi/2$:

$$\begin{aligned} ce_m\left(\frac{\pi}{2} + \varphi\right) &= (-1)^m ce_m\left(\frac{\pi}{2} - \varphi\right), \\ se_m\left(\frac{\pi}{2} + \varphi\right) &= (-1)^{m+1} se_m\left(\frac{\pi}{2} - \varphi\right). \end{aligned} \quad (49)$$

i.e. $ce_{2m}(\varphi)$, $se_{2m+1}(\varphi)$ are even functions and $se_{2m}(\varphi)$, $ce_{2m+1}(\varphi)$ are odd functions. Functions $ce_{2m}(\varphi)$, $se_{2m+1}(\varphi)$, $ce_{2m+1}(\varphi)$ and $se_{2m+2}(\varphi)$ have m real zeros between $\varphi=0$ and $\varphi=\pi/2$ (not considering zeros on edges).

Existing alternation of states (Fig.3) in area along the line of the separatrix is conditioned by the properties of states at the small l . With the help of the expressions (49) it is possible to determine easily, that in the spectrum of the states along the line $E=l$ two (instead of one) even states alternate with odd states and so on. To get the alternation, caused now by properties at major l , two even conditions must degenerate in one even and two odd - in one odd. So we come to the conclusion, that two levels with wave functions $ce_{2m}(\varphi)$ and $se_{2m+1}(\varphi)$ coming nearer amalgamate in one level, and the following two levels --- $ce_{2m+1}(\varphi)$ and $se_{2m+2}(\varphi)$ also in one level. The levels

obtained in this way will be doubly degenerated. The reasons of it are the same as at the research of the similar problem for the states to the left of the separatrix. Not iterating this reasoning, we shall write complex wave functions corresponding to the degenerated condition in the form:

$$\xi_{2n}^{\pm}(\varphi) = ce_{2n}(\varphi) \pm ise_{2n+1}(\varphi) \quad \text{even state,}$$

$$\zeta_{2n+1}^{\pm}(\varphi) = ce_{2n+1}(\varphi) \pm ise_{2n+2}(\varphi) \quad \text{odd state} \quad (50)$$

In the base of complex wave functions ξ_{2n}^{\pm} and ζ_{2n+1}^{\pm} the representation of the subgroup G , (15), consisting from the elements e and b is realized. Evenness of the wave functions ξ and ζ with respect to the transformation $b = G(\varphi \rightarrow \pi - \varphi)$ of the subgroups G , characterizes an important property of wave functions evenness of the quantum oscillatory process.

Let us set about with the calculation of the matrix elements of interaction (32) for the states given by the wave functions (50):

$$W_{\pm\mp}^{2n} = \frac{\delta l}{\pi} \int_0^{2\pi} \xi_{2n}^{\pm} \cos 2\varphi (\zeta_{2n}^{\mp})^* d\varphi \quad (51)$$

and

$$W_{\pm\pm}^{2n} = \frac{\delta l}{\pi} \int_0^{2\pi} \xi_{2n}^{\pm} \cos 2\varphi (\zeta_{2n}^{\mp})^* d\varphi, \quad \delta l < 0. \quad (52)$$

Let us use expansion formulas in the Fourier series [5] for the Mathieu functions with even index

$$ce_{2m} = \sum_{r=0}^{\infty} A_{2r}^{2m} \cos 2r\varphi, \quad (53)$$

$$se_{2m} = \sum_{r=0}^{\infty} B_{2r}^{2m} \sin 2r\varphi,$$

and by recurrence relations

$$(E - 4r^2)A_{2r} - \delta l(A_{2r-2} + A_{2r+2}) = 0$$

$$E = a_{2m}(l) \quad r = 2, 3, \dots \quad (54)$$

and

$$(E - (2r+2)^2)B_{2r} - \delta l(B_{2r} + B_{2r+4}) = 0$$

$$E = b_{2m+2}(l) \quad r = 1, 2, \dots$$

After simple calculations similar to those in the previous section, we shall get:

$$W_{++}^{2m} = W_{--}^{2m} = \frac{1}{2}(a_{2m} + b_{2m}) - \frac{1}{2}(A_0^2 + \tilde{A}^{2m} + \tilde{B}^{2m}), \quad (55)$$

$$W_{+-}^{2m} = W_{-+}^{2m} = \frac{1}{2}(a_{2m} - b_{2m}) - \frac{1}{2}(A_0^2 + \tilde{A}^{2m} + \tilde{B}^{2m}), \quad (56)$$

where

$$\tilde{A}^{2m} = \sum_{r=1}^{\infty} (2r)^2 [A_{2r}^{2m}]^2, \quad \tilde{B}^{2m} = \sum_{r=0}^{\infty} (2r)^2 [B_{2r}^{2m}]^2 \quad (57)$$

For deriving the formulas (55,56) we have used the relations [5,8]:

$$2[A_0]^2 + \sum_{r=1}^{\infty} [A_{2r}]^2 = 1 \quad \text{and} \quad \sum_{r=0}^{\infty} [B_{2r+1}]^2 = 1. \quad (58)$$

Substituting the matrix elements (55) and (56) in the formulas of the secular perturbation theory for the first order terms of the energy eigenvalues and for exact functions of the zero approximation (24) we shall obtain:

$$E_+^{2m} = \frac{\delta l}{l_+^{2m}} \left[a_{2m}(l_+^{2m}) - A_0^2 - \bar{A}^{2m} \right], \quad (59)$$

$$E_-^{2m+1} = \frac{\delta l}{l_+^{2m}} \left[b_{2m+1}(l_+^{2m}) - \bar{B}^{2m+1} \right]$$

$$\psi_1^{(0)} = c e_{2m}(\varphi), \quad \psi_2^{(0)} = i \cdot s e_{2m+1}. \quad (60)$$

From expressions (59) and (60) follows, that going from the right to the left, in the direction of diminution of l , in points $l = l_+^{2m}$ and $l = l_+^{2m+1}$ the removal of degeneration for the levels a_{2m} b_{2m+1} takes place. For determination of the points l_+^{2m} and l_+^{2m+1} we have to solve the equations

$$a_{2m}(l_+^{2m}) = b_{2m+1}(l_+^{2m}), \quad a_{2m+1}(l_+^{2m+1}) = b_{2m+2}(l_+^{2m+1}) \quad (61)$$

This equation can be solved only using numerical method (Table 3).

Table 3. Results of numerical calculations for the coordinates of right branching points

n	Right points of branching	
	l_+^{2n}	l_+^{2n+1}
1	15.0	17.5
2	25.0	32
3	41	51

The similar calculations can be easily done for the odd states (50) ξ_{\pm}^n . As follows from these calculations, at particular values l the degeneration is removed. The results, obtained in this section, are plotted in Fig.4

The Figures 3 and 4 supplement each other: in the field of intersection with the separatrix the curves of the Figures 3 and 4 are

smoothly joined. As a result we get well known diagrams of Mathieu-characteristics [8,9] obtained earlier also with the use of numerical method.

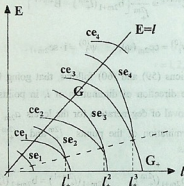


Fig.4. Energy levels as a function of the parameter l on the plane (E, l) to the area right from the separatrix line. The points of branching of curves represent degeneration points of terms in this area.

So, let us summarize the results obtained in this paragraph. The equation of the Mathieu-Shrodinger has an appointed symmetry. The transformations of the symmetry of the Mathieu functions form the group G , which is isomorphic to the quaternary group of Klein. To this symmetry on a plane (E, l) corresponds appointed area along the line of the separatrix $E = l$, containing nondegenerate energy terms. This area is restricted double-sided by the areas of degenerate states. The area of degenerate states is the quantum mechanical analogs of two forms of motion of the classical mathematical pendulum - rotary and oscillatory. Comparing results of quantum reviewing with classical we remark, that these two conditions of motion at quantum reviewing are divided by the area of a finite measure, whereas at the classical reviewing - measure of the separatrix is equal to zero.

In branching points of energy terms the modification of the system's symmetry happens. The area of the nondegenerate states is characterized by the symmetry of quaternary group of Klein G , whereas the areas of the degenerate states are characterized by the symmetries of the subgroups G_2 and G_4 correspondingly.

§ 5. INTEGRALS OF MOTION. AVERAGE VALUES OF SOME OBSERVABLE QUANTITIES

Let us find out the complete set of physical quantities for our system. For this purpose it is necessary to rewrite all transformations, which commute with the Hamiltonian (7). As we already have established (see Table.1), these elements of symmetry form quaternary group of the Klein. In this paragraph each element of this group is compared the appropriate quantum mechanical operators producing these transformations. So, the element of group a is the operator of inversion \hat{I}_0 , ($\hat{I}_0\psi(\varphi) = \psi(-\varphi)$), which commutes with the Hamiltonian \hat{H} (7)

$$\hat{H}\hat{I}_0 - \hat{I}_0\hat{H} = 0, \quad (62)$$

The eigenfunction of the Hamiltonian $\psi(\varphi)$ is also eigenfunction for the operator of the inversion \hat{I}_0

$$\hat{I}_0\psi(\varphi) = I_0\psi(\varphi) \quad (63)$$

Acting once again on the (63) by means of operator \hat{I}_0 one can obtain $\hat{I}_0^2\psi(\varphi) = I_0^2\psi(\varphi) = \psi(\varphi)$. From here follows, that eigenvalues of the operator of inversion are $I_0 = \pm 1$. Thus, the eigenfunctions are having the fixed evenness, which remains invariable in time. The element b of the Klein symmetry group, also commuting with the Hamiltonian, is the operator of inversion relative to the center of the hole (Fig.1) - $I_{\pi/2}$. It is possible to show similarly, that the relevant eigenvalues of the operator are $I_{\pi/2} = \pm 1$.



The element c of the Klain symmetry group, commuting with the Hamiltonian, is the operator of translation \hat{T}_π with respect to the phase on the distance π . The eigenvalues of the operator of translation \hat{T}_π are $T_\pi = \pm 1$.

In the area of nondegenerate states designated in the Fig.3 and 4 by means of G, all four operators component which form the gang: the energy \hat{H} , inversion \hat{I}_0 , inversion concerning to the center of the hole $\hat{I}_{\pi/2}$ and translation with respect to the phase \hat{T}_π are having the same eigenfunctions. For example, to the eigenstate $ce_{2n+1}(l)$ corresponds to the energy term $a_{2n+1}(\varphi)$, $I_0 = 1$, $I_{\pi/2} = -1$, $T_\pi = -1$. We reduce the Table 4 of quantum numbers for eigenfunctions for the nondegenerate states.

Table 4. Table of energy terms and quantum numbers for the eigenfunctions of nondegenerate states ($l > 0$).

	E_0	I_0	$I_{\pi/2}$	T_π
$ce_{2m}(l, \varphi)$	$a_{2m}(l)$	1	1	1
$ce_{2m+1}(l, \varphi)$	$a_{2m+1}(l)$	1	-1	-1
$sc_{2m+1}(l, \varphi)$	$b_{2m+1}(l)$	-1	1	-1
$sc_{2m+2}(l, \varphi)$	$b_{2m+2}(l)$	-1	-1	1

In degenerated area designated by the G_- in Fig.2, where the states are characterized by wave functions ψ_{2m}^\pm and ψ_{2m+1}^\pm (25), operators of symmetry produce transformations

$$\begin{aligned} \hat{I}_0 \psi_{2m}^\pm &= \psi_{2m}^\mp, & \hat{I}_0 \psi_{2m+1}^\pm &= \psi_{2m+1}^\mp, \\ \hat{I}_{\pi/2} \psi_{2m}^\pm &= \psi_{2m}^\mp, & \hat{I}_{\pi/2} \psi_{2m+1}^\pm &= -\psi_{2m+1}^\mp, \end{aligned} \quad (64)$$

$$\hat{T}_\pi \psi_{2m}^\pm = \psi_{2m}^\pm, \quad \hat{T}_\pi \psi_{2m+1}^\pm = -\psi_{2m+1}^\pm. \quad (65)$$

According to the relations (64), the wave functions ψ_{2m}^{\pm} and ψ_{2m+1}^{\pm} are not eigenfunctions for the inversion operators \hat{I}_0 and $\hat{I}_{\pi/2}$, but are eigenfunctions for the (65) operator of translation \hat{T}_{π} .

This result is easy for understanding because, degenerate area G_- corresponds to the rotary motion. Since the rotary motion is valid for the sufficient high energies $E > L > l$, properties of the symmetry (Fig.1), defining the properties of the system at the inversion, are unessential. In this area translation symmetry leading to the infinite motion, i.e. periodic recurrence plays essential role.

As follows from relations (65) two states ψ_{2m}^{\pm} , degenerated with respect to the energy, correspond to the same eigenvalues of the operator \hat{T}_{π} . It means, state ψ_{2m}^{\pm} degenerate with respect to the energy, simultaneously are degenerated with respect to the transition symmetry. The same can be said for the states with odd index ψ_{2m+1}^{\pm} .

From relations (64), (65) follows, that at transition from area G in area G_- the destruction of two integrals of motion (\hat{I}_0 and $\hat{I}_{\pi/2}$ (64)) happens, thus maintaining others two - energy and \hat{T}_{π} (65).

In degenerate area G_+ (Fig.3), in which the states are characterized by wave functions ξ_n^{\pm} and ζ_n^{\pm} (50), the operators of the symmetry produce transformations

$$\hat{I}_0 \xi_{2m}^{\pm} = \xi_{2m}^{\mp}, \quad \hat{I}_0 \zeta_{2m+1}^{\pm} = \zeta_{2m+1}^{\mp}, \quad (66)$$

$$\hat{T}_{\pi} \xi_{2m}^{\pm} = \xi_{2m}^{\mp}, \quad \hat{T}_{\pi} \zeta_{2m+1}^{\mp} = -\zeta_{2m+1}^{\mp},$$

$$\hat{I}_{\pi/2} \xi_{2m}^{\pm} = \xi_{2m}^{\pm}, \quad \hat{I}_{\pi/2} \zeta_{2m}^{\pm} = -\zeta_{2m}^{\pm}. \quad (67)$$

In compliance with relations (67) for the two states ξ_{2m}^{\pm} , degenerate with respect to the energy, correspond the same eigenvalues of the operator $\hat{I}_{\pi/2}$. Therefore states ξ_{2m}^{\pm} degenerated with respect to the

energy simultaneously are degenerated with respect to the operation of inversion concerning the center of the hole. The same must be said with regard to other pair of states - ζ_{2m+1}^{\pm} .

From relations (66) and (67) also follows, that at transition from the area G into the area G_+ the destruction of two integrals of motion (\hat{I}_0 and \hat{T}_π (66)) happens, maintaining thus other two - energy and $\hat{I}_{\pi/2}$ (67). Similar relations for ζ_n^{\pm} for brevity we shall not write out. It can be checked, that everything mentioned for the wave functions ξ_n^{\pm} is valid also for the functions ζ_n^{\pm} .

It is clear from relations (66), that the wave functions ζ_n^{\pm} are not eigenfunctions for the operators \hat{I}_0 and \hat{T}_π . The functions ξ_n^{\pm} are the eigenfunctions for the operator of inversion with respect of symmetry axis of the potential well - $\hat{T}_{\pi/2}$ (Fig. 1.). This result can be understood by assuming that the degenerate area G_+ ($E < l_+ < l$), corresponds to the oscillatory motion made by the particle captured in the potential well. Because the action of operators \hat{I}_0 and \hat{T}_π transfers the particle to the other "potential wells" (i.e. hinders the capture in one of the holes), properties of the system determined by them in the case of oscillatory motion will be inessential. The main role in the area G_+ takes the symmetry relatively to the center of the hole $\hat{I}_{\pi/2}$, describing evenness of the oscillatory states.

Let us proceed to the computation of some important physical quantities characterizing system. Our interest will be fixed on the computation of the average value of the action variation ΔI and its square $(\Delta I)^2$ -

$$\langle \Delta \hat{I} \rangle = -i \frac{\hbar}{2} \langle \psi \left| \frac{\partial}{\partial \varphi} \right| \psi \rangle, \quad \langle (\Delta \hat{I})^2 \rangle = -\frac{\hbar^2}{4} \langle \psi \left| \frac{\partial}{\partial \varphi^2} \right| \psi \rangle, \quad (68)$$

where

$$\langle \psi | \hat{A} | \psi \rangle = \frac{1}{\pi} \int_0^{2\pi} \psi(\varphi) A \psi^*(\varphi) d\varphi.$$

The averaged values calculated with the help of different wave functions of the system, in different areas of the plane (E, l), naturally will be different. Let us begin from the case of the free rotation ($l = 0$). With the help of the wave functions (21) we shall obtain

$$\langle \Psi_{1,2} \left| \frac{\partial}{\partial \varphi} \right| \Psi_{1,2} \rangle = \pm i \cdot n. \quad (69)$$

Two signs in (69) correspond to rotation in two opposite directions. The wave functions $\Psi_{1,2}$ are the eigenfunctions at the same time for the Hamiltonian (16) and for the operator $\frac{\partial}{\partial \varphi}$. Therefore for these states the eigenvalues and the average values coincide. For the computation of average values of the operator $\frac{\partial^2}{\partial \varphi^2}$ it suffices expression (69) raise to the square.

For area G_- the wave functions can be written down in the form of (26). In this area $\frac{\partial}{\partial \varphi}$ does not commute with the Hamiltonian (7) and the appropriate value is not precisely measurable. For the average value $\frac{\partial}{\partial \varphi}$ with the use of wave functions (26) and expansion formulas in the Fourier series (35), (36) we shall get:

$$\langle \Psi_{2n+1}^{\pm} \left| \frac{\partial}{\partial \varphi} \right| \Psi_{2n+1}^{\pm} \rangle = \mp i A^{2n+1} B^{2n+1}, \quad (70)$$

where

$$A^{2n+1} B^{2n+1} = \sum_{r=0}^{\infty} (2r+1) \cdot A_{2r+1} \cdot B_{2r+1}.$$

Two signs before the sum in this case correspond to different directions of rotation too. For the calculation of the average values of $\frac{\partial^2}{\partial \varphi^2}$ we shall take advantage of the energy integral with which it is possible to produce the replacement $\frac{\partial^2}{\partial \varphi^2} \rightarrow -(E_0 - l \cos 2\varphi)$. In view of it we shall get:

$$\langle \Psi_{2n+1}^{\pm} \left| \frac{\partial^2}{\partial \varphi^2} \right| \Psi_{2n+1}^{\pm} \rangle = -E_0 + V_{\pm\pm}. \quad (71)$$

Substituting in (71) results of the previous evaluations for the $V_{\pm\pm}$ (38), we shall obtain:

$$\langle \Psi_{2n+1}^{\pm} \left| \frac{\partial^2}{\partial \varphi^2} \right| \Psi_{2n+1}^{\pm} \rangle = -\frac{1}{2} [\bar{A}^{2n+1} + \bar{B}^{2n+1}]. \quad (72)$$

As was expected, the square of the average (70) does not coincide with the average of square value (72).

Let us calculate average values of quantities for the states of nondegenerate area G. With the help of wave functions (13) we obtain:

$$\langle \Psi_m \left| \frac{\partial}{\partial \varphi} \right| \Psi_m \rangle = \frac{1}{\pi} \int_0^{2\pi} \Psi_m(\varphi) \frac{\partial}{\partial \varphi} \Psi_m^*(\varphi) d\varphi = 0. \quad (73)$$

Having taken advantage of the energy integral (7) for computation of the average value of $\frac{\partial^2}{\partial \varphi^2}$ for the system in the state $\Psi_{2m+1} =$

$= se_{2m+1}(\varphi)$, we shall get:

$$\langle se_{2n+1} \left| \frac{\partial^2}{\partial \varphi^2} \right| se_{2n+1} \rangle = -E_n + \frac{l}{\pi} \int_0^{2\pi} se_{2n+1}^2 \cos 2\varphi d\varphi = -\bar{B}^{2n+1}. \quad (74)$$

And at last, with the help of the state ξ_n^\pm of the degenerated area G_+ for average values we shall obtain

$$\langle \xi_n^\pm \left| \frac{\partial}{\partial \varphi} \right| \xi_n^\pm \rangle = 0, \quad (75)$$

and

$$\begin{aligned} \langle \xi_{2n}^\pm \left| \frac{\partial^2}{\partial \varphi^2} \right| \xi_{2n}^\pm \rangle &= -E_n + \frac{l}{\pi} \int_0^{2\pi} \left[\xi_{2n}^\pm(\varphi) \right]^2 \cos 2\varphi d\varphi = \\ &= -\frac{1}{2} \left[A_0^2 + \bar{A}_{2n} + \bar{B}_{2n+1} \right] \end{aligned} \quad (76)$$

With the help of expressions (68) and the results obtained in this section (69-76), it is possible to make the table of the average values variations of the action and its square with the increase of l .

Table 5. Some average values of variation of the action and its square for the states corresponding to the different areas of the plane (E, l)

	$l \ll E_0$	$l < L < E_0$	$L < l < L_+$	$E_0 < L_+ < l$
	$l = 0$	G_-	G	G_+
$\langle \Delta \bar{l} \rangle_n$	$\mp \frac{\hbar}{2} n$	$\pm \frac{\hbar}{2} \overline{A^{2n+1} B^{2n+1}}$	0	0
$\langle \Delta \bar{l}^2 \rangle_n$	$\frac{\hbar^2}{4} n^2$	$\frac{\hbar^2}{4} \overline{\bar{A}^{2n+1} + \bar{B}^{2n+1}}$	$-\frac{\hbar^2}{4} \bar{B}^{2n+1}$	$\frac{\hbar^2}{4} \overline{A_0^2 + \bar{A}^{2n} + \bar{B}^{2n+1}}$

On the basis of Table 5 possible to infer, that deviation of the action Δl can be measured precisely only at $l=0$. Only for this column are satisfied the condition $\langle \Delta l \rangle_n^2 = \langle (\Delta l)^2 \rangle_n$. In the areas G_+ , G and G_- , $\langle \Delta l \rangle_n^2$ is the quantum mechanical average of the random value, the root-mean-square deviation from the average value

of which is determined by the $\langle (\Delta I)^2 \rangle_n$. The distribution of values is due to the fact that in these areas the system is not in the eigenstate of the operator $\Delta I \sim \partial / \partial \varphi$.

With the growth of the l the diminution of the magnitude $\langle \Delta I \rangle_n$ up to zero happens. The column G is the transitive between G_- and G_+ . In it essential in the column G_- contribution from $cc_{2m+1} \sim \bar{A}^{2n+1}$ in $\langle (\Delta I)^2 \rangle_n$ disappears, and the contribution from $cc_{2m} \sim -(A_0^2 + \bar{A}^{2n})$ in the column G_+ becomes important.

§ 6. QUANTUM ANALOG OF THE STOCHASTIC LAYER

For Hamiltonian systems making finite motion by minimum mesh of phase-space, which carries in itself the germ of the stochasticity, is the stochastic stratum generated in the neighbourhood of the separatrix under the action of arbitrary small perturbation [1]. In this paragraph we shall try to find out, what can be considered as a quantum analog of the stochastic stratum. Studying perturbed state of stationary states of the Mathieu-Schrodinger, we shall look for those quantum singularities, which occur instead of the stochastic layer at transition from the classical to the quantum reviewing.

Let us assume that pumping amplitude is modulated by the slow variable electromagnetic field. The influence of modulation is possible to take into account by means of such replacement in the equation of the Mathieu-Schrodinger (9)

$$l \rightarrow l_0 + \Delta l \cos \nu t \quad \Delta l \ll l_0. \quad (77)$$

Here Δl stands for the amplitude of modulation in dimensionless unit (see (10)), ν is the frequency of modulation. We suppose, that the slow variation of l can embrace some quantity of the branching points on the left and on the right of separatrix line (Figs.2,3)

$$\Delta l \geq \left| l_+^n - l_-^n \right|, \quad n = 1, 2, \dots, N. \quad (78)$$

As a result of replacement (77) in the Hamiltonian (7), we get

$$\hat{H} = \hat{H}_0 + \hat{H}'(t), \quad (79)$$

$$\hat{H}'(t) = \Delta l \cos 2\varphi \cos vt, \quad (80)$$

where H_0 is the universal Hamiltonian (7) and $\hat{H}'(t)$ is the perturbation appearing as a consequence of pumping modulation.

It is easy to see, that the matrix elements of perturbation (80) $\hat{H}'(t)$ for nondegenerate states equal zero. Really, having applied expansion formulas of the Mathieu functions in the Fourier series (35), (36) it is possible to show

$$\langle ce_n | \hat{H}'(t) | se_n \rangle \sim \int_0^{2\pi} ce_n(\varphi) \cos 2\varphi se_n(\varphi) d\varphi = 0 \quad (81)$$

simultaneously for the even and odd n . The expressions of the selection rules (81) will be fulfilled for values l from the area $l_-^n \leq l \leq l_+^n$

Transitions between levels cannot be conditioned by time-dependent perturbation (80). It is expedient to include perturbation in the unperturbed part of the Hamiltonian. The Hamiltonian, obtained in such way, is slowly depending on the parameter l . So, instead of (79) and (80) for the nondegenerated area G we get the Hamiltonian in the form

$$\hat{H} = -\frac{\partial^2}{\partial \varphi^2} + l(t) \cos 2\varphi, \quad (82)$$

$$l(t) = l_0 + \Delta l \cos vt. \quad (83)$$

Springs up the situation, when the system slowly "creeps" along the Mathieu-characteristics, thus enveloping, (78), branching point l_-^n and l_+^n from the left, and on the right of the separatrix line.

At the transition through the branching point from one area to the other area the wave function is not altered, however being

eigenfunction in one area, in other area it won't be eigenfunction any more. Transition probabilities of the system in the eigenstate of another area, in compliance with the common rules of the quantum mechanics are determined by coefficients of expansion of the wave function of one area over the eigenfunctions of another area.

Let us assume at the beginning that, the system was in one of the eigenstates from the nondegenerate area G , for example in the state

ce_{2n} (Fig.5a). After a quarter of the period of modulation $\frac{1}{4} \frac{2\pi}{\nu}$,

having overcome the point I^n , system will appear in the degenerated area G_- . At the same time system turns into the degenerated states ψ_{2n}^{\pm} with the equal probabilities

$$\begin{aligned}
 P(cc_{2n} \rightarrow \psi_{2n}^{\pm}) &= \left| \frac{1}{\pi} \int_0^{2\pi} ce_{2n}(\varphi) \psi_{2n}^{\pm*}(\varphi) d\varphi \right|^2 = \\
 &= \frac{1}{2\pi^2} \cdot \left| \int_0^{2\pi} ce_{2n}(\varphi) (ce_{2n}(\varphi) \pm isc_{2n}(\varphi))^* d\varphi \right|^2 = 1/2. \quad (84)
 \end{aligned}$$

When deriving (84) we used the normalization condition of (12) and orthogonality [5]

$$\int_0^{2\pi} ce_k(\varphi) se_{j+1}(\varphi) d\varphi = 0, \quad l, k = 0, 1, 2, \dots \quad (85)$$

The passage (84) contains a deep physical sense. As is known, in the quantum mechanics symmetry, with respect to the both directions of time is expressed in the invariance of the wave equation with respect to the variation of sign of time t and simultaneous replacement of ψ ψ^* . However it is necessary to remember that this symmetry concerns only the equations, but not the concept of a measurement playing fundamental role in the quantum mechanics [7,10]. "Measurement" is understood as process of interaction of the quantum system with the

classical object usually called "instrument". Let us remind, under the measuring arrangement, consisting from the analyzer and detector one must not imagine laboratorial instrument. The analyzer is presented in our problem in itself and becomes apparent at the passage through the branching point. So, the role of the analyzer in our case plays modulating field, capable to "drag" the system through the branching points. The presence of the analyzer becomes apparent because in the passage happens spectral expansion of the initial wave function belonging to the region of one symmetry over the eigenfunctions belonging to the region of another symmetry. The presence of only analyzer reserves a pure state pure, and the process remains reversible. However, further we shall assume presence of the detector, defining which of the states ψ_n^+ or ψ_n^- is involved in passage. The presence of the detector formally is expressed in averaging with respect to phase and in neglect of interference term appearing usually in expression for a distribution function. As a result the partial loss of information about the condition of the system takes place and mixed state is generated. After that the condition of the system is described by the population of energy levels.

As it follows from (84), after the quarter period degenerated rotary states ψ_{2n}^+ and ψ_{2n}^- will be occupied with the identical probability. After the half period $\frac{1}{2} \frac{2\pi}{v}$ the system again appears in the area G going through the branching point l^n in the reverse direction. At the same time there appear probabilities of the transition into the states cc_{2n} , se_{2n} and both of them are distinct from zero

$$P(\psi_{2n}^{\pm} \rightarrow cc_{2n}) = \frac{1}{2} \left| \frac{1}{\pi} \int_0^{2\pi} (cc_{2n}(\varphi) \pm ise_{2n}(\varphi)) cc_{2n}(\varphi) d\varphi \right|^2 = \frac{1}{2}, \quad (86)$$

$$P(\psi_{2n}^{\pm} \rightarrow se_{2n}) = \frac{1}{2} \left| \frac{1}{\pi} \int_0^{2\pi} (cc_{2n}(\varphi) \pm ise_{2n}(\varphi)) se_{2n}(\varphi) d\varphi \right|^2 = \frac{1}{2}. \quad (87)$$



Here we have used normalization (12) and orthogonality relations (85). It is easy to write transition probability from ce_{2n} into one of the degenerated states ψ_{2n}^{\pm} and back into ce_{2n}

$$P_{-}(ce_{2n} \leftrightarrow ce_{2n}) = P_{-}(ce_{2n} \rightarrow \psi_{2n}^{+} \rightarrow ce_{2n}) = \\ = P(ce_{2n} \rightarrow \psi_{2n}^{+})P(\psi_{2n}^{+} \rightarrow ce_{2n}) + P(ce_{2n} \rightarrow \psi_{2n}^{-})P(\psi_{2n}^{-} \rightarrow ce_{2n}) \quad (88)$$

Here the first item corresponds to the passage through the degenerated state ψ_{2n}^{+} and the second one to the passage through ψ_{2n}^{-} . It is easy to see with the help of previous computations ((84), (86), (87), that contribution of their passages are identical and separately equal 1/4. Therefore finally we have

$$P_{-}(ce_{2n} \leftrightarrow ce_{2n}) = \frac{1}{2}. \quad (89)$$

Similarly it may be shown that transition probability from the state ce_{2n} in one of the degenerated states ψ_{2n}^{\pm} and back in the area G, in state se_{2n} by means of going through the point I_{-}^{n} is

$$P_{-}(ce_{2n} \leftrightarrow se_{2n}) = P(ce_{2n} \rightarrow \psi_{2n}^{+})P(\psi_{2n}^{+} \rightarrow se_{2n}) + \\ + P(ce_{2n} \rightarrow \psi_{2n}^{-}) P(\psi_{2n}^{-} \rightarrow se_{2n}) = \frac{1}{2} \cdot \frac{1}{2} + \frac{1}{2} \cdot \frac{1}{2} = 1/2. \quad (90)$$

Thus, the system being at the initial moment in the eigenstate ce_{2n} , at the end of half-period of modulation appears in the non-eigenstate in one of the $\eta_{2n}^{\pm} = \frac{1}{\sqrt{2}}(ce_{2n} \pm se_{2n})$ (in which namely, the information is lost) and the states ce_{2n} and se_{2n} will be occupied with the identical probability.

After the expiration of quarter of cycle the system will pass from the area G (the state η^{+}) in the area G_{+} , going through the point I_{-}^{n} .

In passages from the area G_+ four states take part

$\xi_{2n}^{\pm} = \frac{1}{\sqrt{2}}(ce_{2n} \pm ise_{2n+1})$ and $\zeta_{2n-1}^{\pm} = \frac{1}{\sqrt{2}}(ce_{2n-1} \pm ise_{2n})$. So, with taking into consideration the above mentioned for the probabilities of transitions we get

$$P(\eta_{2n}^+ \rightarrow \xi_{2n}^{\pm}) = \left| \frac{1}{\pi} \int_0^{2\pi} \eta_{2n}^+(\varphi) \xi_{2n}^{\pm*}(\varphi) d\varphi \right|^2 =$$

$$= \frac{1}{4\pi} \left| \int_0^{2\pi} (ce_{2n}(\varphi) + se_{2n}(\varphi)) \cdot (ce_{2n}(\varphi) \mp ise_{2n+1}(\varphi)) d\varphi \right|^2 = \frac{1}{4}, \quad (91)$$

$$P(\eta_{2n}^+ \rightarrow \zeta_{2n}^{\pm}) =$$

$$= \frac{1}{4\pi} \left| \int_0^{2\pi} (ce_{2n}(\varphi) + se_{2n}(\varphi)) \cdot (ce_{2n-1}(\varphi) \mp ise_{2n}(\varphi)) d\varphi \right|^2 = \frac{1}{4}. \quad (92)$$

For the deriving of the last expressions in addition to the conditions of normalization we have used the conditions of orthogonality [5]:

$$\int_0^{2\pi} ce_n(\varphi) ce_m(\varphi) d\varphi = \int_0^{2\pi} se_{n+1}(\varphi) se_{m+1}(\varphi) d\varphi = 0 \quad m \neq n. \quad (93)$$

On the assumption of (91) and (92) we conclude, that after the time $\frac{3}{4} \frac{2\pi}{v}$, system will be in the area G_+ in one of four oscillatory states

ξ_{2n-1}^{\pm} and ζ_{2n-1}^{\pm} with the identical probability equal to 1/4.

After one cycle $\frac{2\pi}{v}$ the system gets back in the area G , from which it started transition from the level ce_{2n} . At returning, four levels ce_{2n} , se_{2n} , ce_{2n-1} and se_{2n+1} will be involved. Calculating probabilities of



passages from the oscillatory state of the area G_+ , to these four levels we shall obtain

$$P(\xi_{2n}^{\pm} \rightarrow ce_{2n}) = P(\xi_{2n}^{\pm} \rightarrow se_{2n+1}) = 1/2, \quad (94)$$

$$P(\xi_{2n-1}^{\pm} \rightarrow se_{2n}) = P(\xi_{2n-1}^{\pm} \rightarrow se_{2n-1}) = 1/2. \quad (95)$$

The probability of passages from the nondegenerated area to the area G_+ in one of the oscillatory states ξ_{2n}^{\pm} , ξ_{2n-1}^{\pm} and back in the area G will be:

$$\begin{aligned} P_+(\eta_{2n}^{\pm} \leftrightarrow se_{2n}) &= P(\eta_{2n} \rightarrow \xi_{2n}^+)P(\xi_{2n} \rightarrow se_{2n+1}) + \\ &+ P(\eta_{2n} \rightarrow \xi_{2n}^-)P(\xi_{2n}^- \rightarrow se_{2n+1}) = \frac{1}{4} \cdot \frac{1}{2} + \frac{1}{4} \cdot \frac{1}{2} = \frac{1}{4} \end{aligned} \quad (96)$$

Similarly it is possible to show

$$P_+(\eta_{2n} \leftrightarrow ce_{2n}) = P_+(\eta_{2n} \rightarrow se_{2n}) = P_+(\eta_{2n}^{\pm} \rightarrow ce_{2n-1}) = 1/4. \quad (97)$$

Thus, after the lapse of time $\frac{2\pi}{\nu}$ four levels of the nondegenerate area

G will be occupied with the identical probabilities $1/4$ (Fig.5)

Moving of the system upwards on energy terms will be ceased at the reaching the level, for which the of the branching points in Fig.4 are on the distance, at which the condition (78) $|l_-^N - l_+^N| > \Delta l$ is not valid. Moving of the system downwards will be stopped at the reaching of the zero level. In case of assuming, the system being at the initial moment in the state $2n = N/2$, then after of $N/8$ cycles of modulation $\frac{2\pi}{\nu}$ all N levels will be occupied with the probabilities $1/N$. The possibility of such consideration at was first shown in [11].

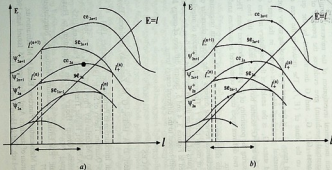


Fig.5. The fragment of the energy terms l , participating in passages calculated in the text.
 a) The initial state. The particle is in the state of cc_{2n} .
 b) The final state. The accessible levels are populated uniformly.

§ 7. CONCLUSIONS

Quantum mechanical investigation of the universal Hamiltonian (the mathematical pendulum) give evidences the presence of three different areas G_+ , G_- and G discriminated by the quantum properties on the plane of (E, I) . The motion in the area of the degenerated states G_- , is the quantum analog of the rotary motion of the mathematical pendulum, while the motion in the area of the degenerated states G_+ is the analog of the oscillatory motion of the pendulum. The area G , located between G_- and G_+ ties two areas, together ensuring the possibility of the passage between them. The area G , dividing two different types can be considered as quantum analog of the separatrix.

The main singularity of the universal Hamiltonian originating at quantum mechanical reviewing consists in the specific character of the dependence of energy terms I . The special alternation of interflowing of different pairs of terms on the left and right side from the separatrix line presented in Figures 3, 4 and 5, ensures diffusion of energy levels population with respect to the different energy terms.

REFERENCES

- 1 R.Z. Sagdeev, D. A. Usikov, G. M. Zaslavsky. Nonlinear Physics, 1988.
2. A.H.Nayfeh, Introduction to Perturbation Techniques, 1981.
3. R.E.Peierls, Quantum Theory of Solids, 1955.
4. G.P.Berman, G.M.Zaslavsky. Phys. Lett., 61A, 1977, 295.
5. H.Bateman, A.Erdelyi. Higher Transcendental Functions, 1955
5. M.Hamermesh, Group Theory and its Application to Physical Problems, 1964.
7. L.P.Landau, E.M.Lifshitz, Quantum Mechanics, Nonrelativistic Theory, 1977.
8. Handbook of Mathematical Functions Edited by M. Abramovitz, National Bureau of standarts Appl. Math.series.55, Issued June 1964.
9. Janke-Emde-Lsch, Tafeln Herer Funktionen, 1960.




10. F. A. Kacmpffer. Concepts in Quantum Mechanics, 1965.
 11. A. Ugulava, L. Chotorlishvili, K. Nikoladze. Phys. Rev. E 68, 2003

Tbilisi State University
 * Telavi State University

ა. უგულავა, ლ. ჭოტორლიშვილი, კ. ნიკოლაძე,
 ზ. როსტომაშვილი

კვანტური ქაოსის თეორიის შესახებ
 დასკვნა

არაწრფივი რეზონანსის ამოცანა დაიყვანება უნივერსალური ჰამილტონიანის შესაბამისი მოძრაობის გამოკვლევაზე. ამ ამოცანის კვანტურშემკვიდრებელ ამოხსნას მიეყავართ მათიე-შრედინგერის განტოლების საკუთარი ფუნქციებისა და საკუთარი მნიშვნელობების შესწავლამდე. კლასიკური სეპარატრისის არეში მათიე-შრედინგერის განტოლების საკუთარი მდგომარეობები გადაუგვარებელი არიან. დამტკმბავი ველის ამპლიტუდის ცვლილების მეშვეობით, როგორც მცირე, ასევე დიდი ამპლიტუდის შემთხვევაში, სისტემა გადადის გადაგვარებული ენერგეტიკული თერმების არეში. გადაგვარება ჩნდება ენერგეტიკული თერმების განშტოებების სახით გადაუგვარებელი ღონეების არეს ორივე მხარეს. დამტკმბავი ველის ნელი ამპლიტუდური მოდულაციის საშუალებით განშტოების წერტილებზე მრავალჯერადი გავლისას სისტემა თანაბარი ალბათობით მოიყავს ენერგეტიკულ თერმებს. სისტემის გადასვლა სხვადასხვა ენერგეტიკულ ღონეებზე, რაც განპირობებულია ენერგეტიკულ თერმებში განშტოების წერტილების არსებობით, წარმოადგენს მათიე-შრედინგერის განტოლების განსაკუთრებულ თვისებას. ის შეიძლება ჩაითვალოს სტოქასტური შრის კვანტურ ანალოგად, რომელიც წარმოიქმნება სეპარატრისის მახლობლობაში იგივე ამოცანის კლასიკური განხილვისას.



COMPUTER PROCESSING OF THE EXPERIMENTAL DATA
OF DEPENDENCE OF DAMPING OF OSCILLATING DISK IN
THE ROTATING He I ON VELOCITY

G. Gujabidze, M. Todua

Accepted for publication July, 2003

ABSTRACT. On the basis of the known experimental data we have studied the dependence of damping of small oscillation of disk on velocity in rotating classical liquid (helium I). The experiment was carried out for the different angular ω_0 velocity at temperature $T = (2.215 \div 2.340)^{\circ}\text{K}$.

The small oscillations of a disk, suspended in rotating classical liquids were theoretically investigated by Yu. Mamaladze and S. Matinyan [1]. The experimental proof of this theory in classical liquid (distilled water) of room temperature was realized by K. Mcsoed and J. Tsakadze [2].

The dependence of oscillations damping of the disk on velocity in low temperature classical liquid (rotating helium I) was studied at the Laboratory of Low Temperatures Physics of the Tbilisi State University by G. Gujabidze and J. Tsakadze under the leadership of academician E. Andronikashvili. The results of their experiment are presented here for the first time.

The oscillating system represented a disk of small size suspended on the elastic fiber. It fulfilled rotation simultaneously with surrounding liquid and small rotary oscillations round the fiber. Logarithmic decrement of oscillations damping was measured using chronometrical method developed by Andronikashvili, Mamaladze and Tsakadze [3].

This method is based on the dependence of amplitude on the time needed for the light spot which is reflected from a small mirror fastened on the pendant of oscillating disk to move between two fixed points: special electronic scheme measures the time interval, during which the light spot passes the distance between two photomultipliers.

According to the theory of this method this time interval increases the damping oscillation of the disk by the law :

$$\ln \tau_n = \ln \tau_1 + \frac{\delta}{2} n \quad (1)$$

if $\tau_n \ll \frac{\theta}{\pi}$; here n is the number of oscillations; τ_1 and τ_2 are the first and n -th time of the movement of light spot between photomultipliers, δ logarithmic decrement of damping; θ denotes period of the oscillation.

Thus, according to this theory, at graphical treatment of experimental data (immediately measured values of τ_n) logarithmic decrement of the damping is determined as double angular coefficient of straight $\ln \tau_n = f(n)$ line.

The experiment was realized by the rough heavy disk, had period of oscillation $\theta_1 = 17.36$ sec in rotary velocity $(0 \div 120)$ sec⁻¹ and temperature $(2,215 \div 2,235)$ °K intervals.

One part of these data, relating to the rotating He I at temperature $T=2,215$ °K, G.Gujabidze and M.Todua processed by computer using program Origin Pro 6.1 in 2002 and the obtained results were published in 2003 [4].

Computer processing of the second part of named data was continued and results are shown in Fig.1, where continuous line represents the theoretical curve, constructed on the ground of the formula Yu.Mamaladze and S.Matinian [1]:

$$\delta - \delta_0 = \frac{\Omega_0}{\Omega} = \frac{\pi^2 \eta R^4}{2I\Omega} \left(\frac{1}{\lambda_+} + \frac{1}{\lambda_-} \right) \left(1 + \frac{2d}{R} + \frac{4}{R} \frac{\lambda_+ + \lambda_-}{\lambda_+ + \lambda_-} \right) \quad (2)$$

Here R and d are radius and thickness of the disk; Ω , δ , and Ω_0 , δ_0 denote frequency and logarithmic decrement of damping, correspondingly in liquid and vacuum; η is viscosity coefficient of liquid.

The experimental points are labelled by the different symbols corresponding to the various temperatures of the He I in the above - mentioned interval. The error of the computer processing is $\pm 0.01 \cdot 10^{-2}$.

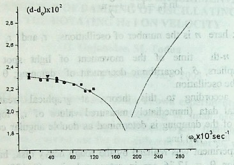


Fig.1. Dependence of logarithmic decrement of damping on rotation velocity for He I at $\theta = 17,36 \text{ wm}^{-1}$ ($R = 1,5\text{cm}$; $d = 0,1\text{cm}$). ■ - $T=2,215^\circ\text{K}$, ● - $T=2,245^\circ\text{K}$, ▲ - $T=2,280^\circ\text{K}$, ▼ - $T=2,315^\circ\text{K}$, ◆ - $T=2,335^\circ\text{K}$.

As can be seen the experimental data of the dependence of oscillation damping on velocity in the rotating He I at the different temperature are in good agreement with the results of theoretical study of analogical question in rotating classical liquid [1].

REFERENCES

1. Yu. Mamaladze, S. Matinyan. PMM, 24, 1960, 473 (Russian).
2. K.Mesoed, J. Tsakadze. Bulletin of the AS GSSR, 26, 1961, 145 (Georgian).
3. E. Andronikashvili, Yu. Mamaladze, J. Tsakadze. Coll. works of AN GSSR, VII, 1960 (Georgian).
4. G.Gujabidze, M.Todua. Bulletin of the Georgian Academy of Sciences, 2, 2003, 167.



მბრუნავ He I-ში რხევადი დისკოს მილვეადობის სიჩქარეზე დამოკიდებულების ექსპერიმენტული კვლევის მონაცემთა კომპიუტერული დამუშავება

დასკვნა

წარმოდგენილია მბრუნავ He-I-ში რხევადი დისკოს მილვეადობის სიჩქარეზე დამოკიდებულების ექსპერიმენტული მონაცემების კომპიუტერული დამუშავების შედეგები გემპერაგურათა (2.215-2.335) °K შუალელში. ისინი ეთანხმება ი. მამალაძისა და ს. მაგინიანის მიერ კლასიკურ სითხეში დისკოს აქსიალურ-გრეხითი რხევების თეორიული კვლევის დასკვნებს.

MODIFIED HYPERSPHERICAL FUNCTION METHOD FOR 3 PARTICLES SYSTEM IN 2D SPACE WITH INVERSE SQUARE POTENTIAL BETWEEN PARTICLES

A. Lomidze, Sh. Tsiklauri

Accepted for publication September, 2002

ABSTRACT. The present investigation reports, that modified hyperspherical function method permits us to advance comparatively simple and nonmodel representation of the solution of three particles problem in 2D space for inverse square of pair interaction. This becomes possible due to the correlation function along with the effective potential there appears r^{-1} potential, leading the ground-state energy to the finite quantity. In a first approximation the problem is decided analytically.

Numerous physical phenomena may be described by singular potentials [1]. Inverse square potential is more interesting, especially in polymers [2], and in the interaction between Rydberg atom and polar molecule [3]. The problem of three particles by pair interaction of $\frac{g}{r^2}$ type in 1D space in a field harmonic oscillator has been worked out analytically [4]. The problem of three particles for pair inverse square interaction in 3D space has been studied [5], the same system in 2D space is considered in the present paper.

Schrodinger equation in a system of center of masses for three nonidentical and nonrelativistic particles in hyperspherical coordinates in 2D space are defined in [6]. When we solve Schrodinger equation we get coupled differential equations system for hyperradial function. We consider only one equation from this system, when $K = K'$ (K is hypermoment of the particles). As a result the following equation have been gotten:

$$\left(\frac{\partial^2}{\partial \rho^2} - \left[\chi^2 + \frac{(K+1)^2 - 0,25}{\rho^2} \right] \right) \varphi_K(\rho) = \frac{2\mu}{\rho^2} J_K \varphi_K(\rho) \quad (1)$$

where:

$$J_K = \int \Phi_K^*(\Omega) \Phi_K(\Omega) (\cos \alpha)^{-2} d\Omega \quad (2)$$

and $\chi^2 = -2\mu E$; $\Phi(\Omega)$ is eigenfunction of the generalized angular-momentum operator which analytical form is known [6],

$$\Phi_K(\Omega) = C_0 \cos \alpha \sin \alpha P_n^{1,1}(\cos^2 \alpha) \quad (3)$$

where:

$$n = \frac{K}{2}, \quad C_0 = \left[\frac{2(1 \cdot 2 \cdot \dots \cdot n) \Gamma(1+n)(1+2n)}{\Gamma(1+n)\Gamma(1+n)} \right]^{1/2}$$

$\Omega = (\alpha, \bar{x}, \bar{y})$ denotes five angles, ρ and α are defined by the expression: $\rho^2 = x^2 + y^2$; \bar{x} and \bar{y} are the Jacoby coordinates; $|\bar{x}| = \rho \cos \alpha$; $|\bar{y}| = \rho \sin \alpha$; ($0 < \rho < \infty$; $0 < \alpha < \frac{\pi}{2}$). $E < 0$ is a binding energy for three particles; μ is a reduced mass. The integral (2) can be calculated analytically [6] and it is equal to

$$J_K = 2^{-(K+1)} \frac{g_{ij} m_i m_j}{(m_i + m_j) \mu} \sum_{k=1}^n \left[\binom{n+1}{k} \binom{n+1}{k+1} \right]^2 B\left(\frac{3}{2}, K-2k+1\right) \times \\ \times \frac{\Gamma(K+2)}{\Gamma(2k+1)\Gamma(K-2k+2)} \quad (4)$$

Simple analysis shows that under these conditions the ground state energy has infinitely large negative value and therefore there is no sense to solve it. To avoid this we use modified hyperspherical function method (MHFM) [7].

The main idea of the MHFM is that wave function Ψ represents the product of two functions, where the first is the main hyperspherical function and the second is the correlation function- $\zeta = \exp(f)$, defined



by singularity and clustering properties of the wave function and it is equal to,

$$f = - \sum_{i=1}^3 \gamma_i r_i, \quad (5)$$

where r_i is a distance between the particles and γ_i is determined according to physical considerations.

Taking into account the relation between three different sets of Jacobi coordinates [8], the expression (5) can be presented as:

$$\sum_{i=1}^3 \gamma_i z_i = \rho(G_1 \cos \alpha + G_2 \sin \alpha), \quad (5')$$

where:

$$G_1 = \gamma_1 + \gamma_2 \cos(\phi_{23} + \phi_{31}) - \gamma_3 \cos \phi_{31};$$

$$G_2 = \gamma_2 \sin(\phi_{23} + \phi_{31}) - \gamma_3 \sin \phi_{31}.$$

If we substitute expression (5') into (1), and carry out some transformations, hyperradial differential equation is obtained but we consider only one equation when $K = K'$:

$$\left(\frac{\partial^2}{\partial \rho^2} + \left(\frac{3}{\rho} - W'_2 \right) \frac{\partial}{\partial \rho} + \frac{3W'_2 + W'_3}{\rho} + \left(\chi^2 + W'_6 \right) - \frac{2\mu K(K+2) + J_0}{\hbar^2 \rho^2} \right) \psi(\rho) = 0 \quad (6)$$

where:

$$W'_2 = (G_1 - G_2) \times \frac{21\sqrt{6}}{8}; \quad W'_6 = G_1^2 + G_2^2;$$

$$W'_3 = W'_2 + 21\sqrt{6}(0,25G_1 + G_2)$$

Taking into account the asymptotic behavior of the equation (6), let us seek a solution as the following:

$$\psi(\rho) = \exp(-\delta\rho)\rho^\sigma\varphi(\rho) \quad (7)$$

where:

$$\sigma = -1 + \sqrt{9 + 2mJ_0}; \quad \delta = \frac{\sqrt{W_2'^2 - 4(\chi^2 + W_6') - W_2'}}{4}$$

Substituting expression (7) into equation (6), then for $\varphi(\rho)$ we obtain the equation of hypergeometrical function:

$$\left(r \frac{\partial^2}{\partial r^2} + (-r + 2\sigma + 3) \frac{\partial}{\partial r} + \frac{(3W_2' + W_3' - 3\delta)}{2\delta + W_2'} - \sigma \right) \varphi(r) = 0, \quad (8)$$

where: $r = (2\delta + W_2')\rho$.

If we take into account that three body system is binded then solution of the (8) equation is represented as the following type of hypergeometrical function:

$$\varphi(\rho) = C_1 F(a, b, r) \quad (9)$$

$$\text{where: } b = 2\sigma + 3; \quad a = \frac{(3W_2' + W_3' - 3\delta)}{2\delta + W_2'} = -N; \quad N = 1, 2, \dots$$

For binding energy we received:

$$E_N = -\frac{\hbar^2}{8\mu} \left[\left(\frac{12W_2' + 4W_3' - W_2'(3 + 2\sigma - 2N)}{3 + 2\sigma - 2N} \right)^2 - W_2'^2 + 4W_6' \right] \quad (10)$$



The dependence of binding energy of three body system on the global quantum number N obtained as a solution results in the expression (10) that is given in the Table.

Table. Dependence of the binding energy of the three body system in 2D space upon the global quantum number N

Global quantum number N	Binding energy $-E$ (a.u.)
1	0.114174
2	0.074499
3	0.005834
4	0.001928
5	0.001256
6	0.001143

(In these results we assume that correlation parameters and interaction constant are the same for all particles. Their variation doesn't give any qualitatively new results).

Thus MHFM permits us to advance comparatively simple and nonmodel representation of the solution of three particles problem in 2D space for inverse square of pair interaction. This is possible due to the correlation function together with effective potential appears to be $\frac{1}{r}$ potential, leading the ground-state energy to finite quantity. In a first approximation the problem is decided analytically.

REFERENCES

1. W.M.Frank, D.Land, R.M.Spector. Rev. Mod.Phys. **43**, 1971, 36; D. Amin. Phys. Today **35**, 1982, 35; Phys. Rev. Lett. **36**, 1976, 323; A. Khare, S. N. Behra, Pramana. J. Phys. **14**, 1980, 327; S. Coleman. Aspects of Symmetry selected Erice Lectures, Cambridge, 1988.
2. E.Marinari, G.Parisi. Europhys. Lett. **15**, 1991, 721.
3. C.Desfranqois, H. Abdoul-Carime, N.Khelifa, J.P.Schermann. Phys.



Rev. Lett. **73**, 1994, 2436.

4. F. Calogero. J. Math. Phys. **10**, 1969, 2191.

5. A.M. Lomidze, Sh.M. Tsiklauri. Bulletin of the Georgian Academy of Sciences, **159** 1, 1999, 52.

6. Georgian Electronic Scientific Journal: Computer Sciences and Telecommunication **1-2002**, 49.

7. A.M. Gorbatov, A.V. Bursak, Yu.N. Krilov, B.V. Rudak, Yad. Fiz. **40**, 1984, 233; M.I. Haftel, V.B. Mandelzweig. Phys. Lett. **A120**, 1987, 232; Ann. Phys. **189**, 1989, 29; Fabre de la Ripelle, Ann. Phys. **147**, 1982, 281.

8. R.I. Jibuty, N.B. Krupennikova. The Hyperspherical Functions Method in Few - Body Quantum Mechanics. Tbilisi, 1984, (Russian).

Tbilisi State University

ა. ლომიძე, შ. წიკლაური

მოდიფიცირებული ჰიპერსფერული ფუნქციების მეთოდი სამ ნაწილაკიანი სისტემისათვის 2D სივრცეში ნაწილაკებს შორის ინვერსიულ-პარმონიული პოტენციალისათვის

მოდიფიცირებული ჰიპერსფერული ფუნქციების მეთოდი შესაძლებლობას იძლევა არამოდულურ წარმოდგენით შედარებით ადვილად გადაწყდეს სამნაწილაკიანი პრობლემა 2D სივრცეში ინვერსიულ-პარმონიული წყვილური ურთიეთქმედებისას, რაც შესაძლებელი გახდა იმის გამო, რომ კორელაციის გათვალისწინებისას ეფექტურ პოტენციალთან ერთად r^{-1} სახის პოტენციალი გაჩნდა, რაც იწვევს ძირითადი მდგომარეობის ენერჯიის სასრულობას.

CONTENTS

G. Kakauridze, V. Shaverdova - The influence of preliminary nonpolarized exposure on the photoanisotropy of mordant azodyes	3
G. Kakauridze, V. Shaverdova - Photoanisotropy in media on the basis of isomeric dyes metanilic yellow and tropocolin 00	8
A. Purtseladze - The degree of light polarization in nonstationary processes	15
Z. Khvedelidze, I. Aladashvili, T. Shalamberidze, E. Tagvadze, R. Chakvaia - Dynamics of atmospheric processes and their role in ecological problems of Georgia	21
L. Tarasashvili, Sh. Kakichashvili - Photoinduced anisotropy in seleno-cadmium glass	31
I. Sikmashvili, Z. Sikmashvili, O. Tsagareishvili - Diffraction radiation of an electron flow moving above the screen with slots	37
K. Tukhashvili, V. Kandashvili - On modeling of the diurnal variation of the coefficient of computation of tilt sounding from vertical sounding of ionosphere	46
S. Tsereteli, V. Bochorishvili, M. Makhviladze, M. Samkharadze - Anthropogenic effect on natural processes and its study using radiocarbon method	57
Sh. Kekutia, N. Chkhaidze, Sh. Ben-Ezra - Equations of motion for superfluid $He^3 - He^4$ solutions filled porous media	62
M. Gochitashvili, B. Kikian, R. Kvizhinadze, R. Lomsadze - The dissociative excitation processes in collisions of electrons and helium ions with oxygen molecules	75
L. Kiknadze, Yu. Mamaladze - Angular momentum caused by any shape vortex line	81
P. Defrance, T. Kereselidze, I. Noselidze, M. Tzulukidze - Electron impact double ionization of helium-like ions in the metastable states	92
A. Ugulava, L. Chotorlishvili, K. Nikoladze, Z. Rostomashvili - On the theory of quantum chaos	109
G. Gujabidze, M. Todua - Computer processing of the experimental dates of dependence of the disk, oscillating in the rotating He I, on velocity	150
A. Lomidze, Sh. Tsiklauri. Modified hyperspherical function method for inverse square potential in 2d space	154

გ. კაკაურიძე, ვ. შავერდოვა - წინასწარი არაპოლარიზებული დასხივე- ბის მოქმედება ამოსალეხბავების ფოტოანიზოტროპიაზე	7
გ. კაკაურიძე, ვ. შავერდოვა - მეტანილის ყვითელი და გროპეოლინი 00 იზომერული სალხბავების ბაზაზე შექმნილი არეების ფოტოანიზოტრო- პია	14
ა. ფურცელაძე - სინათლის პოლარიზაციის ხარისხი არასტაციონარულ პროცესებში	20
ზ. ხვედელიძე, ი. ალადაშვილი, თ. შალამბერიძე, ე. თაგვაძე, რ. ჩახაია - აგმოსფერული პროცესების დინამიკა და მისი როლი საქართველოს ეკოლოგიურ პრობლემებში	30
შ. ყაყიჩაშვილი, ე. გარასაშვილი - ფოტონდუცირებული ანიზოტროპია სელენ-კადმიუმის მინაში	36
ი. სიყმაშვილი, მ. სიყმაშვილი, ო. ცაგარეიშვილი - სასრული სისქის პერფორირებულ ეკრანის შემოთ მოძრავი ელექტრონული ნაკადის დიფრაქციული გამოსხივება	45
ქ. ტუბაშვილი, ვ. ყანდაშვილი, ჯ. მდინარაძე - იონოსფეროს ვერტიკალური ზონდირებიდან დახრილ ზონდირებაზე გადასაანგარიშებელი კოეფიცი- ენტის დღე-ღამური ცვლილების მოდელირების შესახებ	56
ს. წერეთელი, ვ. ბოჭორიშვილი, მ. მახვილაძე, მ. სამხარაძე - ანთროპო- გენური ზემოქმედება ბუნებრივ პროცესებზე და მისი შესწავლა რადიო ნახშირბადული მეთოდით	61
შ. კეკუტია, ნ. ჩხაიძე, შ. ბენ-ემრა - He^3 - He^4 სსნარით შევსებულ ფო- როვან გარემოს მოძრაობის განტოლებები	74
შ. გოჩიაშვილი, ბ. კიკიანი, რ. კვიციანიძე, რ. ლომსაძე - დისოციაციის პრო- დუქტების აღგზნების გამოკვლევა ელექტრონებისა და He^+ იონების ენ- გბადის მოლეკულებთან დაჯახების პროცესში	80
ლ. კიკნაძე, ი. მამალაძე - ნებისმიერი ფორმის გრიგალით განპირობებუ- ლი მოძრაობის რაოდენობის მომენტა	90
პ. ლეფრანსი, თ. კერესელიძე, ი. ნოსელიძე, მ. წულუკიძე - მეტასტაბილურ მდგომარეობაში მყოფი პელიუმისმაგვარი იონების ორჯერადი იონიზა- ცია ელექტრონებით	108
ა. უგულავა, ლ. ჭოგორიშვილი, კ. ნიკოლაძე, ზ. როსტომაშვილი - კვანტური ქაოსის თეორიის შესახებ	149
გ. გუჯაბიძე, მ. თოდუა - მზრუნავ He I-ში რხევადი დისკოს მიღვევადობის სიჩქარეზე დამოკიდებულების ექსპერიმენტული კვლევის მონაცემთა კომპიუტერული დამუშავება	153
ა. ლომიძე, შ. წიკლაური - მოდიფიცირებული პიპერსფერული ფუნქციე- ბის მეთოდი სამნაწილაკიანი სისტემისათვის 2D სივრცეში ნაწილა- კებს შორის ინვერსიულ-პარმონიული პოტენციალისათვის	159

გამომცემლობის რედაქტორი რ. ჩირგაძე
ტექნოლოგიური თ. ფირცხელანი
კორექტორი ნ. მაჭავარიანი
კომპიუტერული უზრუნველყოფა ს. ჩხაიძე

ხელმოწერილია დასაბუქლად 20.11.03

საბეჭდი ქალაქი 60x84

პირ. ნაბეჭდი თაბახი 10.25

სააღრ.-საგამომც. თაბახი 6,6

შეკვეთა № 57

გირაჟი 150

ფასი სახელმწიკრულებო

თბილისის უნივერსიტეტის გამომცემლობა,
0128, თბილისი, ი. ჭავჭავაძის გამზ., 14.



გამომცემლობა „უნივერსალი“

თბილისი, 380028, ი. ჭავჭავაძის გამზ. 1

☎: 29 09 60, 8(99) 17 22 30

E-mail: universal@posta.ge

